Available online at www.sciencedirect.com
SCIENCE DIRECT®

Atomic Data and Nuclear Data Tables 92 (2006) 407–455

Atomic Data AND Nuclear Data Tables

www.elsevier.com/locate/adt

Cross section database for carbon atoms and ions: Electron-impact ionization, excitation, and charge exchange in collisions with hydrogen atoms

Hiroya Suno *, Takako Kato

National Institute for Fusion Science, Toki, Gifu 509-5292, Japan

Abstract

A database has been constructed consisting of the recommended cross sections for electron-impact excitation and ionization of carbon atoms and ions C, C^{+}–C^{5+}, as well as for charge exchange processes between carbon ions C^{+}–C^{6+} and hydrogen atoms. We have collected a large amount of theoretical and experimental cross section data from the literature, and have critically assessed their accuracy. The recommended cross sections, the best values for use, are expressed in the form of simple analytical functions. These are also presented in graphical form.

* Corresponding author. Fax: +81 45 778 5771.
E-mail address: suno@jamstec.go.jp (H. Suno).

0092-640X/$ - see front matter
doi:10.1016/j.adt.2006.01.001

Contents

1. Introduction

The interactions among electrons, ions, and hydrogen atoms are the most important processes which occur in laboratory and astrophysical plasmas. The understanding of these collision processes is essential for diagnosing and modeling plasmas in controlled fusion experiments, plasmas processing, and astrophysics. In addition to the application of studying plasma dynamics, collision processes such as electron-impact excitation, ionization, and charge exchange processes are interesting from the view of fundamental physics, like many-body collision dynamics.

In this paper, we focus attention on carbon atoms and ions C^{q+} ($q = 0$–6). Carbon atoms and ions are abundant in various astrophysical environments, fusion reactors, and plasma-chemistry atmospheres. We consider electron-impact excitation and ionization of these atoms and ions, as well as charge exchange processes in collisions between carbon ions and hydrogen atoms. Therefore, we have collected the data for cross sections from the literature and have critically assessed their accuracy to obtain recommended data. The recommended data have been fitted to simple analytical fit functions. For electron-impact excitation processes, rate coefficients have also been derived. The fit coefficients are presented in the tables. The values derived from fitted functions are presented as the recommended data in the graphs, together with the original data from the literature. We have taken into account the important transitions for excitation, ionization, and charge exchange processes. For these data and the processes which are not shown in this paper, the original data can be found at NIFS Database webpage http://dbshino.nifs.ac.jp: AMDIS for excitation and ionization, and CHART for charge transfer (charge exchange).

This paper is organized as follows. First, we deal with electron-impact excitation of C^{q+} ($q = 0$–5) atoms and ions. Second, electron-impact ionization processes of these atoms and ions are considered. The double-ionization of C^{+} is also presented. Next, charge exchange cross sections between carbon ions C^{q+} ($q = 1$–6) and hydrogen atoms are presented, including state-selective cross sections. Finally, a brief summary of the work is given.

1.1. Electron-impact excitation of carbon ions and atoms

There are numerous theoretical cross section data for electron-impact excitation of carbon ions. Previously, Itikawa et al. [1] compiled cross sections reported until 1985 for carbon ions (C^{+}–C^{5+}) as well as oxygen ions (O^{+}–O^{12+}), critically evaluated the data, and fitted the recommended values to analytical formulae. Before 1985, cross sections were calculated by the distorted-wave method, the Coulomb–Born approximation, the Coulomb–Born Oppenheimer method, and the close-coupling method. These are reported for various excitation processes of all ions C^{+}–C^{5+} in Los Alamos Scientific Reports (1977) [2–5]. McDowell et al. [6] had calculated electron-impact excitation cross sections for C^{5+} and C^{4+} ions using the distorted-wave method. Close-coupling calculations had been carried out for C^{4+} by Foster et al. [7]. Berrington et al. [8,9] had reported cross sections calculated by the *R*-matrix method. In the following, we have compiled cross section and rate coefficient data for electron-impact excitation of carbon atoms and ions reported after 1985 and have given the recommended data. These recommended data are fitted to analytical functions. The references for the data which we adopted as recommended data are shown in Tables 1–6.

For C^{5+}, Aggarwal and Kingston [10] have reported their *R*-matrix calculations of cross sections (collision strengths) and rate coefficients (effective collision strengths) for numerous excitation processes up to $n = 5$, where n is the principal quantum number. The energy region of their calculations is below 50 Ry. All of their data can be found in the NIFS AMDIS Database. Zou and Shirai [11] have calculated cross sections for the $1s \rightarrow 2s$ and $1s \rightarrow 2p$ processes using the close-coupling method with exchange 3-levels, while Fisher et al. [12] have carried out cross section calculations using the convergent close-coupling method for the same transitions. Callaway [13] have reported rate coefficient data calculated by the close-coupling method for $1s \rightarrow 2s$ and $1s \rightarrow 2p$ excitation processes.

For C^{4+} ions, Badnell [14] has reported cross section calculations using the distorted-wave method for several excitation processes among $n = 1$ and $n = 2$ states, where n indicates the principal quantum number of the most excited electron in the initial and final electronic configurations. Cross section calculations have been carried out also with a combination of the distorted-wave method with exchange and the configuration interaction method by Srivastava and Katiyar [15] for the $1s^2\ ^1S \rightarrow 1s2s\ ^1S$ and $1s^2\ ^1S \rightarrow 1s2p\ ^1P$ excitations. Kato and Nakazaki [16] evaluated the data for excitation of He-like ions.

For C^{3+}, experimental cross sections measured by Taylor et al. [17], Bannister et al. [18], Greenwood et al. [19], and Janzen et al. [20] were reported for the $2s\ ^2S \rightarrow 2p\ ^2P$ excitation. Burke [21] and Griffin et al. [22] calculated rate coefficients by using the close-coupling method and the *R*-matrix method, respectively, for several transitions among $n = 1$ to $n = 4$ states.

For C^{2+}, Berrington et al. [23] reported cross sections calculated by the *R*-matrix method for several excitation processes among $n = 2$ and $n = 3$ states. Itikawa and Sakimoto [24] calculated cross sections by using the distorted-wave method for the $2s^2\ ^1S \rightarrow 2s2p\ ^3P$ and $2s^2\ ^1S \rightarrow 2s2p\ ^1P$ transitions. Rate coefficients were calculated using the *R*-matrix method by Berrington et al. [25] for transitions among $n = 2$ and $n = 3$ states.

Unfortunately, we found no new theoretical cross section data published for C^+ since 1985. However, Blum and Pradhan [26] calculated rate coefficients for fine structure transitions among $n = 2$ and $n = 3$ configurations. Experimental measurements by Williams et al. [27] have been reported for the $2s^22p\ ^2P \rightarrow 2s2p^2\ ^4P$ process.

For the C atom, Dunseath et al. [28] reported cross sections calculated by the *R*-matrix method for a large number of excitation processes among $n = 2$ and $n = 3$ states. All of their numerical data can be found in the NIFS AMDIS Database. Cross sections calculated using the close-coupling method were reported by Henry et al. [29] for the $2s^22p^2\ ^3P \rightarrow 2s^22p^2\ ^1D$ and $2s^22p^2\ ^3P \rightarrow 2s^22p^2\ ^1S$ excitation processes. Pindzola et al. [30] calculated cross sections by using the distorted-wave method with exchange for the $2s^22p^2\ ^3P \rightarrow 2s^22p^2\ ^1D$ process. Thomas and Nesbet [31] reported their matrix variational calculations for the $2s^22p^2\ ^3P \rightarrow 2s^22p^2\ ^1S$ and $2s^22p^2\ ^1D \rightarrow 2s^22p^2\ ^1S$ transitions.

In general, electron-impact excitation cross sections calculated by different theoretical methods do not agree well, especially for optically forbidden transitions. Our recommended cross sections are chosen following these criteria: the close-coupling method and *R*-matrix method can lead to more reliable results at lower collision energies, and so can the distorted-wave method and Coulomb–Born method at high energies. Experimental measurements are considered as more reliable than theoretical calculations. For certain transitions we have not found any new cross section data published since [1]. In such cases, we only used the fitted formula given in [1].

In this paper, we fit the collision strength Ω by a fitting formula. The electron-impact excitation cross sections $Q_{\rm if}$ are related in terms of collision strengths $\Omega_{\rm if}$ as follows, where i and f indicate the initial and final states, respectively. For the excitation from state i to f, the cross section is given by

$$Q_{\rm if}[\pi a_0^2] = \frac{\Omega_{\rm if}}{\omega_{\rm i} E_{\rm e}[\rm Ry]} = \frac{1}{\omega_{\rm i} V_{\rm if}[\rm Ry]}\frac{\Omega_{\rm if}}{X}, \tag{1}$$

where $E_{\rm e}$ is the energy of the incident electron, $\omega_{\rm i}$ the statistical weight of the initial state, $V_{\rm if}$ the excitation energy, and $\Omega_{\rm if}$ the collision strength. Here, the cross section is in units of πa_0^2, where a_0 is the Bohr radius and X is the reduced electron energy defined by

$$X = E_{\rm e}/V_{\rm if}. \tag{2}$$

When the cross section and energy are given in units of cm^2 and eV, respectively, we have

$$\begin{aligned} Q_{\rm if}[\rm cm^2] &= 1.1969 \times 10^{-15} \times \frac{\Omega_{\rm if}}{\omega_{\rm i} E_{\rm e}\ [\rm eV]} \\ &= 1.1969 \times 10^{-15} \times \frac{\Omega_{\rm if}}{\omega_{\rm i} V_{\rm if}\ [\rm eV] X}. \end{aligned} \tag{3}$$

With the Maxwellian distribution of electron velocity for temperature $T_{\rm e}$, the rate coefficient is calculated by

$$R_{\rm if}[\rm cm^3\ s^{-1}] = \frac{8.010 \times 10^{-8}}{\omega_{\rm i}\sqrt{T_{\rm e}\ [\rm eV]}}\, y \int_1^\infty {\rm d}X\, \Omega_{\rm if}(X) {\rm e}^{-yX}, \tag{4}$$

where

$$y = V_{\rm if}/T_{\rm e}. \tag{5}$$

We have carefully chosen reliable data from the references. Once the recommended values of cross sections were determined, a fit was made in terms of collision strengths, which facilitates the fit procedure more readily than the cross section because of their energy dependence. Two types of formulae have been used for the fit procedures. The formula of Type 1 is defined by

$$\Omega_{\rm if}(X) = A + \frac{B}{X} + \frac{C}{X^2} + \frac{D}{X^3} + E\ln X, \tag{6}$$

whereas for Type 2 we have

$$\Omega_{\rm if}(X) = \frac{A}{X^2} + B{\rm e}^{-FX} + C{\rm e}^{-2FX} + D{\rm e}^{-3FX} + E{\rm e}^{-4FX}. \tag{7}$$

Here, A, B, C, D, E, and F are adjustable coefficients. Note that, for Type 1, we have $E = 0$ in the case of an optically forbidden transition. For optically allowed transitions, we can drop the term D/X^3 in Eq. (7) since the remaining four terms are sufficient to fit the electron-impact excitation cross sections. With the use of these formulae, the rate coefficients can be calculated in the form

$$R[{\rm cm}^3\ {\rm s}^{-1}] = \frac{8.010\times 10^{-8}}{\omega_{\rm i}\sqrt{T_{\rm e}\ [{\rm eV}]}}{\rm e}^{-y}\gamma. \tag{8}$$

Here, γ is the effective collision strength and is defined by

$$\gamma = y{\rm e}^{y}\int_1^\infty \Omega_{\rm if}{\rm e}^{-yX}\,{\rm d}X. \tag{9}$$

We have

$$\gamma = y\left\{\left(\frac{A}{y} + C\right) + \frac{D}{2}(1-y) + {\rm e}^{y}E_1(y)\left(B - Cy + \frac{D}{2}y^2 + \frac{E}{y}\right)\right\} \tag{10}$$

for Type 1 and

$$\gamma = Ay\{1 - {\rm e}^{y}E_1(y)y\} + \left(\frac{B{\rm e}^{-F}}{F+y} + \frac{C{\rm e}^{-2F}}{2F+y} + \frac{D{\rm e}^{-3F}}{3F+y} + \frac{E{\rm e}^{-4F}}{4F+y}\right)y \tag{11}$$

for Type 2, with

$$E_1(y) = \int_y^\infty \frac{{\rm e}^{-t}}{t}\,{\rm d}t. \tag{12}$$

In most of the cases, the cross section (or collision strength) data are fitted by using the formula in Eq. (6). If Eq. (6) is not good to fit the collision strength, we use Eq. (7). If both of these formulae fail to fit and rate coefficient data are available, we use Eq. (10) or Eq. (11).

When the resonant effects are included in the data and their effects are large, we divide the collision strength into two parts:

$$\Omega = \Omega_{\rm NR}(X) \quad \text{for } X > X_1, \tag{13}$$

$$\Omega_{\rm R}(X) \quad \text{for } 1 \leqslant X \leqslant X_1, \tag{14}$$

where $\Omega_{\rm R}$ and $\Omega_{\rm NR}$ indicate the collision strengths with and without resonance effects, respectively. The reduced energy X_1 defines the boundary of the region where the resonance effects dominate. Note that $\Omega_{\rm R}(X_1)$ is not necessarily equal to $\Omega_{\rm NR}(X_1)$. Since $\Omega_{\rm R}$ has a complicated structure as a function of X, it is almost impossible to fit it to any simple formula. Instead, we assume the collision strength in the form

$$\Omega_R(X) = PX + Q \quad \text{for } 1 \leqslant X \leqslant X_1. \tag{15}$$

The quantities P, Q, and X_1 are determined as fit parameters by equating the rate coefficients calculated with the use of Eqs. (14) and (15) to the rate coefficients given in the literature.

The values of fit parameters A, B, C, D, E, and F for each excitation process are given in Tables 1–6, together with the excitation energies, the references of the adopted data, and the rms percent error (for the definition, see below). When resonance effects are included, the parameters P, Q, and X_1 are also tabulated for $\Omega_{\rm R}(X)$ in Eq. (15).

For most of the excitation processes, the recommended values of collision strengths and rate coefficients, which can be reproduced with the fit parameters, are shown graphically in Graphs 1–124, together with the original data from the literature. The boundary between the resonance and non-resonance regions is also indicated as a dashed line.

In our work, the quality of the fit function is expressed in terms of the rms percent error, which is defined by

$$\text{rms percent error} = \sqrt{\frac{1}{N}\sum_{i=1}^{N}\left(\frac{\Omega_i^{\rm Fit} - \Omega_i^{\rm Data}}{\Omega_i^{\rm Data}}\right)^2}, \tag{16}$$

where N is the number of data points, $\Omega_i^{\rm Fit}$ is the fitted collision strengths, and $\Omega_i^{\rm Data}$ is the collision strengths in the original data. For most of the transitions, the rms percent errors are less than 0.1 and in difficult cases, they are at most 1.46. The rms percent errors are not available for the coefficients that were directly taken from [1].

1.2. Electron-impact ionization of carbon ions and atoms

Electron-impact ionization of carbon ions has been extensively studied both experimentally and theoretically. We selected the data considered to be reliable and they are shown in Graphs 125–138. Experimental measurements of C^{q+} were carried out by Donets and Osvyannikov [34] for the ions C^{q+} with $q = 1, 2, 3, 4$, and 5, in the electron energy range between 1 and 10 keV.

For electron-impact ionization of the C^{5+} ion, experimental measurements were reported by Aichele et al. [35]. Theoretical cross sections calculated by using a semi-empirical method, the distorted-wave method with exchange, relativistic distorted-wave method, and distorted-wave Born method with exchange, were reported respectively by Pattard and Rost [36], Younger [37], Kao et al. [38], and Fang et al. [39]. For C^{5+} as well as the other ions, the experimental data by Donets and Ovsyannikov [34] are larger than the other data.

For C^{4+}, experimental measurements were carried out by Crandall et al. [40]. Theoretical calculations using the binary encounter approximation and distorted-wave Born method with exchange were reported respectively by Salop [41] and Fang et al. [39]. We selected the data from Fang et al. [39] as the recommended data.

For C^{3+}, experimental measurements were performed by Knopp et al. [42] and Crandall et al. [43]. Theoretical calculations using the distorted-wave method with exchange and R-matrix method were carried out respectively by Jakubowicz and Moores [44] and Knopp et al. [42]. The Coulomb–Born method with exchange was employed by Sampson and Golden [45]. Scott et al. [46] and Badnell and Griffin [47] used the R-matrix method with pseudostates. We have selected the data by Knopp et al. [42] as the recommended data. Because of the excitation-autoionization, there are two peaks in the cross section. We fit the cross sections with a sum of two different equations in the form of Eq. (17) (see below for the definition).

For C^{2+}, experimental measurements were reported by Woodruff et al. [48] and Falk et al. [49]. Theoretical calculations using the binary encounter approximation and the Coulomb–Born method were carried out by Salop [41] and Moores [50]. Jakubowicz and Moores [44] and Younger [37] reported cross sections calculated by the distorted-wave method with exchange and the distorted-wave Born method with exchange respectively. We recommend the data by Woodruff et al. [48].

For C^{+}, experiments were carried out by Yamada et al. [51]. Qian and Pan [52] reported theoretical results obtained by R-matrix calculations using the single-channel approximation and the 3-state close coupling approximation. For C^{+}, the cross section measurements by Westermann et al. [53] are reported for the double ionization process $C^{+} + e \rightarrow C^{3+}$.

For the C atom, we found the measurements by Brook et al. [54] and the theoretical calculations using the Born approximation by Omidvar et al. [55]. We choose the data by Brook et al. [54] as the recommended data.

Most of the experimental and theoretical cross sections from different authors agree fairly well with each other. However, the experimental electron-impact ionization cross sections reported by Donets and Ovsyannikov [34] are always larger than the others except for C^{3+}. In general, we have chosen the most recent results as the recommended data. The rms percent errors are at most 1.07 (C^{4+}).

The recommended cross section for electron-impact ionization is parametrized using the expression

$$\sigma[\mathrm{cm}^2] = \frac{10^{-13}}{IE}\left\{A_1 \ln(E/I) + \sum_{i=2}^{N} A_i \left(1 - \frac{I}{E}\right)^{i-1}\right\}, \tag{17}$$

where the collision energy E and ionization potential I are expressed in eV units and A_i are fitting coefficients. Note that the coefficient A_1 can be related to the continuum oscillator strength $\mathrm{d}f/\mathrm{d}\epsilon$ by

$$A_1 = 8.39 \times 10^{-2} I \ [\mathrm{eV}] \int_0^\infty \frac{1}{E+\epsilon}\frac{\mathrm{d}f}{\mathrm{d}\epsilon}\,\mathrm{d}\epsilon, \tag{18}$$

where ϵ is the energy of ejected electrons. However, we do not use this equation to derive the A_1 value. The values of A_i in Eq. (17) are given in Table 7, together with the ionization energy, the references of the adopted data, and the rms percent error. The fitted cross sections are graphically presented as a solid curve in Graphs 125–138.

1.3. Charge exchange in collisions between carbon ions and hydrogen atoms

There are numerous theoretical and experimental results for charge exchange processes in collisions of carbon ions with hydrogen atoms. The references for the recommended data are listed in Table 8 for each process. These data are fitted to analytical functions and the fitting parameters are listed in the tables.

The $C^{6+} + H$ collisions are the most extensively studied processes. State-selective cross sections were calculated by Toshima and Tawara (using the close-coupling method) [56], Belkic et al. (classical distorted-wave method) [57,58], Ryufuku (unitarized distorted-wave approximation) [59], Olson and Schultz (classical trajectory Monte Carlo method) [60], Green et al. (close-coupling method) [61], Harel et al. (molecular orbital approach) [62], Kazanskii and Komarov (molecular orbital approach) [63], Fritsch and Lin (atomic orbital close-coupling method) [64], Fritsch (atomic orbital method) [65], Kimura and Lin (atomic orbital and molecular orbital methods) [66], and Das et al. (classical distorted-wave method) [67]. These authors also obtained the total cross sections for the $C^{6+} + H \rightarrow C^{5+} + H^{+}$ process. Measurements of total cross sections were performed by Panov et al. [68] and Meyer et al. [69]. Janev et al. [70] gave the recommended total charge exchange cross sections.

For $C^{5+} + H$ collisions, state-selective charge exchange cross sections were calculated using the molecular orbital close-coupling method by Shimakura et al. [71] as shown in Graph 159. Since their energy region is too limited to fit the cross sections, only their data are shown in the graph. Total charge exchange cross sections were calculated by Shimakura et al. (molecular orbital close-coupling method) [71] and Shipsey et al. (perturbed-stationary method and classical trajectory Monte Carlo method) [72]. Experimental measurements of total cross sections were carried out by Goffe et al. [73], Panov et al. [68], and Phaneuf et al. [74].

For $C^{4+} + H$ collisions, state-selective charge exchange cross sections were calculated by Errea et al. (using the molecular orbital close-coupling method) [75], Gargaud et al. (molecular orbital approach) [76], and Fritsch and Lin (atomic orbital close-coupling method) [64]. Experimental measurements of state-selective cross sections were carried out by Hoekstra et al. [78]. Total charge exchange cross sections were calculated by Errea et al. [75], Gargaud et al. [76], and Tseng et al. [77]. Experimental measurements of total charge exchange cross sections were performed by Hoesktra et al. [78], Phaneuf et al. [74,79], Crandall et al. [80], Goffe et al. [73], Dijkkamp et al. [81], and Bliek et al. [82]. Since the structures of the state-selective cross sections are too complicated to fit in a formula, we only show their data in graphs.

For $C^{3+} + H$ collisions, state-selective charge exchange cross sections were calculated by Opradolce et al. (using the molecular orbital method) [83] and Bienstock et al. (molecular orbital close-coupling method) [84]. Experimental measurements of state-selective cross sections were carried out by Ciric et al. [85] and McCullough et al. [86]. Total charge exchange cross sections were calculated by Errea et al. (using the molecular orbital close-coupling method) [87], Tseng and Lin (atomic orbital close-coupling method) [88], Heil et al. (molecular orbital close-coupling method) [89], and Bienstock et al. (molecular orbital close-coupling method) [84]. Experimental measurements of total charge exchange cross sections were carried out by Phaneuf et al. [74,79], Goffe et al. [73], Sant'Anna et al. [90], McCullough et al. [86], and Ciric et al. [85].

For $C^{2+} + H$ collisions, total charge exchange cross sections were calculated by Gu et al. (using the classical trajectory Monte Carlo method) [91] and Errea et al. (molecular orbital close-coupling method) [92]. Experimental measurements of total charge exchange cross sections were carried out by Goffe et al. [73], Nutt et al. [93], Phaneuf et al. [79], and Gardner et al. [94]. We have selected the data by Goffe et al. [73] and Nutt et al. [93] as the recommended data.

For $C^{+} + H$ collisions, total charge exchange cross sections were calculated using the classical trajectory Monte Carlo method by Stancil et al. [95]. Experimental measurements of total charge exchange cross sections were carried out by Phaneuf et al. [79], Nutt et al. [93], Goffe et al. [73], and Stancil et al. [95]. Stancil et al. [95] also gave the recommended values of total charge exchange cross sections.

Here, we also consider charge exchange cross sections in $C^{+} + C$ collisions. Cross sections were measured experimentally by Belyaev et al. [96], and calculated theoretically by Duman et al. [97]. Since their energy region is too limited to fit the cross sections, only their data are shown in graphs.

The recommended (total and state selective) cross sections are fitted to the following analytic functions:

$$\sigma[\mathrm{cm}^2] = 10^{-16} \times \begin{cases} \dfrac{a_1 \exp[-(a_2/E)^{a_3}]}{1+(E/a_4)^{a_5}+(E/a_6)^{a_7}+(E/a_8)^{a_9}} \\ \dfrac{a_1 \exp[-(a_2/E)^{a_3}]}{1+(E/a_4)^{a_5}+(E/a_6)^{a_7}+(E/a_8)^{a_9}} \\ \quad + \dfrac{a_{10} \exp[-(a_{11}/E)^{a_{12}}]}{1+(E/a_{13})^{a_{14}}} \\ \dfrac{a_1 \exp[-(a_2/E)^{a_3}]}{1+(E/a_4)^{a_5}+(E/a_6)^{a_7}+(E/a_8)^{a_9}} \\ \quad + \dfrac{a_{10} \exp[-(a_{11}/E)^{a_{12}}]}{1+(E/a_{13})^{a_{14}}+(E/a_{15})^{a_{16}}} \end{cases}, \tag{19}$$

where the collision energy E is expressed in eV/amu and a_i, $i = 1$–14 are fitting parameters. The values of a_i in Eq. (19) are given in Tables 8 and 9, together with the references of the adopted data and the rms percent error. The recommended cross sections are shown graphically in Graphs 139–175. We did not find enough data for fitting certain state-selective charge exchange processes. In such cases, we show only the original data in graphs. This is the case for Graphs 159, 161–167, 169–171, and 175. The rms percent errors are at most 1.33 in our fitting.

2. Summary

We have compiled and critically assessed cross sections for electron-impact excitation and ionization of carbon ions, as well as charge exchange in collisions between carbon ions and hydrogen atoms. The recommended cross sections are expressed in terms of simple analytic functions. These can immediately lead to applications in fusion science.

Acknowledgments

We thank Prof. Hiroshi Sato for providing us the code for fitting the cross sections to analytic functions. Useful discussions with Profs. Mineo Kimura, Akinori Igarashi, and Prof. Ratko Janev are also appreciated.

Appendix A. Supplementary data

Supplementary data associated with this article can be found, in the online version, at doi:10.1016/j.adt.2006.01.001.

References

[1] Y. Itikawa, S. Hara, T. Kato, S. Nakazaki, M.S. Pindzola, D.H. Crandall, At. Data Nucl. Data Tables 33 (1985) 149.
[2] J.M. Peak, quoted in Los Alamos Scientific Laboratory Report LA-6691-MS, edited by N.H. Magee, J.B. Mann, A.L. Merts, W.D. Robb (1977DW).
[3] J.B. Mann, quoted in Los Alamos Scientific Laboratory Report LA-6691-MS, edited by N.H. Magee, J.B. Mann, A.L. Merts, W.D. Robb (1977CB).
[4] J.B. Mann, quoted in Los Alamos Scientific Laboratory Report LA-6691-MS, edited by N.H. Magee, J.B. Mann, A.L. Merts, W.D. Robb (1977CBO).
[5] W.D. Robb, quoted in Los Alamos Scientific Laboratory Report LA-6691-MS, edited by N.H. Magee, J.B. Mann, A.L. Merts, W.D. Robb (1977CC).

[6] M.R.C. McDowell, L.A. Morgan, V.P. Myerscough, T. Scott, J. Phys. B 10 (1977) 2727.
[7] G. Foster, D.G. Hummer, D.W. Norcross, Information Quarterly No. 6 (1977).
[8] K.A. Berrington, P.G. Burke, P.L. Dufton, A.E. Kingston, J. Phys. B 10 (1977) 1465.
[9] K.A. Berrington, P.G. Burke, P.L. Dufton, A.E. Kingston, At. Data Nucl. Data Tables 26 (1981) 1.
[10] K.M. Aggarwal, A.E. Kingston, J. Phys. B 24 (1991) 4583.
[11] Y. Zou, T. Shirai, Phys. Rev. A 45 (1992) 6902.
[12] V.I. Fisher, Y.V. Ralchenko, V.A. Bernshtam, A. Goldgirsh, Y. Maron, L.A. Vainshtein, I. Bray, H. Golten, Phys. Rev. A 55 (1997) 329.
[13] J. Callaway, At. Data Nucl. Data Tables 57 (1994) 9.
[14] N.R. Badnell, J. Phys. B 18 (1985) 955.
[15] R. Srivastava, A.K. Katiyar, Phys. Rev. A 35 (1987) 1080.
[16] T. Kato, S. Nakazaki, At. Data Nucl. Data Tables 42 (1989) 313.
[17] P.O. Taylor, D. Gregory, G.H. Dunn, R.A. Phaneuf, D.H. Crandall, Phys. Rev. Lett. 39 (1977) 1256.
[18] M.E. Bannister, Y.-S. Chung, N. Djuric, B. Wallbank, O. Woitke, S. Zhou, G.H. Dunn, A.C.H. Smith, Phys. Rev. A 57 (1998) 278.
[19] J.B. Greenwood, S.J. Smith, A. Chutjian, Phys. Rev. A 59 (1999) 1348.
[20] P.H. Janzen, L.D. Gardner, D.B. Reisenfeld, D.W. Savin, J.L. Kohl, K. Bartschat, Phys. Rev. A 59 (1999) 4821.
[21] V.M. Burke, J. Phys. B 25 (1992) 4917.
[22] D.C. Griffin, N.R. Badnell, M.S. Pindzola, J. Phys. B 33 (2000) 1013.
[23] K.A. Berrington, P.G. Burke, P.L. Dufton, A.E. Kingston, At. Data Nucl. Data Tables 33 (1985) 195.
[24] Y. Itikawa, K. Sakimoto, Phys. Rev. A 31 (1985) 1319.
[25] K.A. Berrington, V.M. Burke, P.G. Burke, S. Scialla, J. Phys. B 22 (1989) 665.
[26] R.D. Blum, A. Pradhan, Astrophys. J. Suppl. 80 (1992) 425.
[27] I.D. Williams, J.B. Greenwood, P. McGuiness, J. Phys. B 28 (1995) L555.
[28] K.M. Dunseath, V.M. Burke, P.G. Burke, A.E. Kingston, R.H.G. Reid, J.H. Tait, JET Order No. JP2/11566 (1993).
[29] R.J.W. Henry, P.G. Burke, A.-L. Sinfailam, Phys. Rev. 178 (1969) 218.
[30] M.S. Pindzola, A.K. Bhatia, A. Temkin, Phys. Rev. A 15 (1977) 35.
[31] L.D. Thomas, R.K. Nesbet, Phys. Rev. A 12 (1975) 2378.
[32] J.B. Mann, private communication (1981).
[33] D.R. Flower, J.M. Launay, Astron. Astrophys. 29 (1973) 321.
[34] E.D. Donets, V.P. Ovsyannikov, Sov. Phys.-JETP 53 (1981) 466.
[35] K. Aichele, U. Hartenfeller, D. Hathiramani, G. Hofmann, V. Schafer, M. Steidl, M. Stenke, E. Salzborn, T. Pattard, J.M. Rost, J. Phys. B 31 (1998) 2369.
[36] T. Pattard, J.M. Rost, Phys. Scr. T80 (1999) 295.
[37] S.M. Younger, Phys. Rev. A 22 (1980) 111.
[38] H.C. Kao, T.Y. Kuo, H.P. Yen, C.M. Wei, K.N. Huang, Phys. Rev. A 45 (1992) 4646.
[39] D. Fang, W. Hu, C. Chen, Y. Wang, F. Lu, J. Tang, F. Yang, At. Data Nucl. Data Tables 61 (1995) 91.
[40] D.H. Crandall, R.A. Phaneuf, D.C. Gregory, ORNL/TM-7029 (1979).
[41] A. Salop, Phys. Rev. A 14 (1976) 2095.
[42] H. Knopp, H. Teng, S. Ricz, S. Schippers, A. Müller, Phys. Scr. T92 (2001) 379.
[43] D.H. Crandall, R.A. Phaneuf, D.C. Gregory, ORNL/TM-9501 (1985).
[44] H. Jakubowicz, D.H. Moores, J. Phys. B 14 (1981) 3733.
[45] D.H. Sampson, L.B. Golden, J. Phys. B 12 (1979) L785.
[46] M.P. Scott, H. Teng, P.G. Burke, J. Phys. B 33 (2000) L63.
[47] N.R. Badnell, D.C. Griffin, J. Phys. B 33 (2000) 2955.
[48] P.R. Woodruff, M.-C. Hublet, M.F.A. Harrison, E. Brook, J. Phys. B 11 (1978) L679.
[49] R.A. Falk, G. Stefani, R. Camilloni, G.H. Dunn, R.A. Phaneuf, D.C. Gregory, D.H. Crandall, Phys. Rev. A 28 (1983) 91.
[50] D.L. Moores, J. Phys. B 11 (1978) L403.
[51] I. Yamada, A. Danjo, T. Hirayama, A. Matsumoto, S. Ohtani, H. Suzuki, T. Takayanagi, H. Tawara, K. Wakita, M. Yoshino, J. Phys. Soc. Jpn. 58 (1989) 1585.
[52] X.Z. Qian, S.F. Pan, Phys. Lett. A 239 (1988) 363.
[53] M. Westermann, F. Scheuermann, K. Aichele, U. Hartenfeller, D. Hathiramani, M. Steidl, E. Salzborn, Phys. Scr. T80 (1999) 285.
[54] E. Brook, M.F.A. Harrison, A.C.H. Smith, J. Phys. B 11 (1978) 3115.
[55] K. Omidvar, H.L. Kyle, E.C. Sullivan, Phys. Rev. A 5 (1972) 1174.
[56] N. Toshima, H. Tawara, NIFS-DATA 26 (1995).
[57] D. Belkic, R. Gayet, A. Salin, At. Data Nucl. Data Tables 51 (1992) 59.
[58] D. Belkic, private communication.
[59] H. Ryufuku, JAERI-M 82-031 42 (1982).
[60] R.E. Olson, D.R. Schultz, Phys. Scr. T28 (1989) 71.
[61] T. Green, E.J. Shipsey, J.C. Browne, Phys. Rev. A 25 (1982) 1364.
[62] C. Harel, H. Jouin, B. Pons, At. Data Nucl. Data Tables 68 (279) (1998).
[63] A.K. Kazanskii, I.V. Komarov, Sov. Phys. Tech. Phys. 27 (1982) 1064.
[64] W. Fritsch, C.D. Lin, J. Phys. B 17 (1984) 3271.
[65] W. Fritsch, J. Phys. C1 (1989) 87.
[66] M. Kimura, C.D. Lin, Phys. Rev. A 32 (1985) 1357.
[67] M. Das, N.C. Deb, S.C. Mukherjee, Phys. Scr. 54 (1996) 44.
[68] M.N. Panov, A.A. Baselaev, K.O. Lozhkin, Phys. Scr. T3 (1983) 124.
[69] F.W. Meyer, A.M. Howald, C.C. Havener, R.A. Phaneuf, Phys. Rev. A 32 (1985) 3310.
[70] R.K. Janev, R.A. Phaneuf, H. Tawara, At. Data Nucl. Data Tables 55 (1993) 201.
[71] N. Shimakura, S. Koizumi, S. Suzuki, M. Kimura, Phys. Rev. A 45 (1992) 7876.
[72] E.J. Shipsey, J.C. Browne, R.E. Olson, J. Phys. B 14 (1981) 869.
[73] T.V. Goffe, M.B. Shah, H.B. Gilbody, J. Phys. B 12 (1979) 3763.
[74] R.A. Phaneuf, Phys. Rev. A 24 (1981) 1138;
R.A. Phaneuf, I. Alvarez, F.W. Meyer, D.H. Crandall, Phys. Rev. A 26 (1982) 1892.
[75] L.F. Errea, J.D. Gorfinkiel, C. Harel, H. Jouin, A. Macias, L. Mendez, B. Pons, A. Riera, J. Phys. B 32 (1999) L673.
[76] M. Gargaud, R. McCarroll, P. Valion, J. Phys. B 20 (1987) 1555.
[77] H.C. Tseng, C.D. Lin, Phys. Rev. A 58 (1998) 1966.
[78] R. Hoekstra, J.P.M. Beijers, A.R. Schlatmann, R. Morgenstern, Phys. Rev. A 41 (1990) 4800.
[79] R.A. Phaneuf, F.W. Meyer, R.H. McKnight, Phys. Rev. A 17 (1978) 534.
[80] D.H. Crandall, R.A. Phaneuf, F.W. Meyer, Phys. Rev. A 19 (1979) 504.
[81] D. Dijkkamp, D. Ciric, E. Flieg, A. de Boer, F.J. de Heer, J. Phys. B 18 (1985) 4763.
[82] F.W. Bliek, R. Hoekstra, M.E. Bannister, C.C. Havener, Phys. Rev. A 56 (1997) 426.
[83] L. Opradolce, L. Benmeuraiem, R. McCarroll, R.D. Piacentini, J. Phys. B 21 (1988) 503.
[84] S. Bienstock, T.G. Heil, C. Bottcher, A. Dalgarno, Phys. Rev. A 25 (1982) 2850.
[85] D. Ciric, A. Brazuk, D. Dijkkamp, F.J. de Heer, H. Winter, J. Phys. B 18 (1985) 3629.
[86] R.W. McCullough, F.G. Wilkie, H.B. Gilbody, J. Phys. B 17 (1984) 1373.
[87] L.F. Errea, B. Herrero, L. Mendez, A. Riera, J. Phys. B 24 (1991) 4061.
[88] H.C. Tseng, C.D. Lin, J. Phys. B 32 (1999) 5271.
[89] T.G. Heil, S.E. Butler, A. Dalgarno, Phys. Rev. A 23 (1981) 1100.
[90] M.M. Sant'Anna, W.S. Melo, A.C.F. Santos, M.B. Shah, E.C. Montenegro, J. Phys. B 33 (2000) 353.

[91] J.P. Gu, G. Hirsch, R.J. Buenker, M. Kimura, C.M. Dutta, P. Nordlander, Phys. Rev. A 57 (1998) 4483.
[92] L.F. Errea, A. Macias, L. Mendez, A. Riera, J. Phys. B 33 (2000) 1369.
[93] W.L. Nutt, R.W. McCullough, H.B. Gilbody, J. Phys. B 12 (1979) L157.
[94] L.D. Gardner, J.E. Bayfield, P.M. Koch, I.A. Sellin, D.J. Pegg, R.S. Peterson, D.H. Crandall, Phys. Rev. A 21 (1980) 1397.
[95] P.C. Stancil, J.-P. Gu, C.C. Havener, P.S. Krstić, D.R. Schultz, M. Kimura, B. Zygelman, G. Hirsch, R.J. Buenker, M.E. Bannister, J. Phys. B 31 (1998) 3647.
[96] V.A. Belyaev, B.G. Brezhnev, E.M. Erastov, Sov. Phys. JETP 27 (1968) 924.
[97] E.L. Duman, B.M. Smirnov, Sov. Phys. Tech. Phys. 15 (1970) 61.

Explanation of Tables

Table 1. Values of the fit parameters for electron-impact excitation of the C^{5+} ion (H like)

V_{if}	Excitation energy in eV
A, B, C, D, E, F	Fit parameters in Eqs. (6), (7), (10), and (11)
P, Q, X_1	Additional fit parameters, when resonance effects are included by means of Eq. (14)
rms	rms percent error defined by Eq. (16)
Ref.	The reference number(s) indicate the original data from the literature

Fit parameters are tabulated for each excitation process and each ion species. The notation $1s^2\ ^1S$–$1s2s\ ^3S$, for example, means the excitation from the lower state $1s^2\ ^1S$ to the upper state $1s2s\ ^3S$.

Table 2. Values of the fit parameters for electron-impact excitation of the C^{4+} ion (He like). Same as Table 1

Table 3. Values of the fit parameters for electron-impact excitation of the C^{3+} ion (Li like). Same as Table 1

Table 4. Values of the fit parameters for electron-impact excitation of the C^{2+} ion (Be like). Same as Table 1

Table 5. Values of the fit parameters for electron-impact excitation of the C^{+} ion (B like). Same as Table 1

Table 6. Values of the fit parameters for electron-impact excitation of the C atom. Same as Table 1

Table 7. Values of the fitting parameters for electron-impact ionization in Eq. (17)

I	Ionization energy in eV
$A_i\ (i = 1, \ldots, 5)$	Fit parameters in Eq. (17)
rms	rms percent error defined by Eq. (16)
Ref.	The reference number(s) indicate the original data from the literature

Fit parameters are tabulated for each ion species. The notation $C^{5+} \rightarrow C^{6+}$, for example, means the ionization of the C^{5+} ion into the C^{6+} ion.

Table 8. Values of the fitting parameters in Eq. (19) for charge exchange in C^{6+} + H collisions

$a_i\ (i = 1, \ldots, 16)$

rms

Ref.

Fit parameters are tabulated for each charge exchange process and each ion species in Tables 8 and 9. The notation $C^{6+} + H \rightarrow C^{5+}(4s) + H^{+}$, for example, means the charge exchange between the C^{6+} ion and the H atom into the proton and the C^{5+} in the 4s state.

Table 9. Values of the fitting parameters in Eq. (19) for charge exchange in C^{q+} + H collisions. Same as for Table 8

Fit parameters are tabulated for each charge exchange process and each ion species in Tables 8,9. The notation $C^{6+} + H \rightarrow C^{5+}(4s) + H^{+}$, for example, means the charge exchange between the C^{6+} ion and the H atom into the proton and the C^{5+} in the 4s state.

Explanation of Graphs

Graphs 1–124. Recommended collision strengths and rate coefficients for electron-impact excitation
Excitation collision strengths Ω (dimensionless) are plotted against reduced electron energy $X = E_e/V_{if}$ (dimensionless), where E_e is the electron energy and V_{if} the excitation energy for each transition. Excitation rate coefficients [$cm^3\ s^{-1}$] are plotted against electron temperature [eV]. The initial and final states are given at the top of each graph using the same notation as that in Tables 1–6 together with the ion species. Recommended collision strengths and rate coefficients are given as solid curves. Original data from recent references (after 1985) are shown as empty circles, empty squares, etc., as indicated in the graphs. At the end of each reference, theoretical data are labeled as "T" and experimental data as "E." When resonance effects are included by means of Eq. (14), the position of X_1 is also indicated as a dashed line.

Graphs 125–138. Recommended electron-impact ionization cross sections
Ionization cross sections [cm^2] are plotted against electron energy [eV]. At the top of each graph the notation $C^{5+} \rightarrow C^{6+}$, for example, means the ionization of the C^{5+} ion into the C^{6+} ion as in Table 7. Recommended cross sections are given as solid curves. Original data from references are shown as empty circles, empty squares, etc., as indicated in the graph. At the end of each reference, theoretical data are labeled as "T" and experimental data as "E." Recommended cross sections and original data are plotted in logarithmic vertical scale as well as in linear vertical scale.

Graphs 139–175. Recommended charge exchange cross sections
Charge exchange cross sections are plotted against electron energy [eV/amu]. The initial and final states are given at the top of each graph using the same notation as that in Tables 8 and 9. Recommended cross sections are given as solid curves. Original data from references are shown as empty circles, empty squares, etc., as indicated in the graphs. At the end of each reference, theoretical data are labeled as "T" and experimental data as "E."

Table 1
Values of the fit parameters for electron-impact excitation of the C^{5+} ion (H like). See page 415 for Explanation of Tables

Transition	$V_{\rm if}$ [eV]	Fit Eq.	Fit parameters	rms	Ref.
1s–2s	367	(6)	$A = 2.446(-2)$[a], $B = -1.567(-2)$, $C = 1.010(-2)$, $D = 0.0$, $E = 0.0$	0.004	[6,11]
1s–2p	367	(6)	$A = 1.040(-2)$, $B = 1.720(-2)$, $C = 4.370(-2)$, $D = 0.0$, $E = 1.259(-1)$	—[b]	[1]
1s–3s	435	(6)	$A = 4.866(-3)$, $B = -2.522(-3)$, $C = 3.158(-3)$, $D = -1.765(-3)$, $E = 0.0$	—	[1]
1s–3p	435	(6)	$A = 4.248(-3)$, $B = 8.978(-3)$, $C = 4.082(-3)$, $D = 0.0$, $E = 2.130(-2)$	0.01	[2,10]
1s–3d	435	(6)	$A = 3.874(-3)$, $B = -6.100(-3)$, $C = 3.909(-3)$, $D = 2.143(-3)$, $E = 0.0$	0.01	[3,10]
1s–4s	459	(6)	$A = 1.814(-3)$, $B = -1.035(-3)$, $C = 1.515(-3)$, $D = -9.157(-4)$, $E = 0.0$	0.001	[4]
1s–4p	459	(6)	$A = 1.106(-3)$, $B = 2.965(-3)$, $C = 3.247(-3)$, $D = 0.0$, $E = 7.915(-3)$	0.02	[4,10]
1s–5p	470	(6)	$A = 6.869(-4)$, $B = 1.166(-3)$, $C = 2.120(-3)$, $D = 0.0$, $E = 3.711(-3)$	0.02	[4,10]

[a] $x(\pm y) = x \times 10^{\pm y}$.
[b] rms is not available for the coefficients taken from [1].

Table 2
Values of the fit parameters for electron-impact excitation of the C^{4+} ion (He like). See page 415 for Explanation of Tables

Transition	V_{if} [eV]	Fit Eq.	Fit parameters	rms	Ref.
$1s^2\ ^1S$–$1s2s\ ^3S$	299	(6)	$A = -1.820(-5)$[a], $B = 1.093(-3)$, $C = 1.675(-2)$, $D = -8.788(-3)$, $E = 0.0$, $P = -1.777$, $Q = 1.826$, $X_1 = 1.02$	—[b]	[1]
$1s^2\ ^1S$–$1s2s\ ^1S$	304	(6)	$A = 2.830(-2)$, $B = -3.159(-2)$, $C = 2.694(-2)$, $D = -1.063(-2)$, $E = 0.0$	—	[1]
$1s^2\ ^1S$–$1s2p\ ^3P$	304	(6)	$A = 8.926(-5)$, $B = -2.824(-3)$, $C = 7.379(-2)$, $D = -2.670(-2)$, $E = 0.0$	0.70	[2,7,14]
$1s^2\ ^1S$–$1s2p\ ^1P$	308	(6)	$A = 1.642(-2)$, $B = -7.345(-2)$, $C = 9.320(-2)$, $D = 0.0$, $E = 1.247(-1)$	0.06	[2,5]
$1s^2\ ^1S$–$1s3d\ ^3D$	354	(6)	$A = 5.061(-5)$, $B = -5.619(-4)$, $C = 2.116(-3)$, $D = 7.710(-4)$, $E = 0.0$	—	[1]
$1s^2\ ^1S$–$1s3p\ ^1P$	355	(6)	$A = 1.286(-2)$, $B = -2.133(-2)$, $C = 1.656(-2)$, $D = 0.0$, $E = 2.107(-2)$	—	[1]
$1s2s\ ^3S$–$1s2s\ ^1S$	5.4	(6)	$A = -3.821(-3)$, $B = 7.199(-1)$, $C = -1.671$, $D = 1.393$, $E = 0.0$	1.46	[14]
$1s2s\ ^3S$–$1s2p\ ^3P$	5.4	(6)	$A = 9.507$, $B = 1.195(1)$, $C = -7.559$, $D = 0.0$, $E = 4.417$	0.008	[5,14]
$1s2s\ ^3S$–$1s2p\ ^1P$	8.94	(6)	$A = -5.935(-3)$, $B = 6.629(-1)$, $C = -7.935(-1)$, $D = 2.695(-1)$, $E = 0.0$	—	[1]
$1s2s\ ^3S$–$1s3p\ ^3P$	54.5	(6)	$A = -7.449(-1)$, $B = 1.335$, $C = -3.423(-1)$, $D = 0.0$, $E = 1.011$	—	[1]
$1s2s\ ^1S$–$1s2p\ ^3P$	0.022	(7)	$A = 1.187(-2)$, $B = 4.767(-2)$, $C = -3.971(-2)$, $D = 3.753(-2)$, $E = 1.534(-1)$, $F = 6(-4)$	—	[1]
$1s2s\ ^1S$–$1s2p\ ^1P$	3.5	(6)	$A = 1.508$, $B = 3.987$, $C = -1.245$, $D = 0.0$, $E = 1.652$	0.004	[14]
$1s2p\ ^3P$–$1s2p\ ^1P$	3.2	(7)	$A = 2.487(-2)$, $B = 1.042$, $C = -3.304$, $D = 6.244$, $E = -3.249$, $F = 2(-2)$	—	[1]
$1s2p\ ^3P$–$1s3s\ ^3S$	47.7	(6)	$A = -1.091(-1)$, $B = 2.359(-1)$, $C = -5.644(-2)$, $D = 0.0$, $E = 1.758(-1)$	—	[1]

[a] $x(\pm y) = x \times 10^{\pm y}$.
[b] rms is not available for the coefficients taken from [1].

Table 3
Values of the fit parameters for electron-impact excitation of the C^{3+} ion (Li like). See page 415 for Explanation of Tables

Transition	V_{if} [eV]	Fit Eq.	Fit parameters	rms	Ref.
2s ^{2}S–2p ^{2}P	8.0	(6)	$A = 4.744$[a], $B = 4.440$, $C = 5.971(-1)$, $D = 0.0$, $E = 4.519$	0.01	[4]
2s ^{2}S–3s ^{2}S	37.6	(6)	$A = 4.846(-1)$, $B = -2.743(-1)$, $C = 4.768(-1)$, $D = -3.971(-1)$, $E = 0.0$, X_1=1.072, $P = 7.390(-1)$, $Q = 2.460(-1)$	—[b]	[1]
2s ^{2}S–3p ^{2}P	40.0	(6)	$A = -5.731(-1)$, $B = 9.548(-1)$, $C = -8.931(-2)$, $D = 0.0$, $E = 5.638(-1)$, X_1=1.019, $P = -3.412$, $Q = 9.141$	—	[1]
2s ^{2}S–3d ^{2}D	40.0	(6)	$A = 1.252$, $B = -1.243$, $C = 4.93(-1)$, $D = 1.326(-1)$, $E = 0.0$	—	[1]
2s ^{2}S–4p ^{2}P	50.6	(10)	$A = 2.775(-1)$, $B = -6.663(-1)$, $C = 4.959(-1)$, $D = 0$, $E = 3.530(-6)$	0.02	[22]
2p ^{2}P–3s ^{2}S	29.4	(10)	$A = 1.273$, $B = -5.038$, $C = 5.374$, $D = 0$, $E = 2.270(-3)$	0.05	[22]
2p ^{2}P–3d ^{2}D	32.1	(10)	$A = 1.899(+1)$, $B = -4.193(+1)$, $C = 2.857(+1)$, $D = 0$, $E = 4.027(-3)$	0.04	[22]
2p ^{2}P–4s ^{2}S	41.8	(10)	$A = 1.964(-1)$, $B = -6.743(-1)$, $C = 7.166(-1)$, $D = 0$, $E = 2.411(-4)$	0.04	[22]

[a] $x(\pm y) = x \times 10^{\pm y}$.
[b] rms is not available for the coefficients taken from [1].

Table 4
Values of the fit parameters for electron-impact excitation of the C^{2+} ion (Be like). See page 415 for Explanation of Tables

Transition	V_{if} [eV]	Fit Eq.	Fit parameters	rms	Ref.
$2s^2\ ^1S$–$2s2p\ ^3P$	6.5	(6)	$A = -4.024(-2)$[a], $B = 2.914$, $C = -4.344$, $D = 2.121$, $E = 0.0$, X_1=2.0, $P = 5.434(-1)$, $Q = 3.453(-1)$	—[b]	[1]
$2s^2\ ^1S$–$2s2p\ ^1P$	12.7	(6)	$A = 6.261(-1)$, $B = 3.044$, $C = 5.384(-1)$, $D = 0.0$, $E = 4.364$	0.04	[8,23,32]
$2s^2\ ^1S$–$2p^2\ ^3P$	17.2	(6)	$A = -5.732(-3)$, $B = 8.467(-2)$, $C = -1.676(-1)$, $D = 1.307(-1)$, $E = 0.0$, X_1=2.0, $P = 5.389(-3)$, $Q = 7.167(-3)$	0.01	[23]
$2s^2\ ^1S$–$2p^2\ ^1D$	18.2	(6)	$A = 2.915(-1)$, $B = 1.655(-1)$, $C = -3.445(-1)$, $D = 3.720(-1)$, $E = 0.0$	0.03	[23,33]
$2s^2\ ^1S$–$2p^2\ ^1S$	22.9	(6)	$A = 2.092(-2)$, $B = 2.289(-1)$, $C = -4.268(-1)$, $D = 2.137(-1)$, $E = 0.0$	0.01	[9,23]
$2s^2\ ^1S$–$2s3s\ ^3S$	29.5	(6)	$A = 3.910(-3)$, $B = 2.740(-1)$, $C = 1.120$, $D = 1.110$, $E = 0$	0.36	[25]
$2s^2\ ^1S$–$2s3s\ ^1S$	30.6	(6)	$A = 4.260(-1)$, $B = 4.350(-1)$, $C = -2.280$, $D = 1.760$, $E = 0$	0.0004	[25]
$2s^2\ ^1S$–$2s3p\ ^1P$	32.1	(6)	$A = -1.140(-1)$, $B = -5.230(-1)$, $C = 8.110(-1)$, $D = 0$, $E = 3.730(-1)$	0.0005	[25]
$2s^2\ ^1S$–$2s3p\ ^3P$	32.2	(6)	$A = -2.190(-2)$, $B = 3.660(-1)$, $C = -1.030$, $D = 8.240(-1)$, $E = 0$	0.20	[25]
$2s^2\ ^1S$–$2s3d\ ^3D$	33.5	(6)	$A = 4.190(-2)$, $B = 6.490(-2)$, $C = 1.100(-2)$, $D = 1.050(-1)$, $E = 0$	0.0005	[25]
$2s^2\ ^1S$–$2s3d\ ^1D$	34.3	(6)	$A = 7.330(-1)$, $B = 5.400(-2)$, $C = -2.110$, $D = 1.490$, $E = 0$	0.0005	[25]
$2s2p\ ^3P$–$2p^2\ ^3P$	10.6	(6)	$A = 9.842$, $B = -8.660$, $C = 2.184(+1)$, $D = 0.0$, $E = 1.631$	—	[1]
$2s2p\ ^3P$–$2p^2\ ^1D$	11.7	(6)	$A = -1.822(-1)$, $B = 4.490$, $C = -4.889$, $D = 2.056$, $E = 0.0$	0.06	[5,9]
$2s2p\ ^3P$–$2p^2\ ^1S$	16.5	(6)	$A = 3.280(-4)$, $B = 1.676(-1)$, $C = 2.778(-1)$, $D = -4.524(-1)$, $E = 0.0$	0.02	[9]
$2s2p\ ^3P$–$2s3s\ ^1S$	24.1	(6)	$A = -1.200(-2)$, $B = 1.310$, $C = -4.030$, $D = 3.590$, $E = 0$	0.88	[25]
$2s2p\ ^3P$–$2s3p\ ^1P$	25.6	(6)	$A = -1.310(-2)$, $B = 1.580$, $C = -4.800$, $D = 4.270$, $E = 0$	0.0004	[25]
$2s2p\ ^3P$–$2s3p\ ^3P$	25.7	(6)	$A = 1.980$, $B = 1.490(+1)$, $C = -4.330(+1)$, $D = 3.170(+1)$, $E = 0$	0.0004	[25]
$2s2p\ ^3P$–$2s3d\ ^3D$	27.0	(6)	$A = -2.900(-1)$, $B = 2.090$, $C = 7.110$, $D = 0$, $E = 1.010(+1)$	0.80	[25]
$2s2p\ ^3P$–$2s3s\ ^1D$	27.8	(6)	$A = 9.840(-3)$, $B = 5.080(-1)$, $C = -7.040(-1)$, $D = 9.550(-1)$, $E = 0$	0.0004	[25]
$2s2p\ ^1P$–$2p^2\ ^3P$	4.3	(6)	$A = -8.624(-3)$, $B = 4.141$, $C = -7.089$, $D = 3.824$, $E = 0.0$, X_1=1.85, $P = 7.072(-1)$, $Q = 2.899(-1)$	—	[1]
$2s2p\ ^1P$–$2p^2\ ^1D$	4.3	(6)	$A = 3.762$, $B = 9.351$, $C = -3.004$, $D = 0.0$, $E = 7.320$	—	[1]
$2s2p\ ^1P$–$2p^2\ ^1S$	10.1	(6)	$A = 3.032$, $B = -2.375$, $C = 2.675$, $D = 0.0$, $E = 2.991$	—	[1]
$2p^2\ ^3P$–$2p^2\ ^1D$	1.01	(6)	$A = 1.925$, $B = 1.440(+1)$, $C = -3.560(+1)$, $D = 2.727(+1)$, $E = 0.0$	—	[1]
$2p^2\ ^3P$–$2p^2\ ^1S$	5.8	(6)	$A = 4.319(-2)$, $B = 1.004$, $C = -1.037$, $D = 3.630(-1)$, $E = 0.0$	—	[1]
$2p^2\ ^1D$–$2p^2\ ^1S$	4.79	(6)	$A = 8.948(-1)$, $B = -8.607(-1)$, $C = 1.007$, $D = -4.136(-1)$, $E = 0.0$	—	[1]

[a] $x(\pm y) = x \times 10^{\pm y}$.
[b] rms is not available for the coefficients taken from [1].

Table 5
Values of the fit parameters for electron-impact excitation of the C^+ ion (B like). See page 415 for Explanation of Tables

Transition	V_{if} [eV]	Fit Eq.	Fit parameters	rms	Ref.
$2s^22p\ ^2P$–$2s2p^2\ ^4P$	4.74	(7)	$A = 4.360(-1)$[a], $B = 1.627$, $C = -2.923$, $D = 1.094(+1)$, $E = -6.580$, $F = 5.769(-2)$	—[b]	[1]
$2s^22p\ ^2P$–$2s2p^2\ ^2D$	9.27	(6)	$A = -2.155$, $B = 1.374(+1)$, $C = -6.562$, $D = 0.0$, $E = 1.018$	—	[1]
$2s^22p\ ^2P$–$2s2p^2\ ^2S$	12.0	(6)	$A = 8.572(-1)$, $B = 2.079(-1)$, $C = 7.058(-1)$, $D = 0.0$, $E = 4.136$	—	[1]
$2s^22p\ ^2P$–$2s2p^2\ ^2P$	13.7	(6)	$A = -6.883(-1)$, $B = 4.106$, $C = 3.435(-1)$, $D = 0.0$, $E = 1.631(+1)$	—	[1]
$2s^22p\ ^2P$–$2s^23s\ ^2S$	14.4	(6)	$A = -9.843(-1)$, $B = 2.983$, $C = -9.975(-1)$, $D = 0.0$, $E = 8.910(-1)$	—	[1]
$2s^22p\ ^2P$–$2s^23p\ ^2P$	16.3	(6)	$A = 1.678$, $B = -2.238$, $C = 4.829$, $D = 0.0$, $E = 0.0$	—	[1]
$2s^22p\ ^2P$–$2s^23d\ ^2D$	18.0	(6)	$A = -1.703$, $B = 2.675$, $C = 1.165$, $D = 0.0$, $E = 5.791$	—	[1]

[a] $x(\pm y) = x \times 10^{\pm y}$.
[b] rms is not available for the coefficients taken from [1].

Table 6
Values of the fit parameters for electron-impact excitation of the C atom. See page 415 for Explanation of Tables

Transition	V_{if} [eV]	Fit Eq.	Fit parameters	rms	Ref.
$2s^22p^2\ ^3P–2s^22p^2\ ^1D$	1.26	(11)	$A = 1.277$[a], $B = 1.304(+1)$, $C = -3.314(+1)$, $D = 6.357(+1)$, $E = -4.621(+1)$, $F = 4(-2)$	0.01	[28]
$2s^22p^2\ ^3P–2s^22p^2\ ^1S$	2.68	(10)	$A = 1.598(-1)$, $B = 2.836$, $C = -9.813$, $D = -1.012(+1)$, $E = 1.233(-1)$	0.01	[28]
$2s^22p^2\ ^3P–2s2p^3\ ^5S$	4.18	(11)	$A = -2.302$, $B = 8.923$, $C = -2.873(+1)$, $D = 4.555(+1)$, $E = -2.431(+1)$, $F = 1.323(-1)$	0.003	[28]
$2s^22p^2\ ^3P–2s^22p3s\ ^3P$	7.48	(6)	$A = -6.117$, $B = 2.989$, $C = 4.148$, $D = 0$, $E = 1.222(+1)$	0.07	[28]
$2s^22p^2\ ^3P–2s^22p3s\ ^1P$	7.68	(11)	$A = 2.423$, $B = 7.590(-1)$, $C = -6.486$, $D = 3.143$, $E = -2.074(+1)$, $F=6.744(-1)$	0.01	[28]
$2s^22p^2\ ^3P–2s2p^3\ ^3D$	7.94	(6)	$A = 1.307(+1)$, $B = -3.052(+1)$, $C = 1.835(+1)$, $D = 0$, $E = 1.001(+1)$	0.20	[28]
$2s^22p^2\ ^3P–2s^22p3p\ ^1P$	8.53	(7)	$A = 1.909$, $B = -6.101(-1)$, $C = -2.336$, $D = -3.093(+2)$, $E = 7.450(+2)$, $F = 1.491$	0.06	[28]
$2s^22p^2\ ^3P–2s^22p3p\ ^3D$	8.64	(10)	$A = 9.753(-1)$, $B = 1.908$, $C = 2.161$, $D = -4.891$, $E = 0$	0.01	[28]
$2s^22p^2\ ^3P–2s^22p3p\ ^3S$	8.77	(10)	$A = 1.886(-3)$, $B = 2.263(-1)$, $C = 8.836(-1)$, $D = -1.031$, $E = 0$	0.001	[28]
$2s^22p^2\ ^3P–2s^22p3p\ ^3P$	8.85	(6)	$A = 7.728$, $B = 8.661(-1)$, $C = -1.640(+1)$, $D = 7.754$, $E = 0$	0.22	[28]
$2s^22p^2\ ^3P–2s^22p3p\ ^1D$	9.00	(7)	$A = -1.389$, $B = 1.062$, $C = -3.742(-1)$, $D = 4.786$, $E = -4.126$, $F = 2.606(-1)$	0.18	[28]
$2s^22p^2\ ^3P–2s^22p3p\ ^1S$	9.20	(7)	$A = 3.567(-2)$, $B = 5.081(-1)$, $C = -7.062(-1)$, $D = 1.463$, $E = -2.569$, $F = 4.101(-1)$	0.33	[28]
$2s^22p^2\ ^3P–2s2p^3\ ^3P$	9.33	(6)	$A = 1.146(+1)$, $B = -2.477(+1)$, $C = 1.281(+1)$, $D = 0$, $E = 6.328$	0.11	[28]
$2s^22p^2\ ^3P–2s^22p3d\ ^1D$	9.63	(6)	$A = 5.747(-2)$, $B = -1.444(-1)$, $C = 1.793$, $D = -1.719$, $E = 0$	0.52	[28]
$2s^22p^2\ ^3P–2s^22p3d\ ^3F$	9.69	(11)	$A = -3.067$, $B = 2.352$, $C = -3.127$, $D = -9.123$, $E = 1.656(+1)$, $F = 1.476(-1)$	0.007	[28]
$2s^22p^2\ ^3P–2s^22p3d\ ^3D$	9.71	(6)	$A = 4.081$, $B = -9.274$, $C = 5.423$, $D = 0$, $E = 4.970$	0.02	[28]
$2s^22p^2\ ^3P–2s^22p3d\ ^1F$	9.73	(11)	$A = 1.183$, $B = -8.798(-1)$, $C = 7.839$, $D = -1.718(+1)$, $E = -8.149(-1)$, $F = 5.66(-1)$	0.01	[28]
$2s^22p^2\ ^3P–2s^22p3d\ ^3P$	9.83	(6)	$A = 1.247$, $B = -5.247$, $C = 3.983$, $D = 0$, $E = 3.876$	0.02	[28]
$2s^22p^2\ ^3P–2s2p^3\ ^1D$	12.2	(7)	$A = -3.820$, $B = 2.082$, $C = 2.801$, $D = -9.506$, $E = 1.552(+1)$, $F = 2.937(-1)$	0.16	[28]
$2s^22p^2\ ^3P–2s2p^3\ ^3S$	13.1	(6)	$A = 8.801(-1)$, $B = -9.630$, $C = 8.179$, $D = 0$, $E = 1.199(+1)$	1.95	[28]
$2s^22p^2\ ^3P–2s2p^3\ ^1P$	14.9	(11)	$A = 2.975$, $B = -4.065$, $C = -2.943(-1)$, $D = 7.361(+1)$, $E = -3.359(+2)$, $F = 1.40$	0.10	[28]
$2s^22p^2\ ^1D–2s^22p^2\ ^1S$	1.42	(10)	$A = 2.029$, $B = -1.093(+1)$, $C = 2.049(+1)$, $D = -1.221(+1)$, $E = 0.0$	0.01	[28]
$2s^22p^2\ ^1D–2s2p^3\ ^3D$	6.68	(7)	$A = 1.003(+2)$, $B = -5.439(+1)$, $C = -1.260(+2)$, $D = 1.861(+2)$, $E = -9.357(+2)$, $F = 6.9(-1)$	0.09	[28]
$2s^22p^2\ ^1D–2s^22p3s\ ^3P$	6.22	(7)	$A = 9.576$, $B = -6.855(-1)$, $C = 2.121$, $D = 3.983$, $E = -7.383(+1)$, $F = 4.750(-1)$	0.19	[28]
$2s^22p^2\ ^1D–2s^22p3s\ ^1P$	6.42	(6)	$A = -1.795$, $B = -1.134$, $C = 2.995$, $D = 0$, $E = 4.794$	0.20	[28]

[a] $x(\pm y) = x \times 10^{\pm y}$.

Table 7
Values of the fitting parameters for electron-impact ionization in Eq. (17). See page 415 for Explanation of Tables

	I	A_1	A_2	A_3	A_4	A_5	rms	Ref.
$C^{5+} \to C^{6+}$	490	2.489(−1)[a]	1.847(−1)	4.475(−2)	−9.432(−2)	5.122(−1)	0.02	[36]
$C^{4+} \to C^{5+}$	392	9.205(−1)	−6.297(−1)	1.316	−9.156(−2)	0.0	1.07	[39]
$C^{3+} \to C^{4+}$ [b]	64.5	1.350	−8.748(−1)	−1.444	2.330	−2.730	0.11	[42]
	285	−2.777	5.376	−8.748	1.766(+1)	−9.086		
$C^{2+} \to C^{3+}$	41.4	4.009(−1)	−3.518(−1)	2.375	−3.992	2.794	0.08	[48]
$C^{+} \to C^{2+}$	24.4	8.390(−1)	−7.950(−1)	3.263	−5.382	3.476	0.24	[51]
$C^{+} \to C^{3+}$ [b]	70.0	1.674(−1)	−1.583(−1)	1.941(−2)	1.200(−1)	−3.559(−1)	0.430	[53]
	320	−7.904(−1)	1.315	7.235(−1)	−7.621(−1)	2.485		
$C \to C^{+}$	10.6	1.829	−1.975	1.149	−3.583	2.451	0.61	[54]

[a] $x(\pm y) = x \times 10^{\pm y}$.
[b] A sum of two sets of Eq. (17) were needed to fit these cross sections.

Table 8
Values of the fitting parameters in Eq. (19) for charge exchange in $C^{6+} + H$ collisions. See page 415 for Explanation of Tables

Transition	Parameters	rms and Ref.
$C^{6+} + H \rightarrow C^{5+}(1s) + H^+$	$a_1 = 8.775(+3)$[a], $a_2 = 2.203(+6)$, $a_3 = 7.199(-1)$, $a_4 = 4.031(+3)$, $a_5 = -3.389$, $a_6 = 3.785(+2)$, $a_7 = 2.211$, $a_8 = 4.927(+4)$, $a_9 = 5.159$, $a_{10} = 5.556(+1)$, $a_{11} = 1.362(+4)$, $a_{12} = 5.824(-1)$, $a_{13} = 2.211(-9)$, $a_{14} = 7.417(-1)$	rms = 1.33 [56,57]
$C^{6+} + H \rightarrow C^{5+}(2s) + H^+$	$a_1 = 6.077(+1)$, $a_2 = 1.203(+6)$, $a_3 = 4.784(-1)$, $a_4 = 3.421(+3)$, $a_5 = 1.388$, $a_6 = 9.320(+3)$, $a_7 = 1.093$, $a_8 = 4.930(+4)$, $a_9 = 4.448$, $a_{10} = 1.120(+2)$, $a_{11} = 2.781(+3)$, $a_{12} = 1.194$, $a_{13} = 1.732(+2)$, $a_{14} = 8.134$	rms = 0.44 [56,57]
$C^{6+} + H \rightarrow C^{5+}(2p) + H^+$	$a_1 = 4.400(+4)$, $a_2 = 4.203(+6)$, $a_3 = 4.630(-1)$, $a_4 = 4.108(+3)$, $a_5 = 2.529$, $a_6 = 9.326(+3)$, $a_7 = 2.430$, $a_8 = 4.929(+4)$, $a_9 = 5.889$, $a_{10} = 4.900(-2)$, $a_{11} = 1.360(+2)$, $a_{12} = 6.767(-1)$, $a_{13} = 2.132(+1)$, $a_{14} = 2.553$	rms = 2.18 [56,57]
$C^{6+} + H \rightarrow C^{5+}(n = 2) + H^+$	$a_1 = 7.553(+1)$, $a_2 = 1.203(+6)$, $a_3 = 4.747(-1)$, $a_4 = 3.766(+3)$, $a_5 = 9.873(-1)$, $a_6 = 9.294(+3)$, $a_7 = 8.192(-1)$, $a_8 = 4.928(+4)$, $a_9 = 3.779$, $a_{10} = 4.900(-2)$, $a_{11} = 1.360(+2)$, $a_{12} = 6.760(-1)$, $a_{13} = 2.132(+1)$, $a_{14} = 2.010$	rms = 0.24 [56]
$C^{6+} + H \rightarrow C^{5+}(3s) + H^+$	$a_1 = 9.197(-1)$, $a_2 = 1.203(+6)$, $a_3 = -7.438(-2)$, $a_4 = 5.026(+3)$, $a_5 = -3.446$, $a_6 = 4.364(+4)$, $a_7 = 2.946$, $a_8 = 2.290(+5)$, $a_9 = 5.395$	rms = 0.28 [56,57]
$C^{6+} + H \rightarrow C^{5+}(3p) + H^+$	$a_1 = 1.606$, $a_2 = 1.267(+6)$, $a_3 = -3.948(-1)$, $a_4 = 6.026(+3)$, $a_5 = -3.064$, $a_6 = 4.684(+4)$, $a_7 = 2.461$, $a_8 = 1.941(+5)$, $a_9 = 5.264$	rms = 0.17 [57,62,70]
$C^{6+} + H \rightarrow C^{5+}(3d) + H^+$	$a_1 = 8.680$, $a_2 = 1.192(+6)$, $a_3 = 1.436(-1)$, $a_4 = 7.064(+4)$, $a_5 = 2.995$, $a_6 = 6.849(+3)$, $a_7 = -2.652$, $a_8 = 1.545(+5)$, $a_9 = 5.895$	rms = 0.21 [57,62,70]
$C^{6+} + H \rightarrow C^{5+}(n = 3) + H^+$	$a_1 = 1.121(+1)$, $a_2 = 1.195(+6)$, $a_3 = 6.029(-2)$, $a_4 = 6.088(+4)$, $a_5 = 2.798$, $a_6 = 5.994(+3)$, $a_7 = -2.943$, $a_8 = 1.547(+5)$, $a_9 = 5.436$	rms = 0.16 [57,62,70]
$C^{6+} + H \rightarrow C^{5+}(4s) + H^+$	$a_1 = 2.570(+1)$, $a_2 = 1.334(+6)$, $a_3 = -4.311(-1)$, $a_4 = 9.667(+4)$, $a_5 = -8.384(-1)$, $a_6 = 3.104(+3)$, $a_7 = 7.322(-1)$, $a_8 = 2.051(+5)$, $a_9 = 2.951$	rms = 0.20 [57,62,70]
$C^{6+} + H \rightarrow C^{5+}(4p) + H^+$	$a_1 = 3.654(+2)$, $a_2 = 2.932(+6)$, $a_3 = 1.646(-1)$, $a_4 = 1.328(+4)$, $a_5 = 3.086$, $a_6 = 2.879(+3)$, $a_7 = 1.233$, $a_8 = 9.395(+4)$, $a_9 = 6.076$	rms = 0.10 [57,62,70]
$C^{6+} + H \rightarrow C^{5+}(4d) + H^+$	$a_1 = 9.718(+2)$, $a_2 = 2.930(+6)$, $a_3 = 1.749(-1)$, $a_4 = 1.481(+4)$, $a_8 = 8.098(+4)$, $a_5 = 3.120$, $a_6 = 2.204(+3)$, $a_7 = 1.038$, $a_9 = 6.391$	rms = 0.17 [57,61,70]
$C^{6+} + H \rightarrow C^{5+}(4f) + H^+$	$a_1 = 3.705(+1)$, $a_2 = 3.080(+5)$, $a_3 = 1.880(-1)$, $a_4 = 7.779(+4)$, $a_5 = 1.992$, $a_6 = 6.461(+4)$, $a_7 = 5.695$, $a_8 = 9.590(+4)$, $a_9 = 1.631$, $a_{10} = 7.417(+1)$, $a_{11} = 4.791(+3)$, $a_{12} = -5.261(-1)$, $a_{13} = 1.515(+3)$, $a_{14} = -1.121$, $a_{15} = 7.601(+3)$, $a_{16} = -6.016(-2)$	rms = 0.18 [57,62,70]
$C^{6+} + H \rightarrow C^{5+}(n = 4) + H^+$	$a_1 = 4.570(+3)$, $a_2 = 1.201(+6)$, $a_3 = 1.936(-1)$, $a_4 = 6.222(+2)$, $a_5 = 8.580(-1)$, $a_6 = 1.683(+4)$, $a_7 = 3.534$, $a_8 = 5.590(+4)$, $a_9 = 5.735$	rms = 0.08 [57,61,70]
$C^{6+} + H \rightarrow C^{5+}(5s) + H^+$	$a_1 = 3.960(+4)$, $a_2 = 8.690(+5)$, $a_3 = -1.380$, $a_4 = 6.004(+3)$, $a_5 = 4.215$, $a_6 = 5.845(+2)$, $a_7 = 2.676$, $a_8 = 1.968(+4)$, $a_9 = 5.396$, $a_{10} = 8.126(-1)$, $a_{11} = 4.121(+4)$, $a_{12} = 4.196(-1)$, $a_{13} = 1.656(+3)$, $a_{14} = 1.956(+3)$, $a_{15} = 6.126(+4)$, $a_{16} = 3.048$	rms = 0.38 [57,62,70]
$C^{6+} + H \rightarrow C^{5+}(5p) + H^+$	$a_1 = 3.230(+1)$, $a_2 = 5.615(+3)$, $a_3 = -3.934(-1)$, $a_4 = 1.302(+4)$, $a_5 = -1.240$, $a_6 = 2.084(+4)$, $a_7 = -1.240$, $a_8 = 2.084(+4)$, $a_9 = 1.625$, $a_{10} = 9.971(+1)$, $a_{11} = 1.800(+5)$, $a_{12} = 2.287(-1)$, $a_{13} = 1.142(+3)$, $a_{14} = 3.097$	rms = 0.22 [57,62,70]
$C^{6+} + H \rightarrow C^{5+}(5d) + H^+$	$a_1 = 3.960(+4)$, $a_2 = 8.690(+5)$, $a_3 = 4.461(-1)$, $a_4 = 6.140(+3)$, $a_5 = -5.379(-1)$, $a_6 = 4.690(+2)$, $a_7 = 1.793$, $a_8 = 1.960(+4)$, $a_9 = 5.644$, $a_{10} = 2.906$, $a_{11} = 4.120(+4)$, $a_{12} = -6.217(-1)$, $a_{13} = 1.311(+3)$, $a_{14} = -4.244(-2)$, $a_{15} = 6.110(+4)$, $a_{16} = 1.688$	rms = 0.24 [57,62,70]
$C^{6+} + H \rightarrow C^{5+}(5f) + H^+$	$a_1 = 3.965(+4)$, $a_2 = 8.690(+5)$, $a_3 = 3.591(-1)$, $a_4 = 6.133(+3)$, $a_5 = -1.572$, $a_6 = 4.456(+2)$, $a_7 = 1.662$, $a_8 = 2.022(+4)$, $a_9 = 5.796$, $a_{10} = 3.904$, $a_{11} = 4.129(+4)$, $a_{12} = -7.814(-1)$, $a_{13} = 1.550(+3)$, $a_{14} = -2.499(-2)$, $a_{15} = 6.113(+4)$, $a_{16} = 1.070$	rms = 0.14 [57,61,70]
$C^{6+} + H \rightarrow C^{5+}(5g) + H^+$	$a_1 = 3.960(+4)$, $a_2 = 8.690(+5)$, $a_3 = 3.379(-1)$, $a_4 = 6.141(+3)$, $a_5 = -3.628$, $a_6 = 4.376(+2)$, $a_7 = 1.392$, $a_8 = 1.963(+4)$, $a_9 = 5.969$, $a_{10} = 7.954$, $a_{11} = 4.120(+4)$, $a_{12} = 9.565(-2)$, $a_{13} = 1.296(+3)$, $a_{14} = -4.248(-2)$, $a_{15} = 6.111(+4)$, $a_{16} = 5.873$	rms = 1.90 [57,61,70]
$C^{6+} + H \rightarrow C^{5+}(n = 5) + H^+$	$a_1 = 5.196(+1)$, $a_2 = 1.870(+4)$, $a_3 = 3.448(-1)$, $a_4 = 5.788(+4)$, $a_5 = 4.234$, $a_6 = 2.991(+4)$, $a_7 = 1.498$, $a_8 = 9.741(+4)$, $a_9 = 4.707$, $a_{10} = 2.709(+1)$, $a_{11} = 2.119(+3)$, $a_{12} = 1.947(-1)$, $a_{13} = 8.518(+2)$, $a_{14} = 3.159$	rms = 0.11 [56,57,62]
$C^{6+} + H \rightarrow C^{5+} + H^+$	$a_1 = 2.301(+2)$, $a_2 = 5.983(+3)$, $a_3 = 3.117(-1)$, $a_4 = 1.300(+4)$, $a_5 = 6.613(-1)$, $a_6 = 7.299(+4)$, $a_7 = 4.895$, $a_8 = 2.100(+4)$, $a_9 = 1.557$, $a_{10} = 3.355(-2)$, $a_{11} = 1.800(+5)$, $a_{12} = -9.768(-2)$, $a_{13} = 4.500(+3)$, $a_{14} = 3.584$	rms = 0.20 [58,70]

[a] $x(\pm y) = x \times 10^{\pm y}$.

Table 9
Values of the fitting parameters in Eq. (19) for charge exchange in $C^{q+} + H$ collisions. See page 415 for Explanation of Tables

Transition	Parameters	rms and Ref.
$C^{5+} + H \rightarrow C^{4+} + H^+$	$a_1 = 1.397(+2)$, $a_2 = 1.897(+4)$, $a_3 = 2.697(-1)$, $a_4 = 5.814(+4)$, $a_5 = 3.761$, $a_6 = 3.211(+4)$, $a_7 = 1.477$, $a_8 = 9.750(+4)$, $a_9 = 5.583$, $a_{10} = 9.227(+2)$, $a_{11} = 5.496(+2)$, $a_{12} = -4.044(-1)$, $a_{13} = 7.590(-7)$, $a_{14} = 1.755(-1)$	rms = 0.02 [71,73,79]
$C^{4+} + H \rightarrow C^{3+} + H^+$	$a_1 = 9.600(+1)$, $a_2 = 3.088(+5)$, $a_3 = 1.218(-1)$, $a_4 = 7.784(+4)$, $a_5 = 2.059$, $a_6 = 6.458(+4)$, $a_7 = 5.498$, $a_8 = 9.596(+4)$, $a_9 = 1.690$, $a_{10} = 1.270(+2)$, $a_{11} = 2.080(+2)$, $a_{12} = -2.589(-1)$, $a_{13} = 2.830(+2)$, $a_{14} = -3.554(-1)$, $a_{15} = 7.157(+1)$, $a_{16} = -1.956$	rms = 0.09 [73,79]
$C^{3+} + H \rightarrow C^{2+} + H^+$	$a_1 = 6.239(+1)$, $a_2 = 1.873(+4)$, $a_3 = 2.589(-1)$, $a_4 = 5.783(+4)$, $a_5 = 4.767$, $a_6 = 3.026(+4)$, $a_7 = 1.492$, $a_8 = 9.744(+4)$, $a_9 = 4.254$, $a_{10} = 3.847(+2)$, $a_{11} = 1.946(+2)$, $a_{12} = -1.814(-1)$, $a_{13} = 4.743(-3)$, $a_{14} = 3.457(-1)$	rms = 0.09 [73,79]
$C^{2+} + H \rightarrow C^+ + H^+$	$a_1 = 3.719(+1)$, $a_2 = 1.086(+4)$, $a_3 = 3.514(-1)$, $a_4 = 3.785(+4)$, $a_5 = 9.584(-1)$, $a_6 = 3.462(+4)$, $a_7 = 3.442$, $a_8 = 4.597(+4)$, $a_9 = 8.611(-1)$	rms = 0.08 [73,93]
$C^+ + H \rightarrow C{+}H^+$	$a_1 = 3.016(+3)$, $a_2 = 2.941(+6)$, $a_3 = 2.283(-1)$, $a_4 = 9.976(+3)$, $a_5 = 2.911$, $a_6 = 2.497(+3)$, $a_7 = 1.604$, $a_8 = 4.969(+4)$, $a_9 = 4.980$	rms = 0.24 [95]

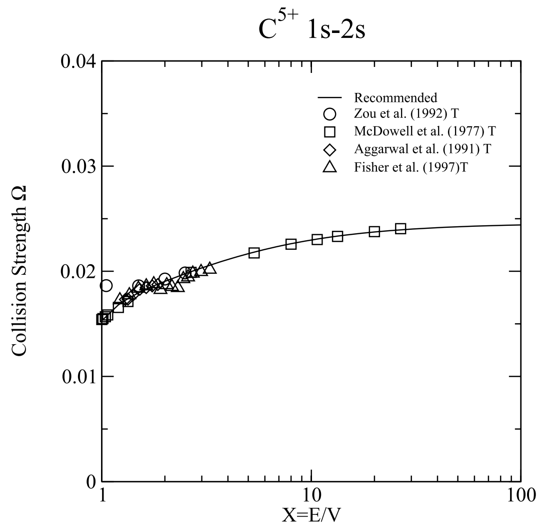

Graph 1: Collision strength for electron-impact excitation.

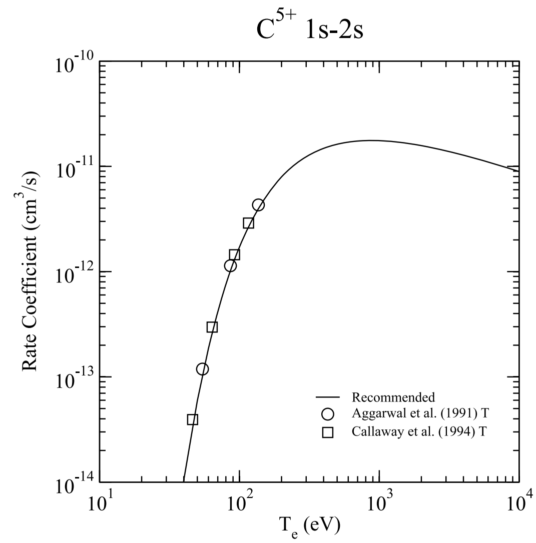

Graph 2: Rate coefficient for electron-impact excitation.

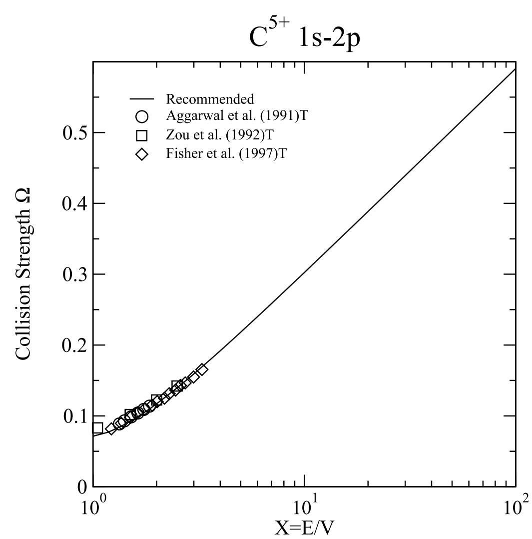

Graph 3: Collision strength for electron-impact excitation.

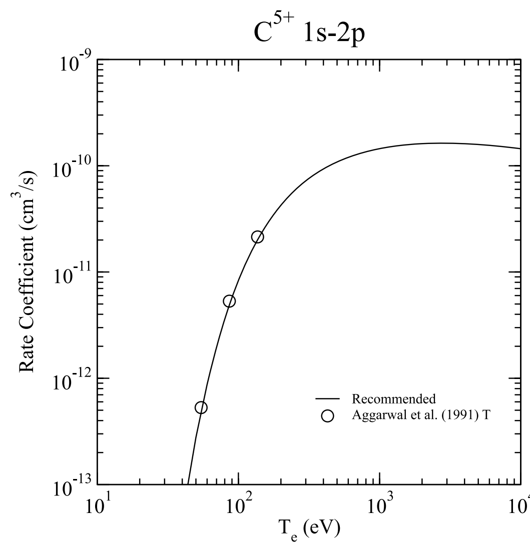

Graph 4: Rate coefficient for electron-impact excitation.

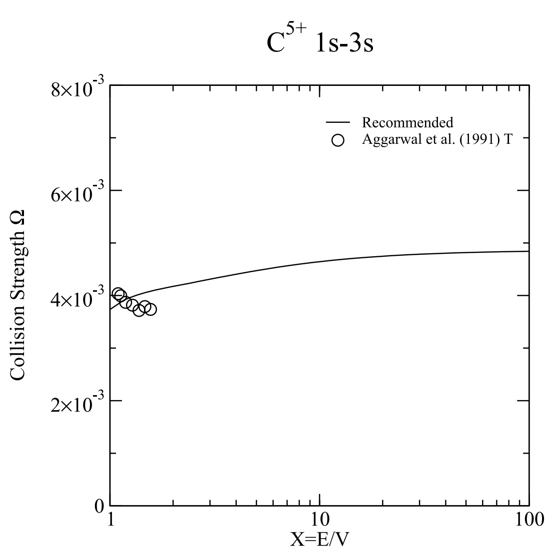

Graph 5: Collision strength for electron-impact excitation.

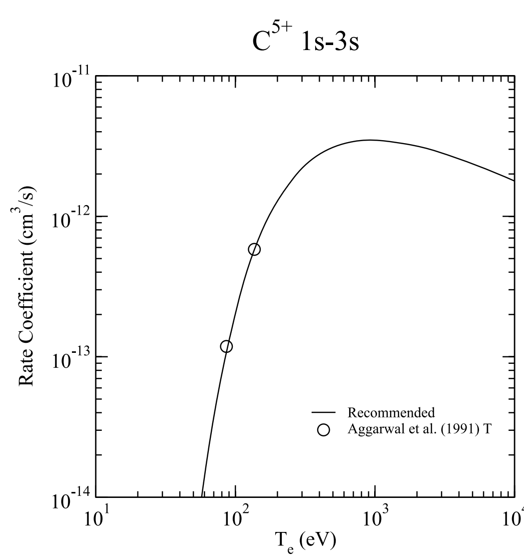

Graph 6: Rate coefficient for electron-impact excitation.

Graphs 1–124. Recommended collision strengths and rate coefficients for electron-impact excitation. See page 416 for Explanation of Graphs.

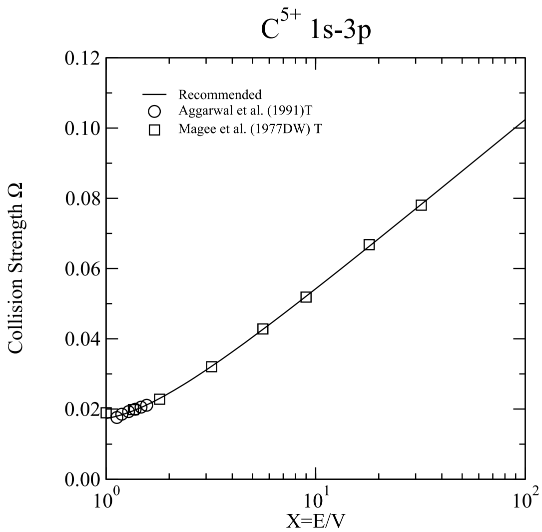

Graph 7: Collision strength for electron-impact excitation.

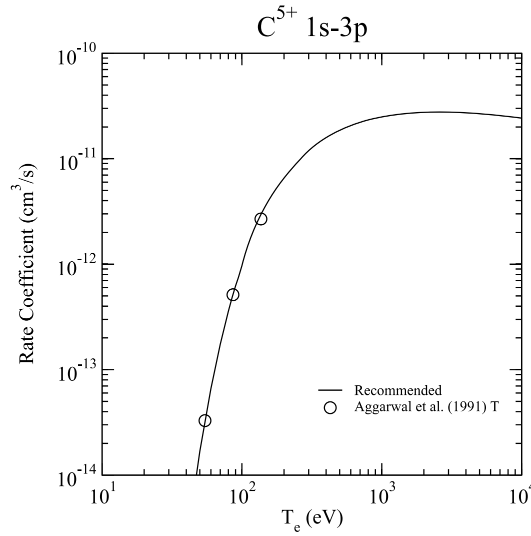

Graph 8: Rate coefficient for electron-impact excitation.

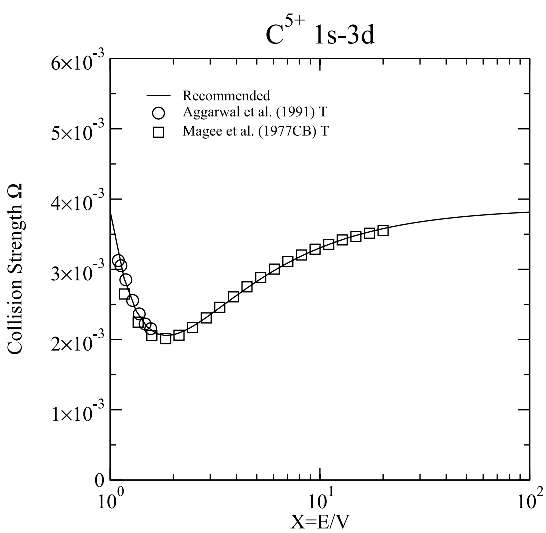

Graph 9: Collision strength for electron-impact excitation.

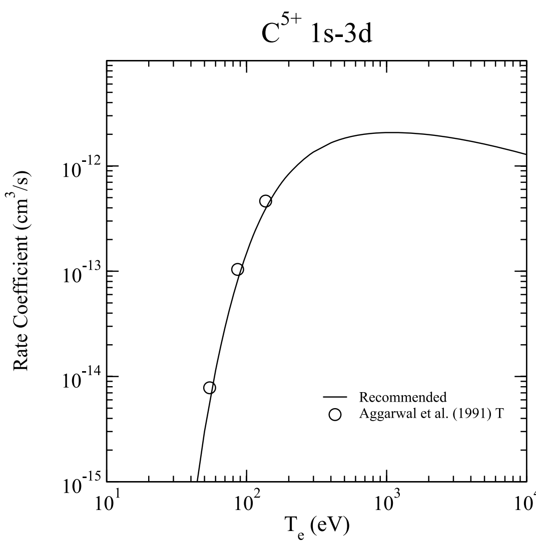

Graph 10: Rate coefficient for electron-impact excitation.

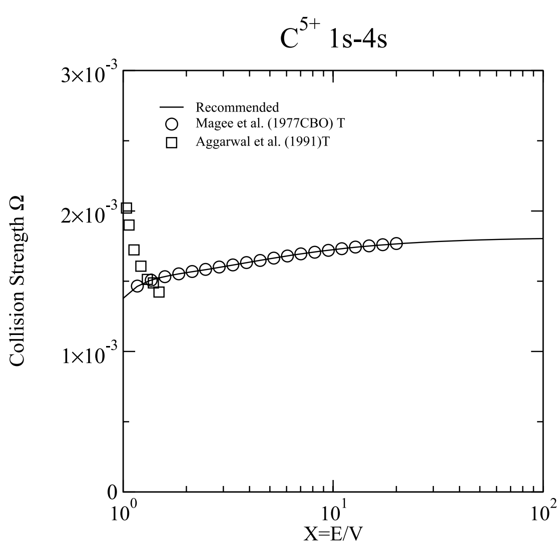

Graph 11: Collision strength for electron-impact excitation.

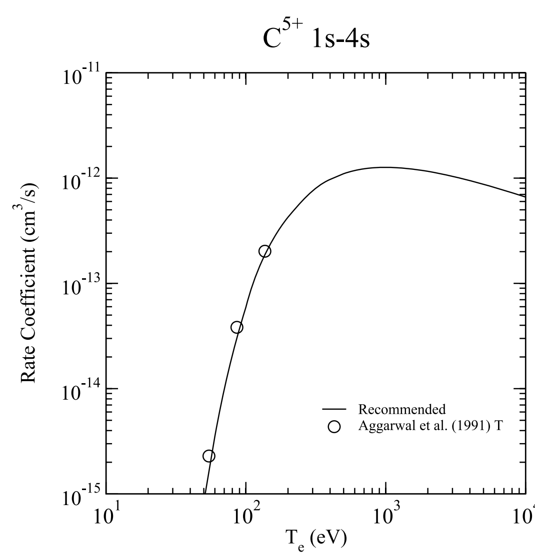

Graph 12: Rate coefficient for electron-impact excitation.

Graphs 1–124. (*continued*)

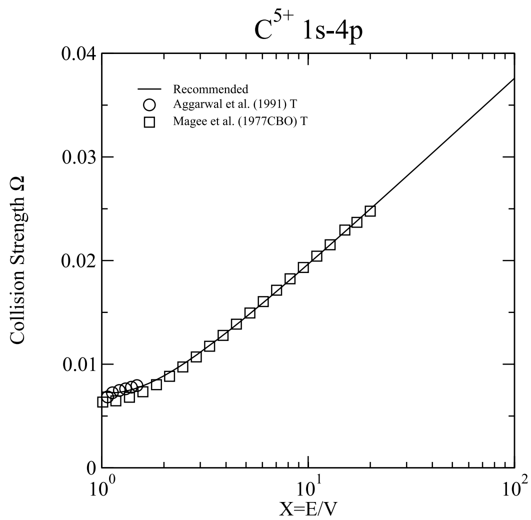

Graph 13: Collision strength for electron-impact excitation.

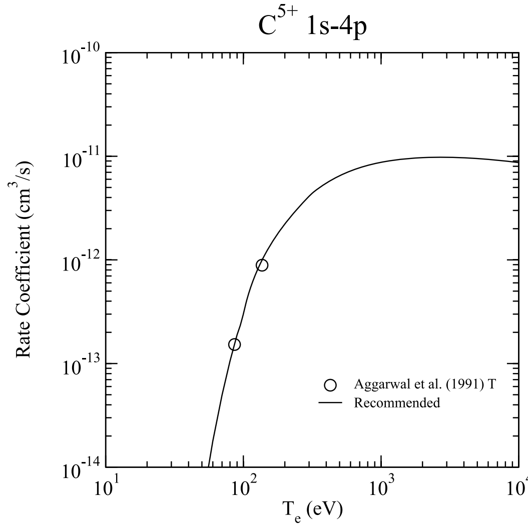

Graph 14: Rate coefficient for electron-impact excitation.

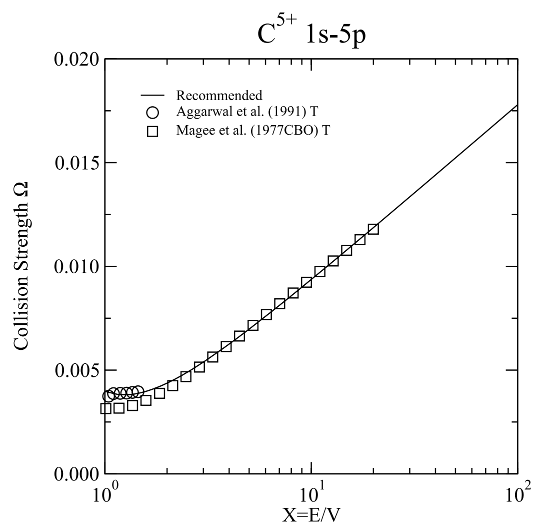

Graph 15: Collision strength for electron-impact excitation.

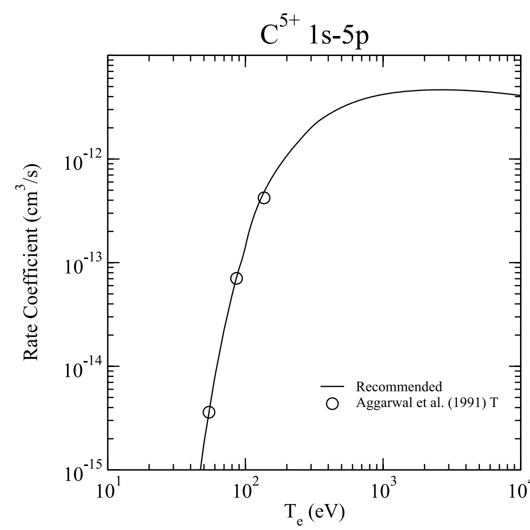

Graph 16: Rate coefficient for electron-impact excitation.

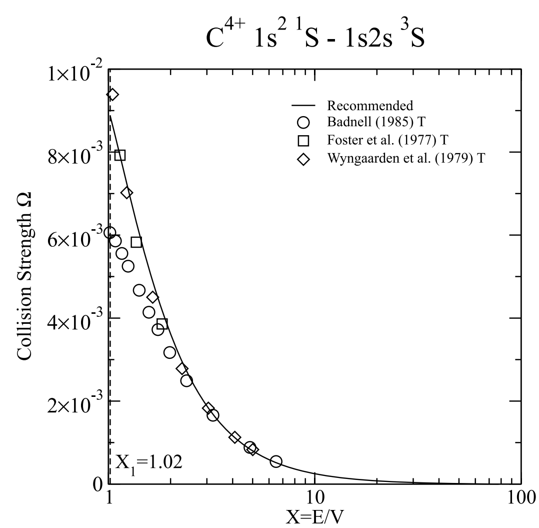

Graph 17: Collision strength for electron-impact excitation.

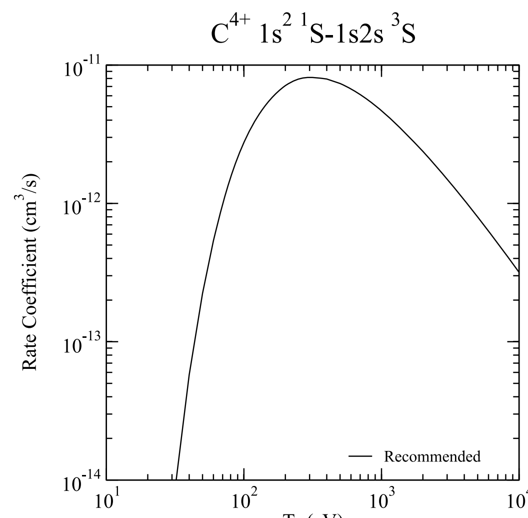

Graph 18: Rate coefficient for electron-impact excitation.

Graphs 1–124. (*continued*)

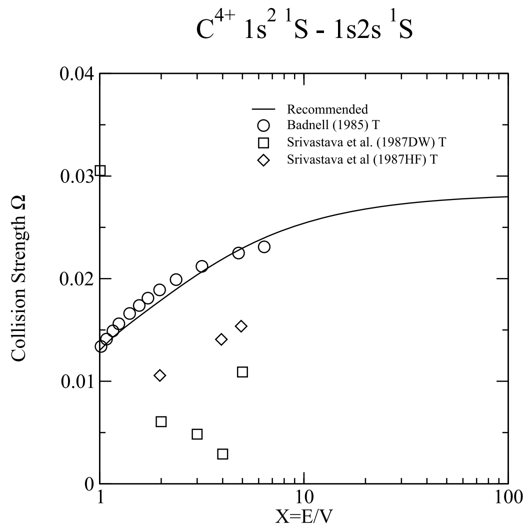

Graph 19: Collision strength for electron-impact excitation.

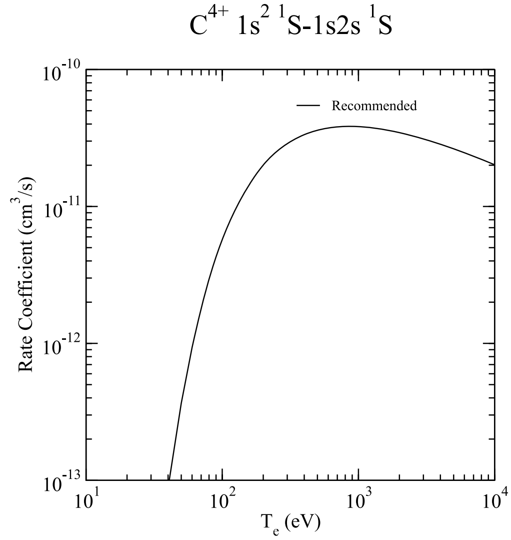

Graph 20: Rate coefficient for electron-impact excitation.

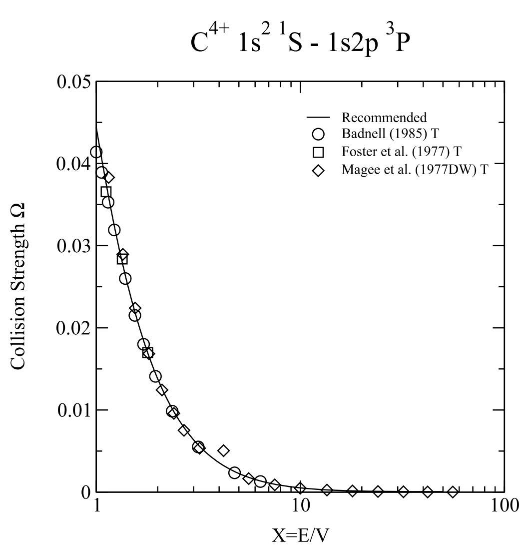

Graph 21: Collision strength for electron-impact excitation.

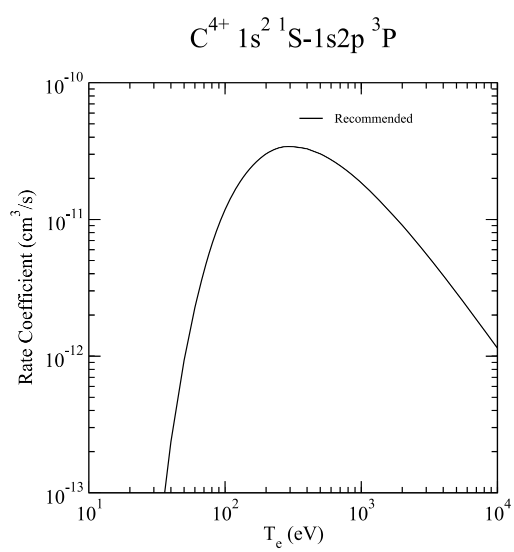

Graph 22: Rate coefficient for electron-impact excitation.

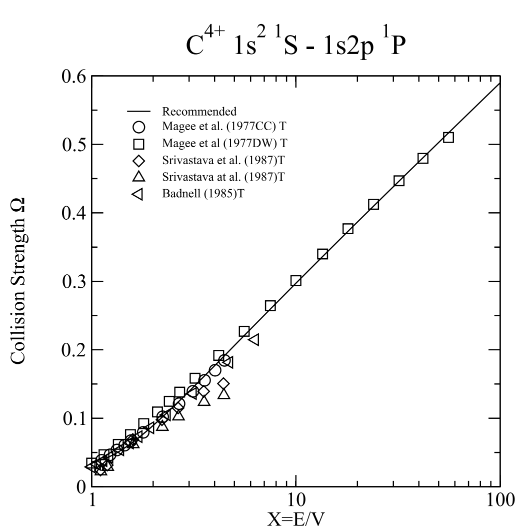

Graph 23: Collision strength for electron-impact excitation.

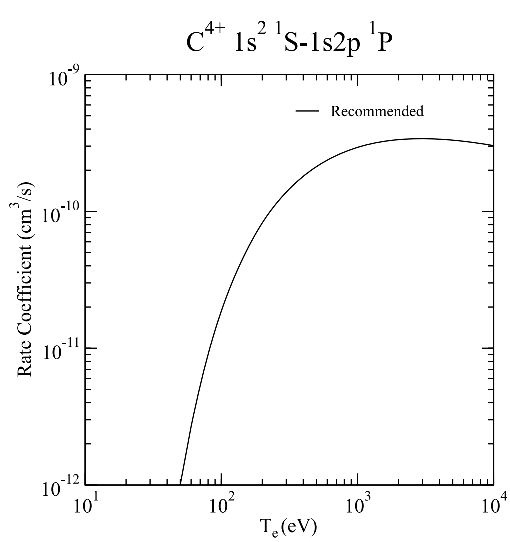

Graph 24: Rate coefficient for electron-impact excitation.

Graphs 1–124. (*continued*)

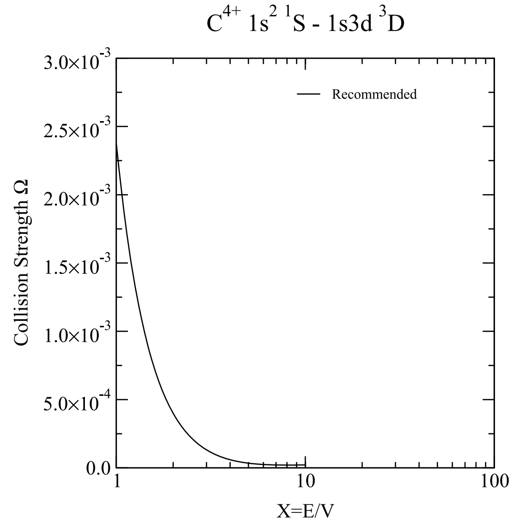

Graph 25: Collision strength for electron-impact excitation.

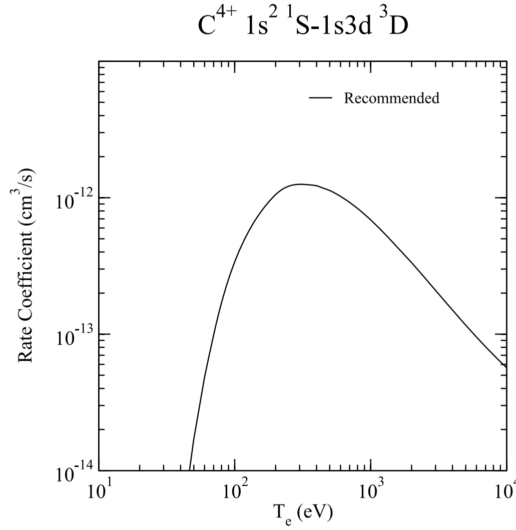

Graph 26: Rate coefficient for electron-impact excitation.

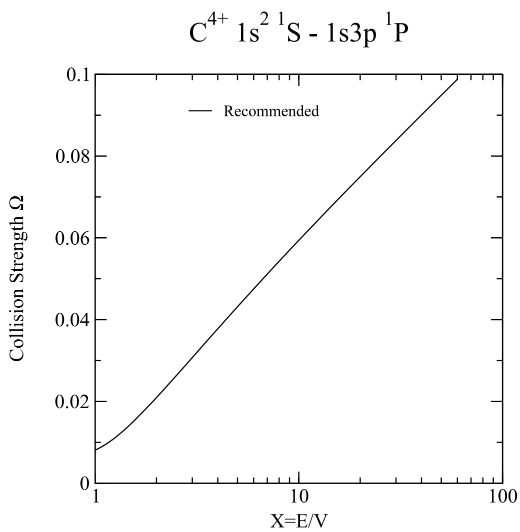

Graph 27: Collision strength for electron-impact excitation.

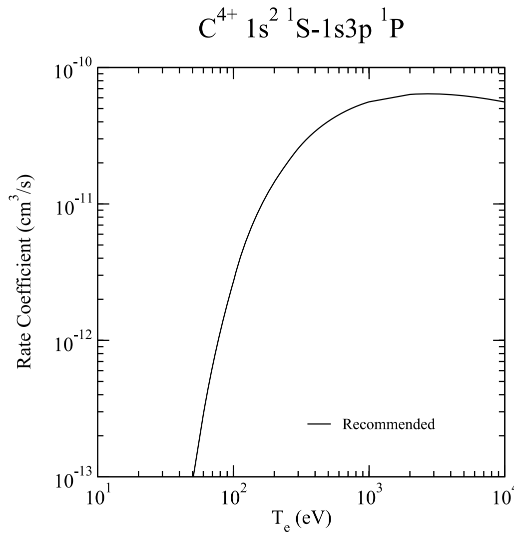

Graph 28: Rate coefficient for electron-impact excitation.

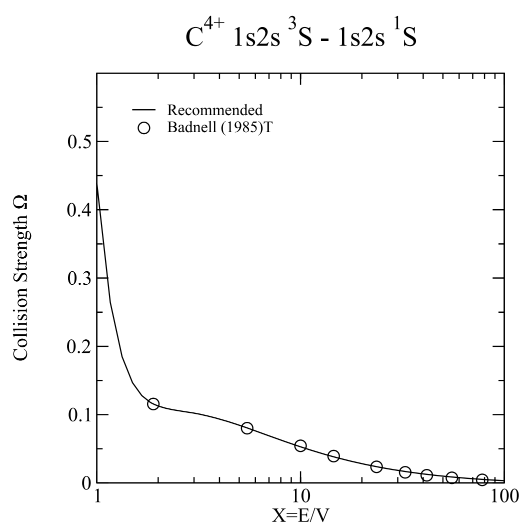

Graph 29: Collision strength for electron-impact excitation.

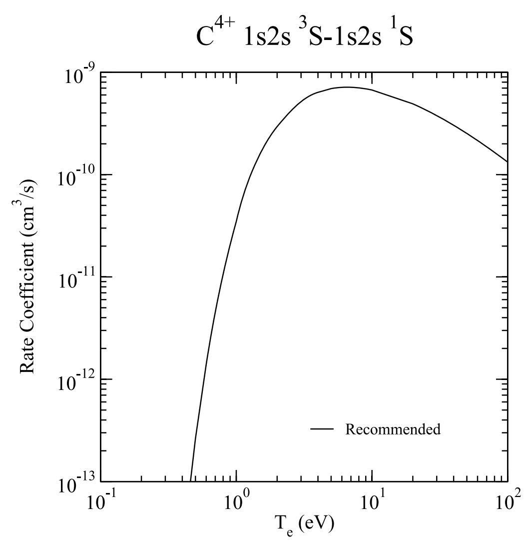

Graph 30: Rate coefficient for electron-impact excitation.

Graphs 1–124. (*continued*)

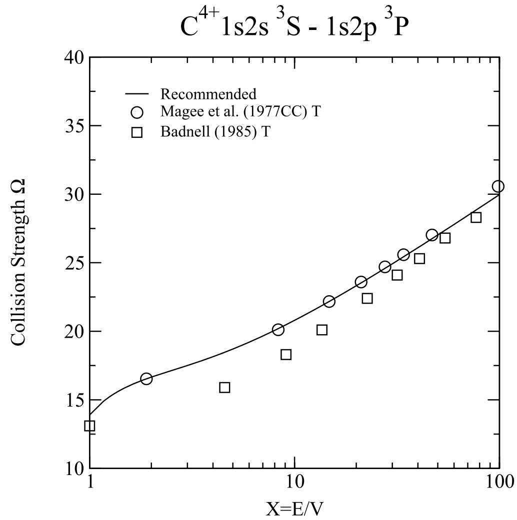

Graph 31: Collision strength for electron-impact excitation.

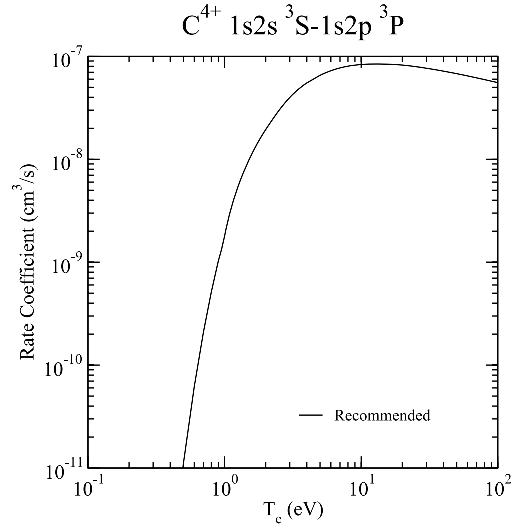

Graph 32: Rate coefficient for electron-impact excitation.

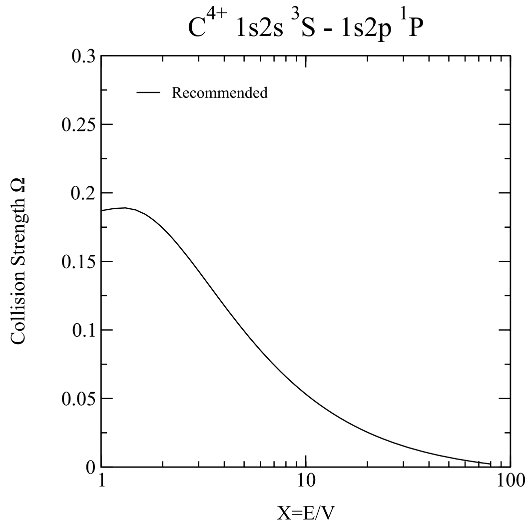

Graph 33: Collision strength for electron-impact excitation.

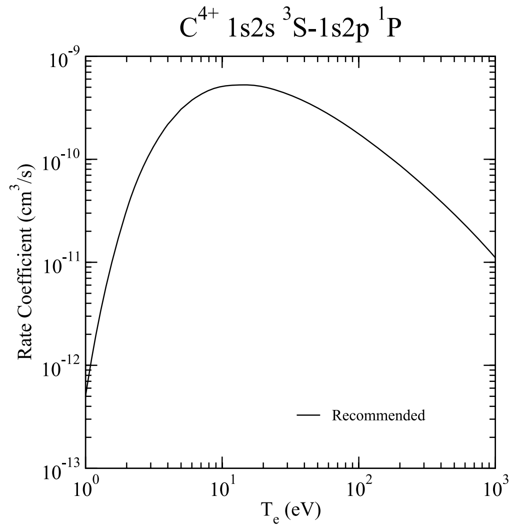

Graph 34: Rate coefficient for electron-impact excitation.

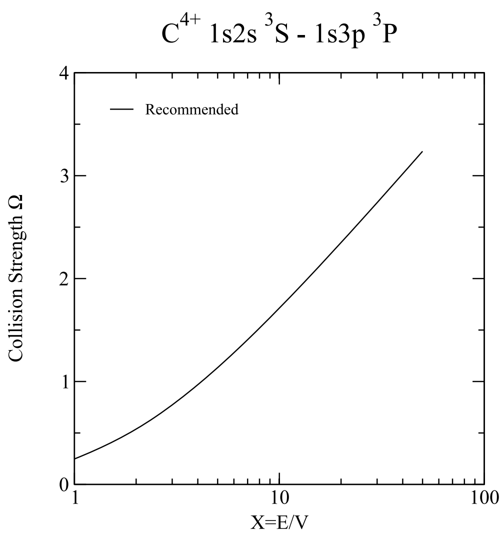

Graph 35: Collision strength for electron-impact excitation.

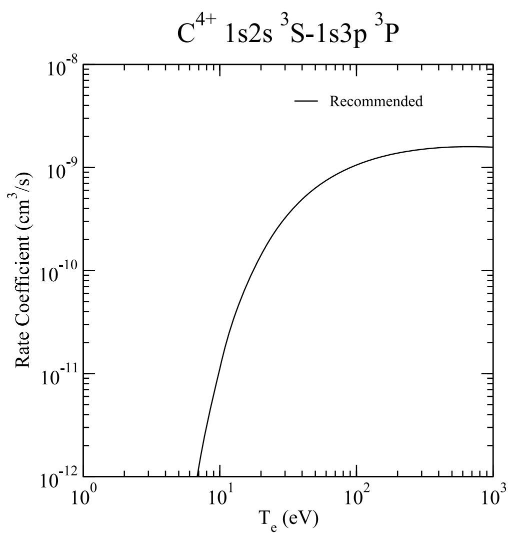

Graph 36: Rate coefficient for electron-impact excitation.

Graphs 1–124. (*continued*)

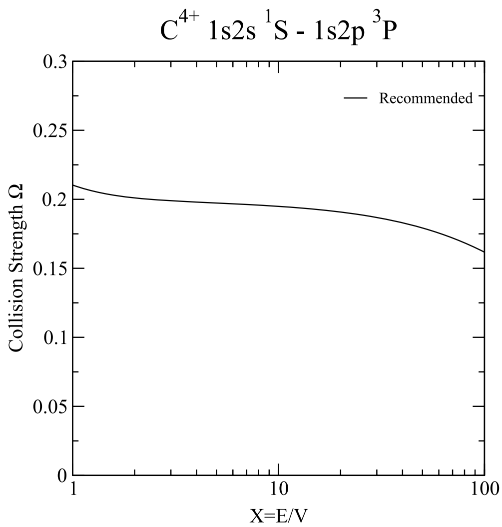

Graph 37: Collision strength for electron-impact excitation.

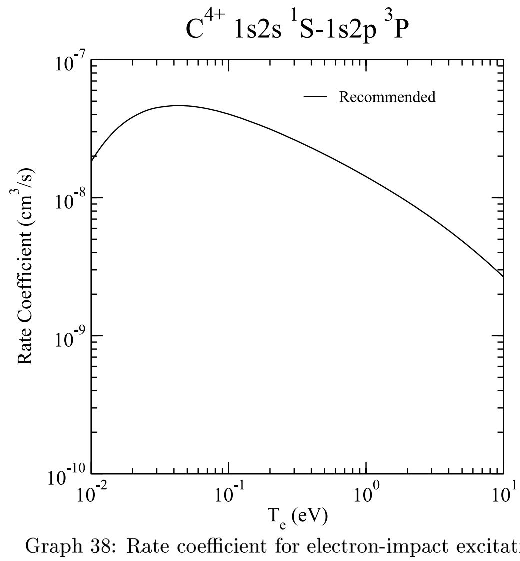

Graph 38: Rate coefficient for electron-impact excitation.

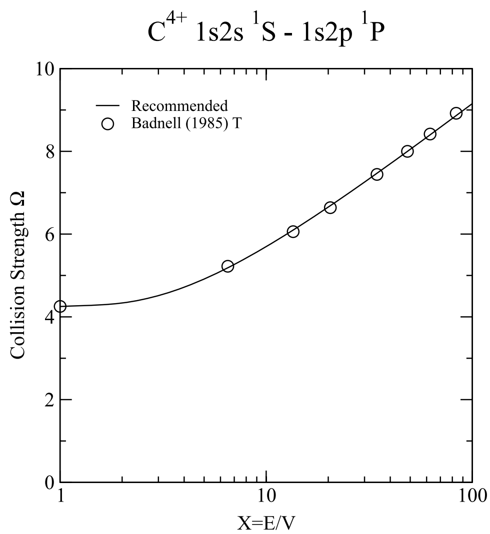

Graph 39: Collision strength for electron-impact excitation.

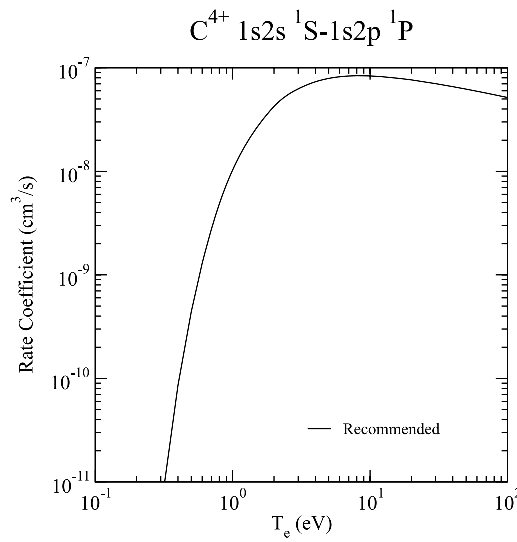

Graph 40: Rate coefficient for electron-impact excitation.

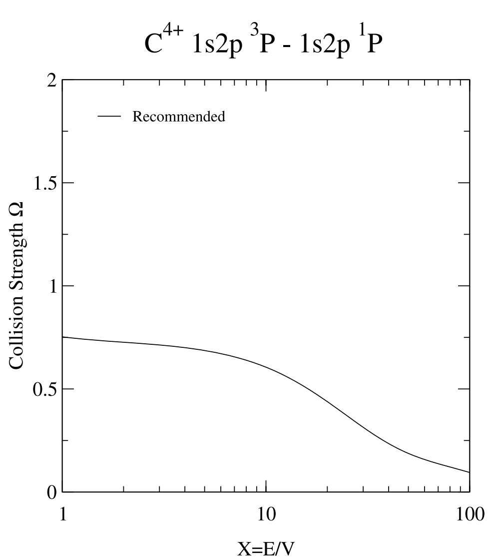

Graph 41: Collision strength for electron-impact excitation.

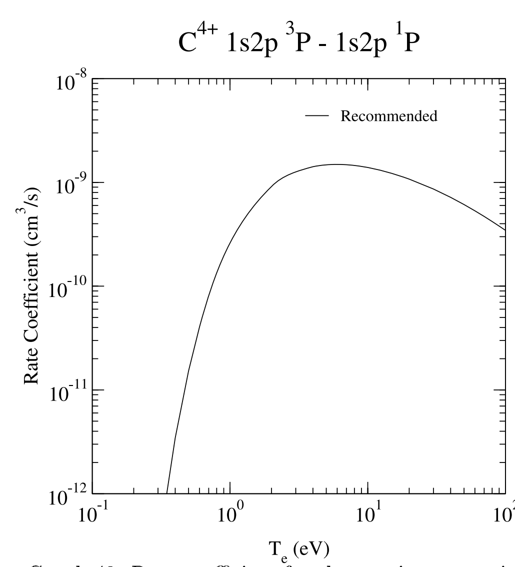

Graph 42: Rate coefficient for electron-impact excitation.

Graphs 1–124. (*continued*)

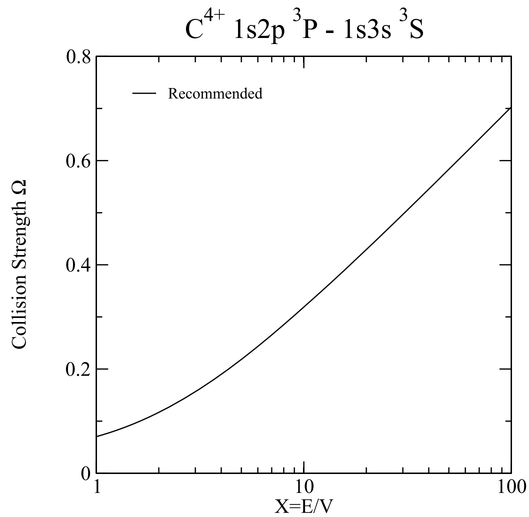

Graph 43: Collision strength for electron-impact excitation.

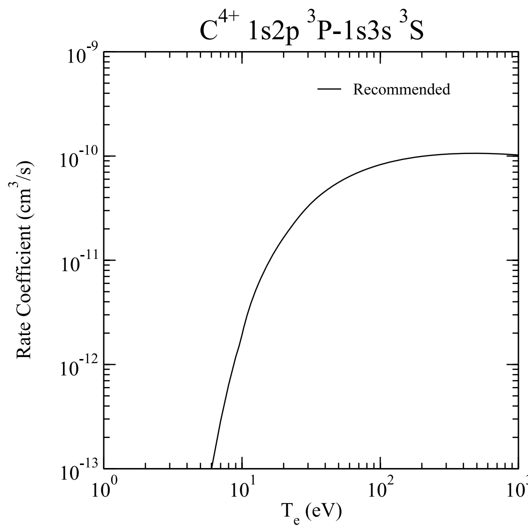

Graph 44: Rate coefficient for electron-impact excitation.

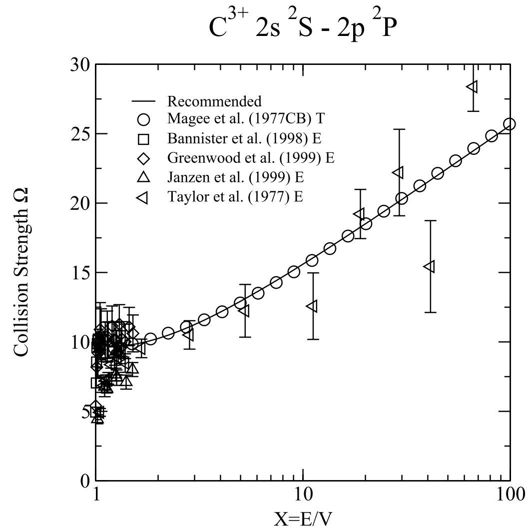

Graph 45: Collision strength for electron-impact excitation.

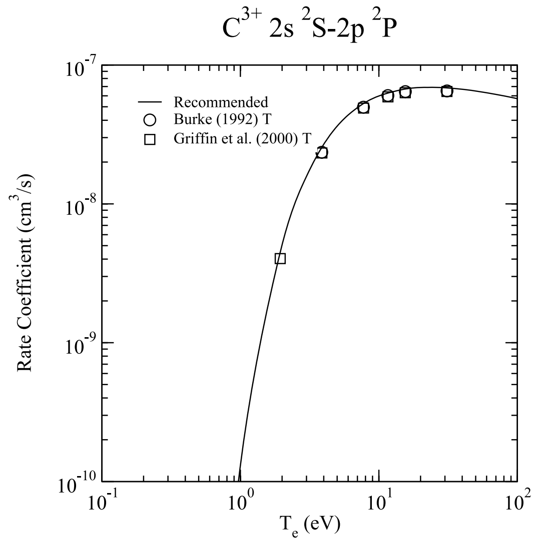

Graph 46: Rate coefficient for electron-impact excitation.

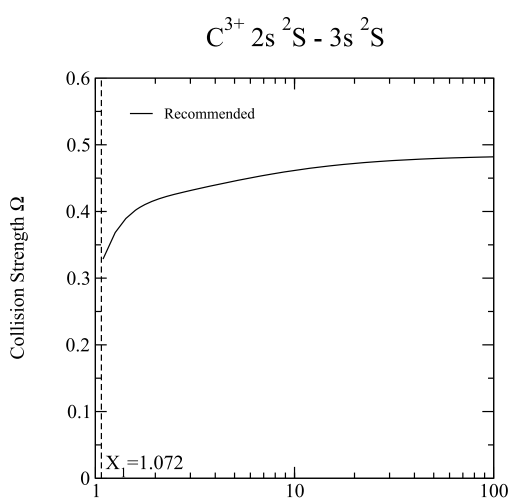

Graph 47: Collision strength for electron-impact excitation.

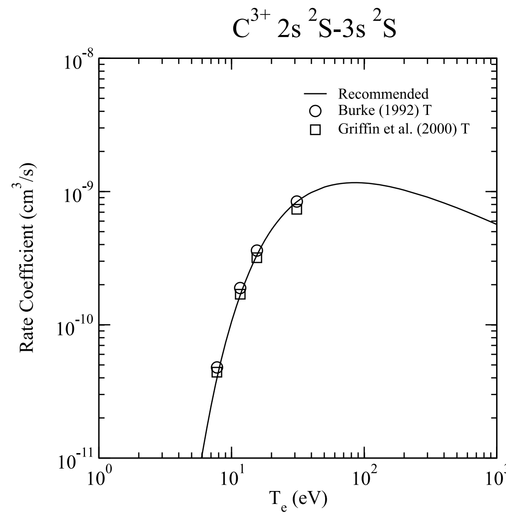

Graph 48: Rate coefficient for electron-impact excitation.

Graphs 1–124. (*continued*)

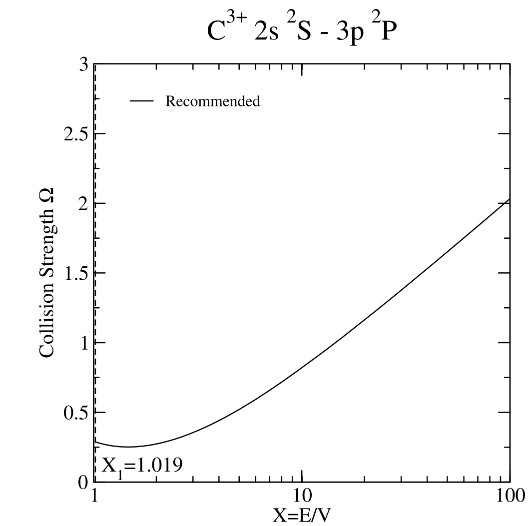

Graph 49: Collision strength for electron-impact excitation.

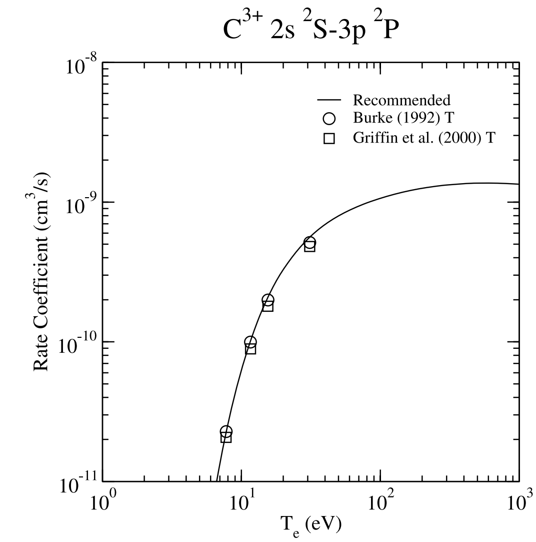

Graph 50: Rate coefficient for electron-impact excitation.

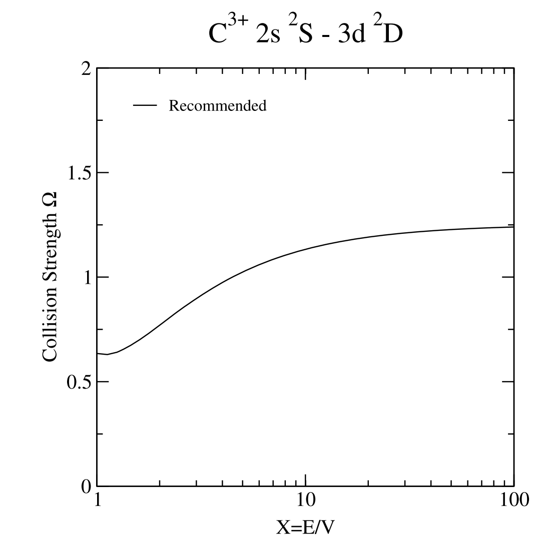

Graph 51: Collision strength for electron-impact excitation.

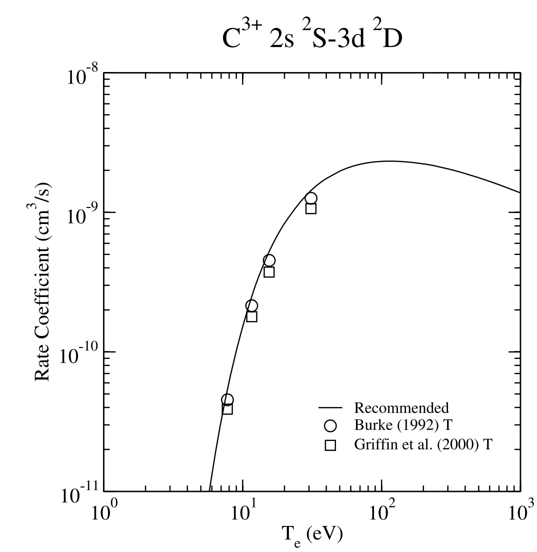

Graph 52: Rate coefficient for electron-impact excitation.

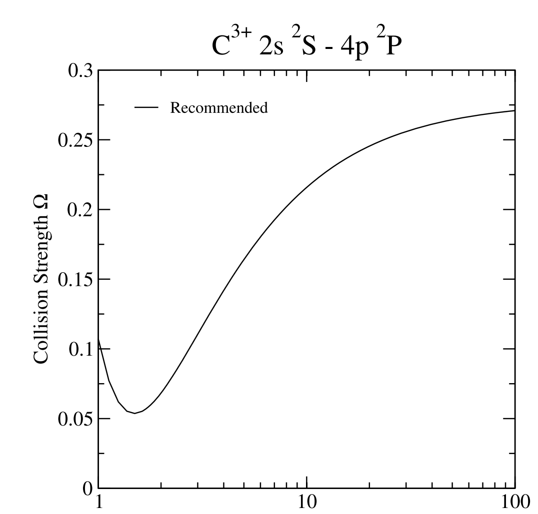

Graph 53: Collision strength for electron-impact excitation.

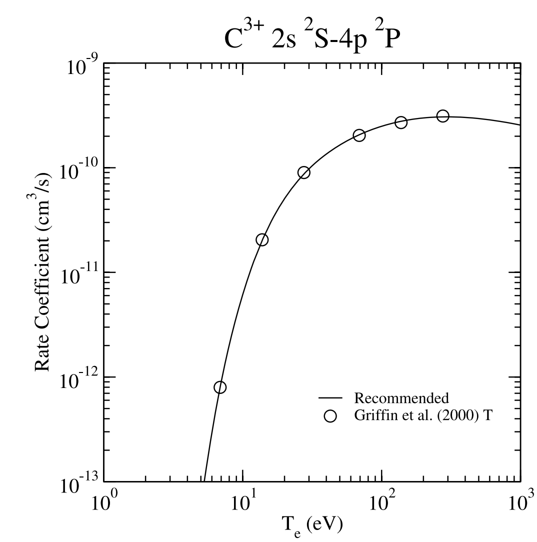

Graph 54: Rate coefficient for electron-impact excitation.

Graphs 1–124. (*continued*)

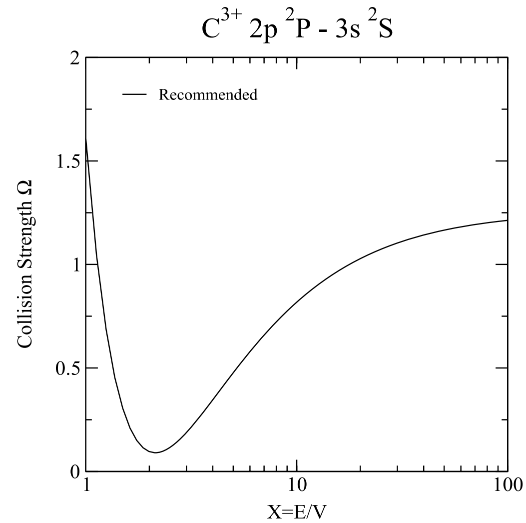

Graph 55: Collision strength for electron-impact excitation.

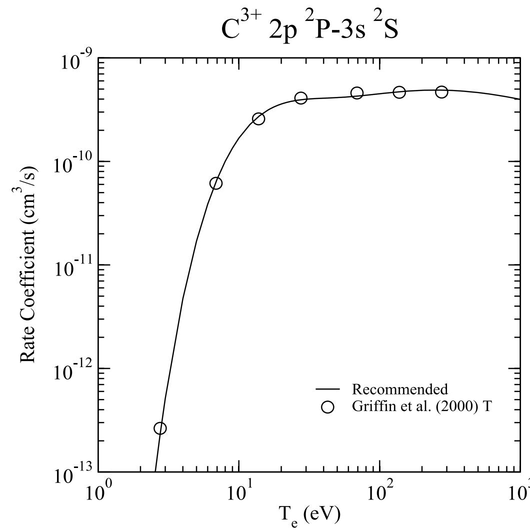

Graph 56: Rate coefficient for electron-impact excitation.

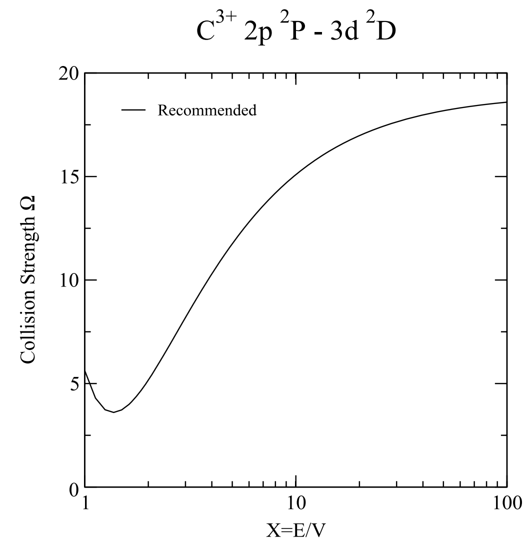

Graph 57: Collision strength for electron-impact excitation.

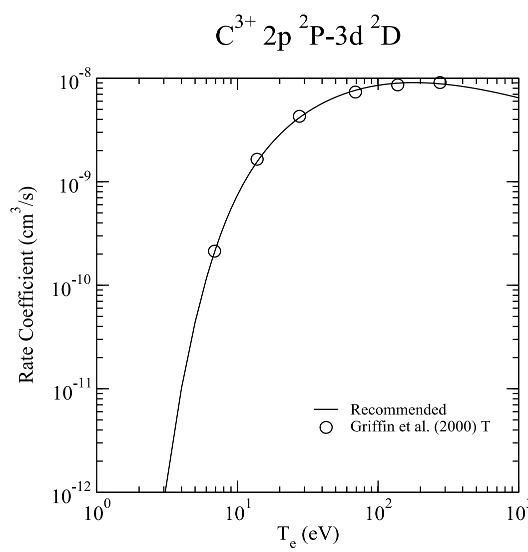

Graph 58: Rate coefficient for electron-impact excitation.

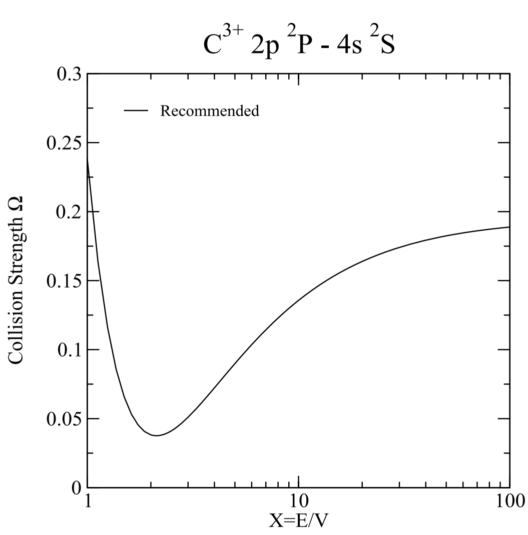

Graph 59: Collision strength for electron-impact excitation.

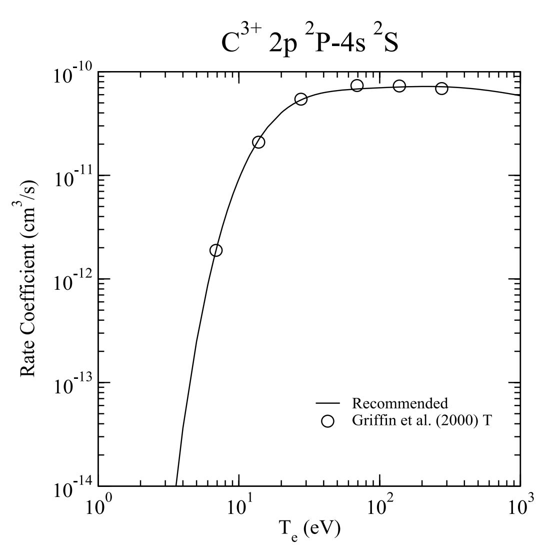

Graph 60: Rate coefficient for electron-impact excitation.

Graphs 1–124. (*continued*)

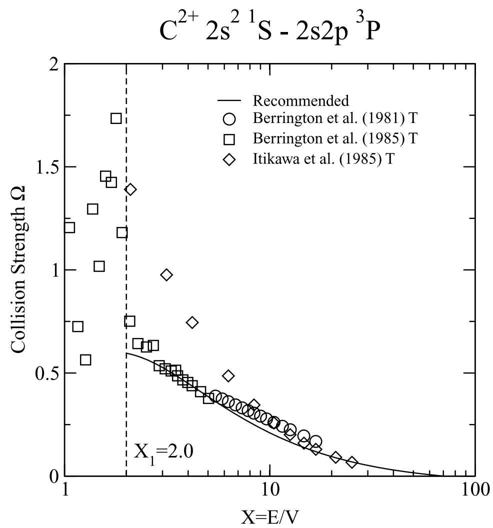

Graph 61: Collision strength for electron-impact excitation.

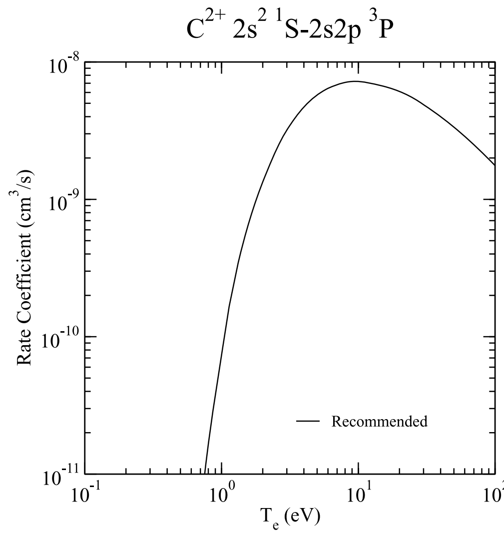

Graph 62: Rate coefficient for electron-impact excitation.

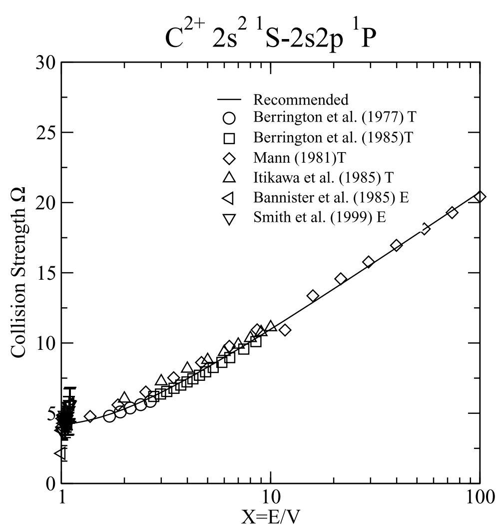

Graph 63: Collision strength for electron-impact excitation.

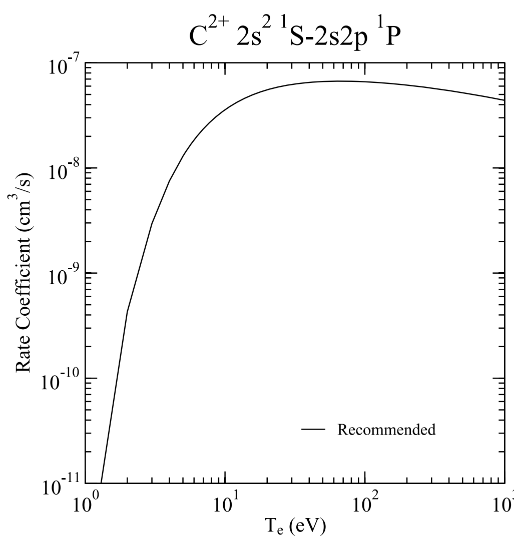

Graph 64: Rate coefficient for electron-impact excitation.

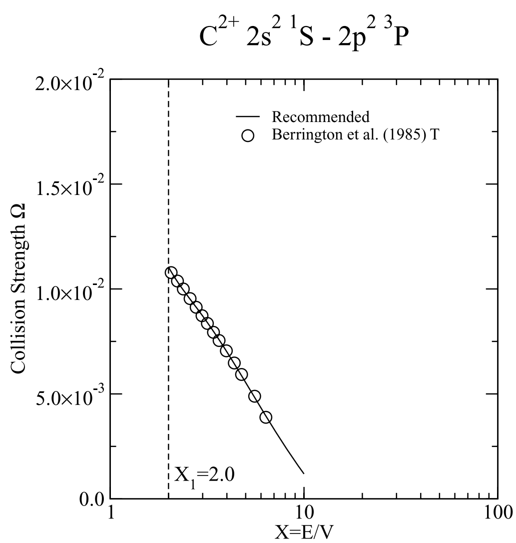

Graph 65: Collision strength for electron-impact excitation.

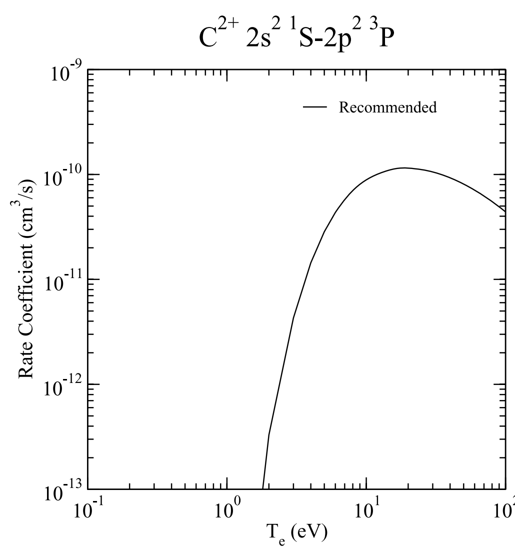

Graph 66: Rate coefficient for electron-impact excitation.

Graphs 1–124. (*continued*)

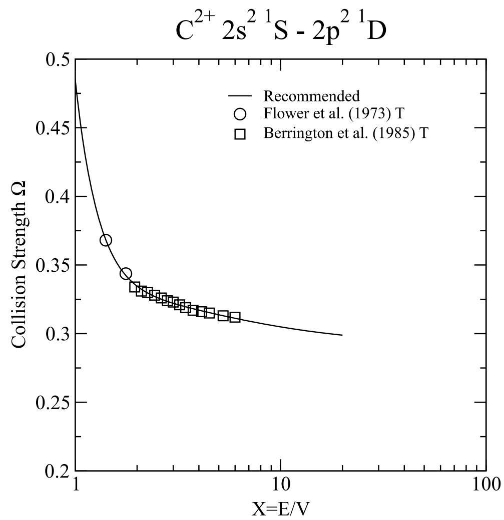

Graph 67: Collision strength for electron-impact excitation.

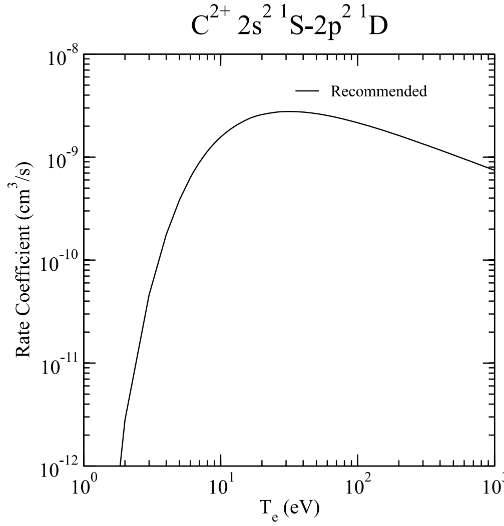

Graph 68: Rate coefficient for electron-impact excitation.

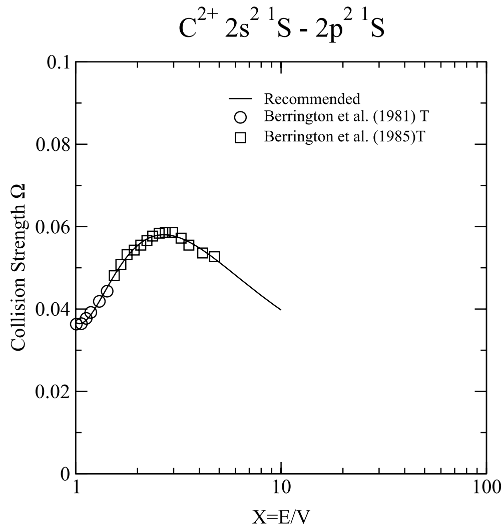

Graph 69: Collision strength for electron-impact excitation.

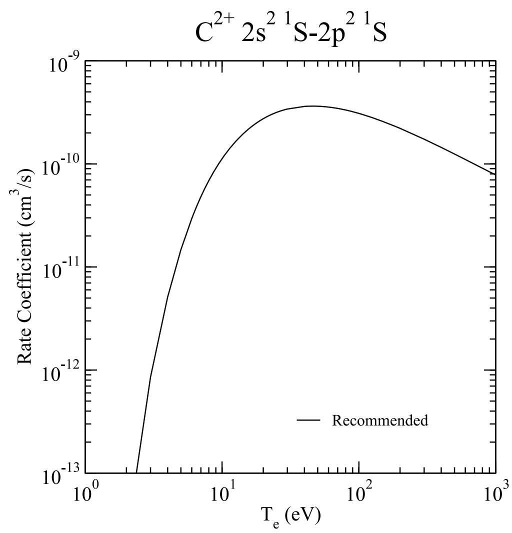

Graph 70: Rate coefficient for electron-impact excitation.

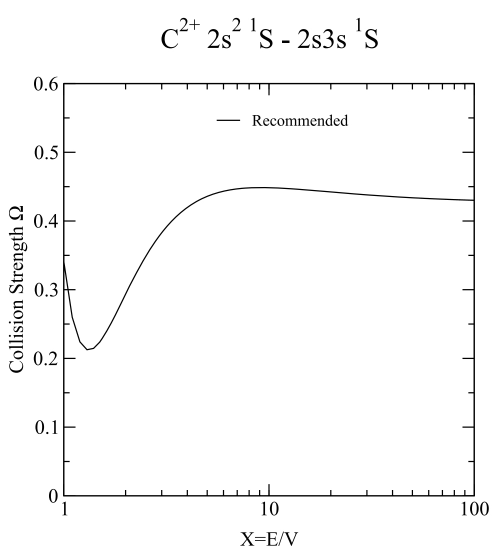

Graph 71: Collision strength for electron-impact excitation.

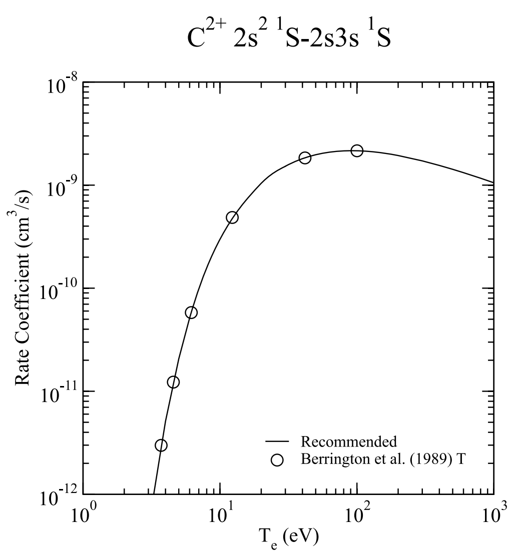

Graph 72: Rate coefficient for electron-impact excitation.

Graphs 1–124. (*continued*)

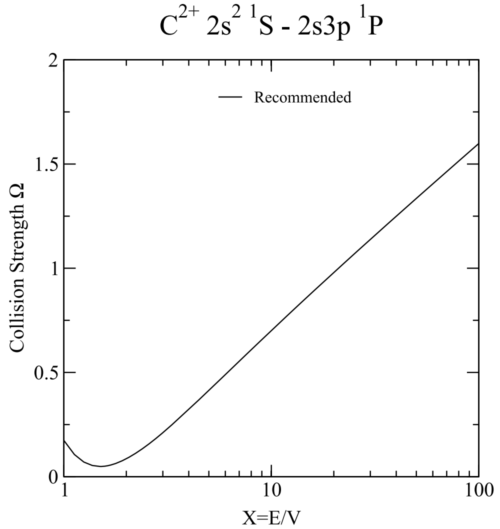

Graph 73: Collision strength for electron-impact excitation.

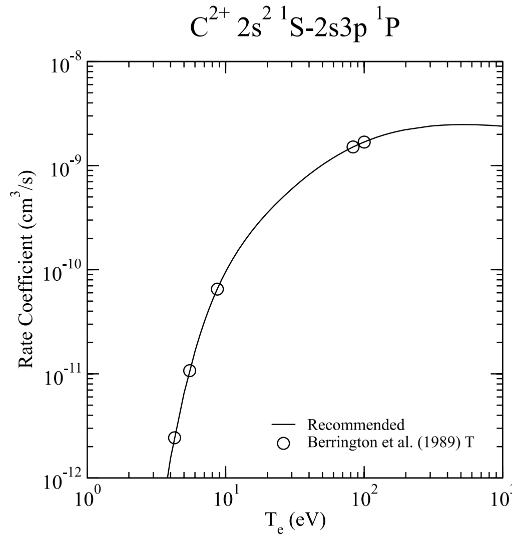

Graph 74: Rate coefficient for electron-impact excitation.

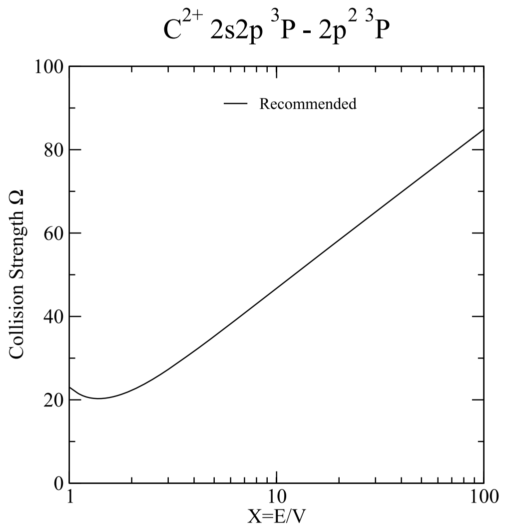

Graph 75: Collision strength for electron-impact excitation.

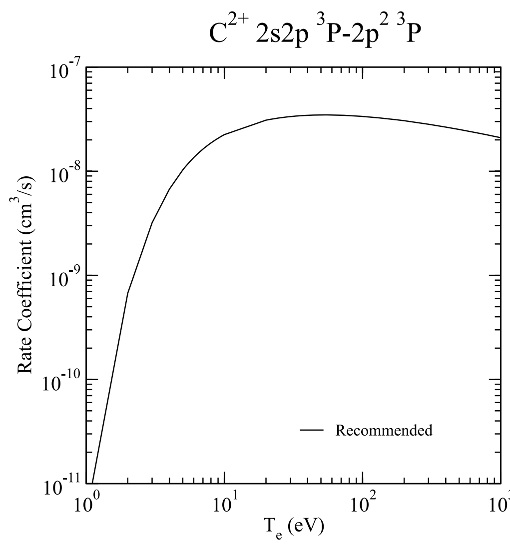

Graph 76: Rate coefficient for electron-impact excitation.

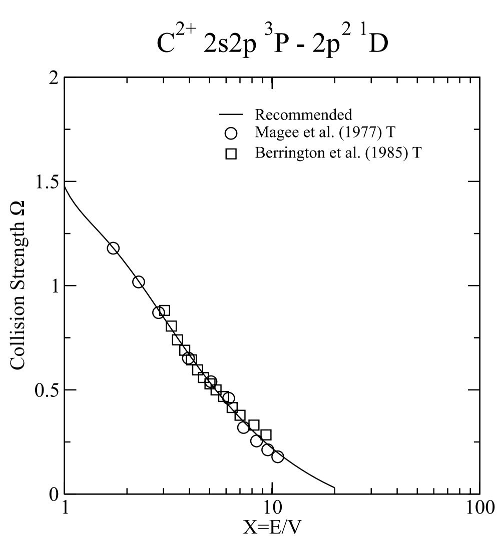

Graph 77: Collision strength for electron-impact excitation.

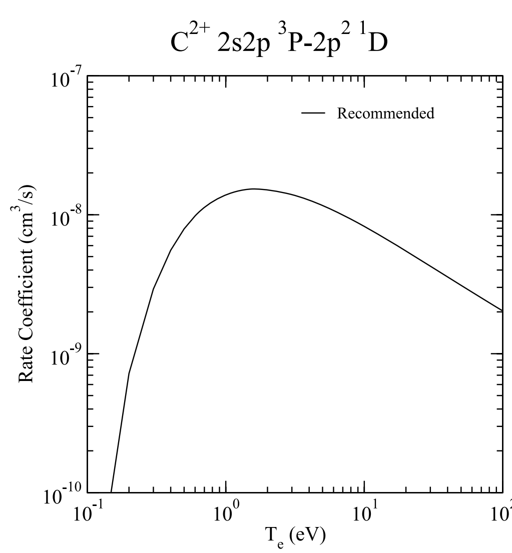

Graph 78: Rate coefficient for electron-impact excitation.

Graphs 1–124. (*continued*)

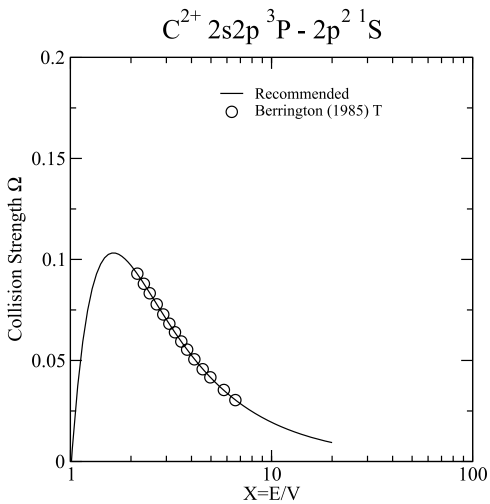

Graph 79: Collision strength for electron-impact excitation.

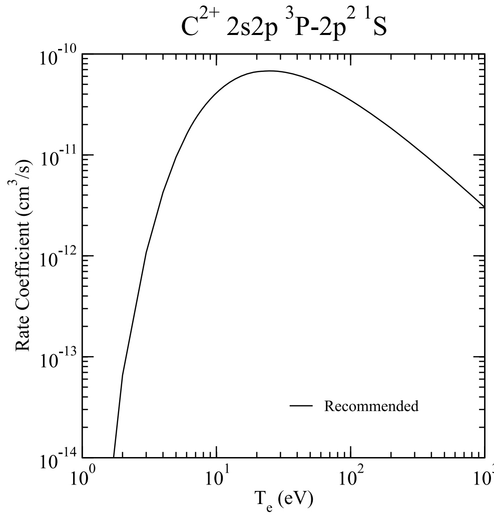

Graph 80: Rate coefficient for electron-impact excitation.

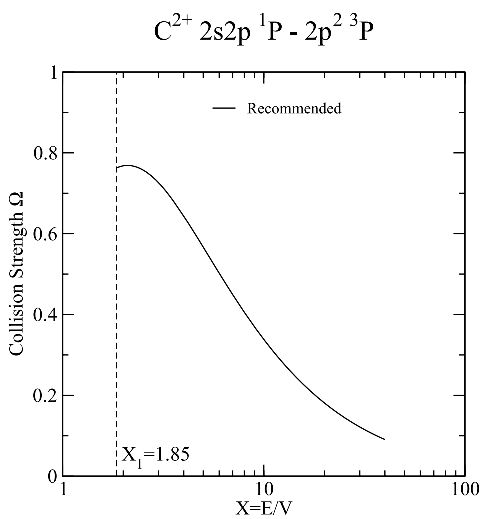

Graph 81: Collision strength for electron-impact excitation.

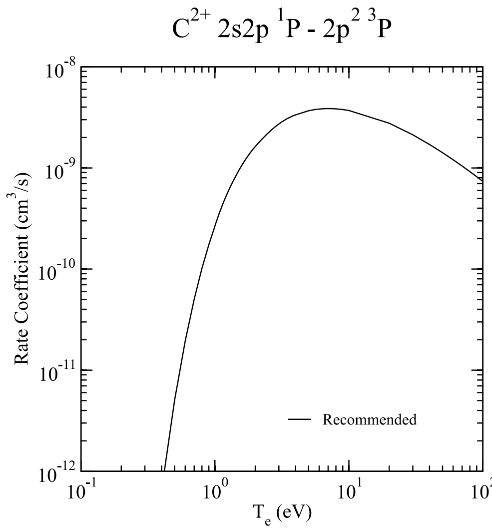

Graph 82: Rate coefficient for electron-impact excitation.

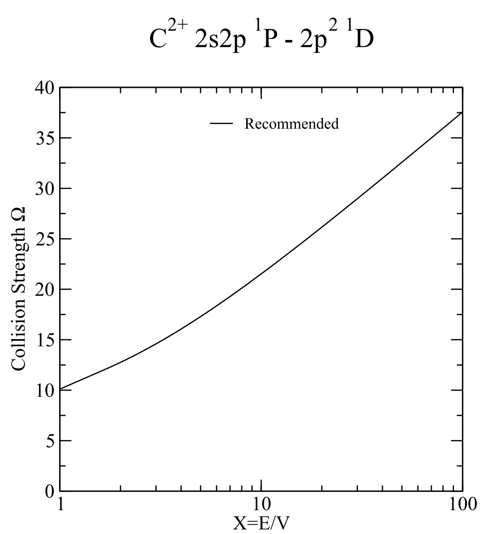

Graph 83: Collision strength for electron-impact excitation.

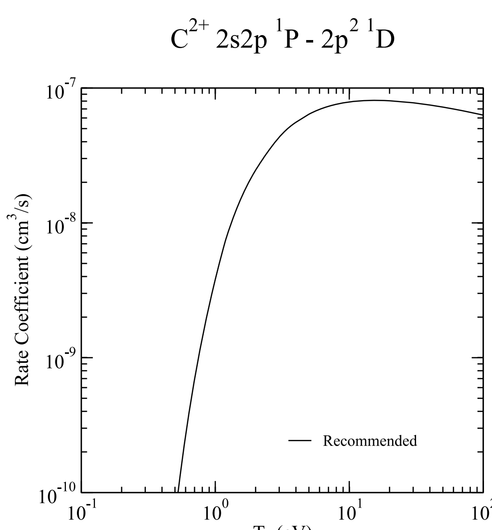

Graph 84: Rate coefficient for electron-impact excitation.

Graphs 1–124. (*continued*)

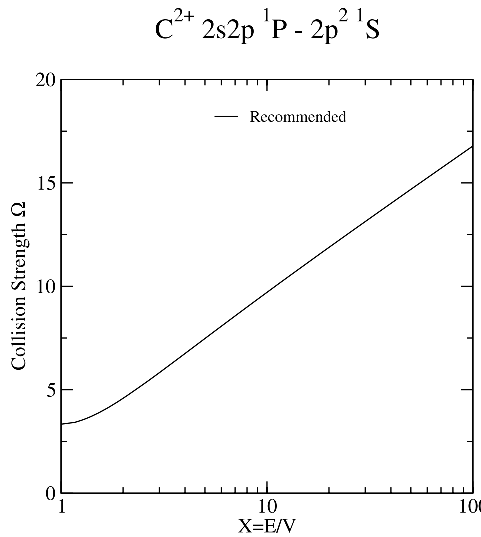

Graph 85: Collision strength for electron-impact excitation.

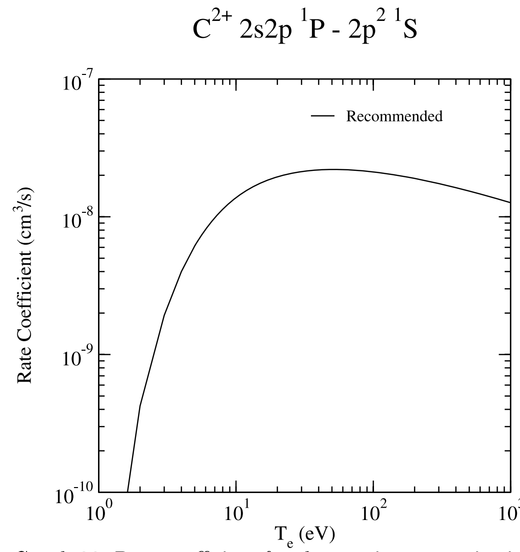

Graph 86: Rate coefficient for electron-impact excitation.

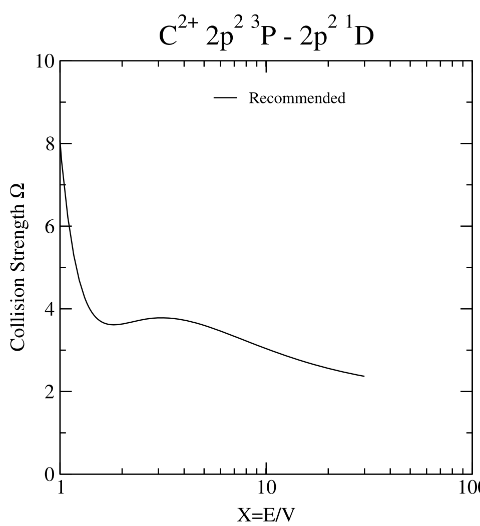

Graph 87: Collision strength for electron-impact excitation.

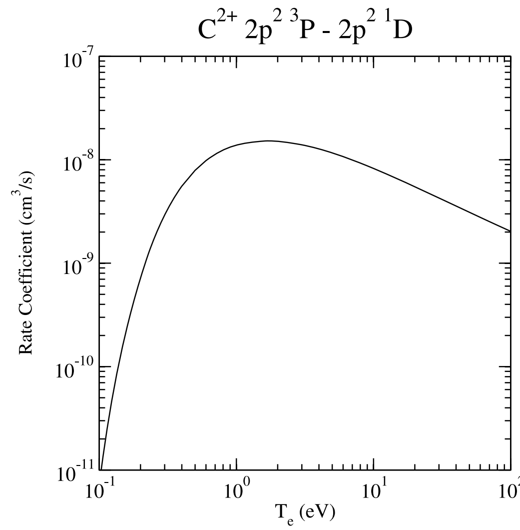

Graph 88: Rate coefficient for electron-impact excitation.

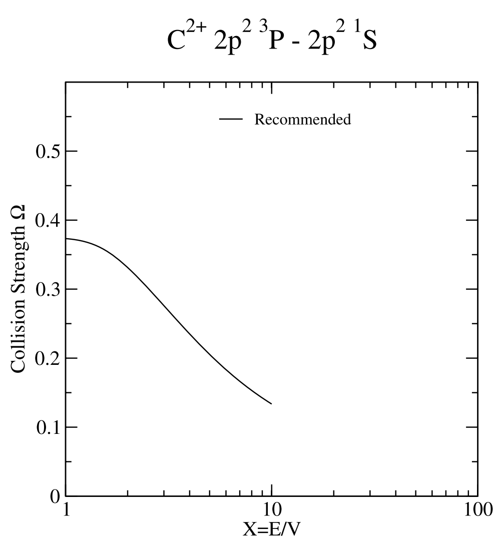

Graph 89: Collision strength for electron-impact excitation.

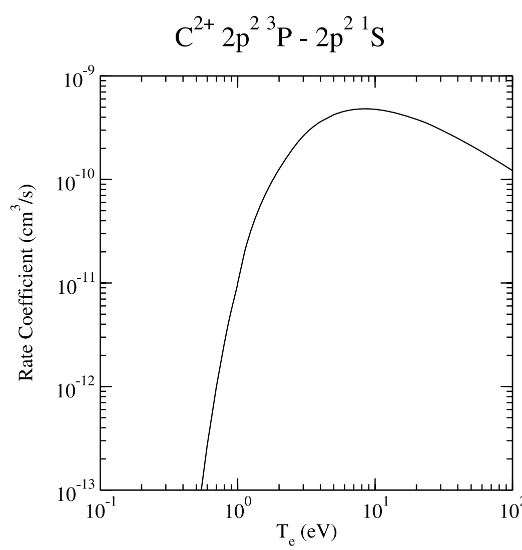

Graph 90: Rate coefficient for electron-impact excitation.

Graphs 1–124. (*continued*)

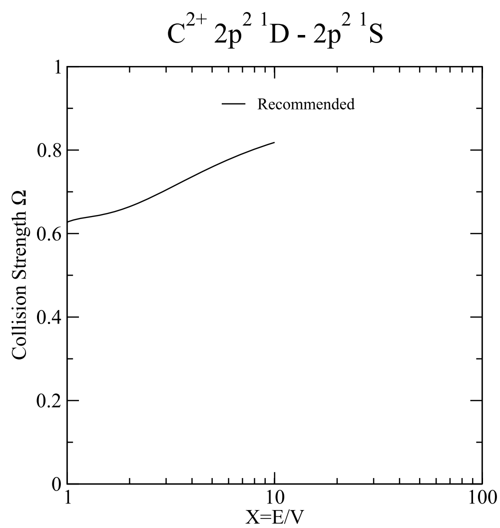

Graph 91: Collision strength for electron-impact excitation.

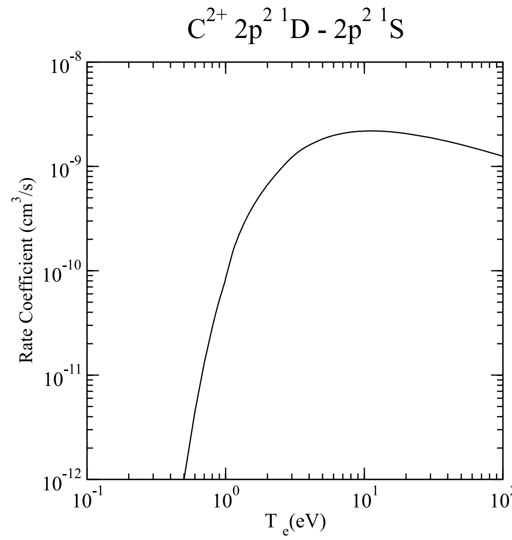

Graph 92: Rate coefficient for electron-impact excitation.

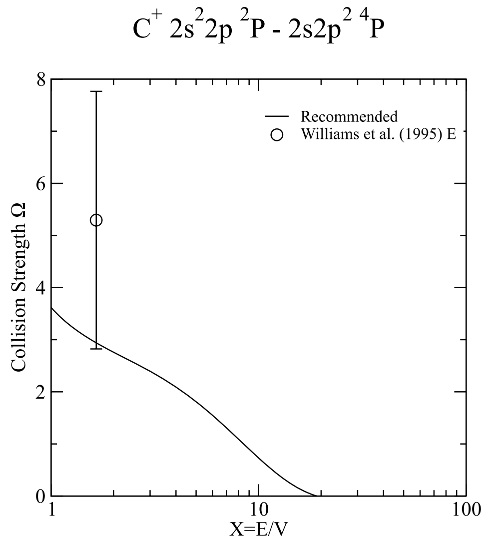

Graph 93: Collision strength for electron-impact excitation.

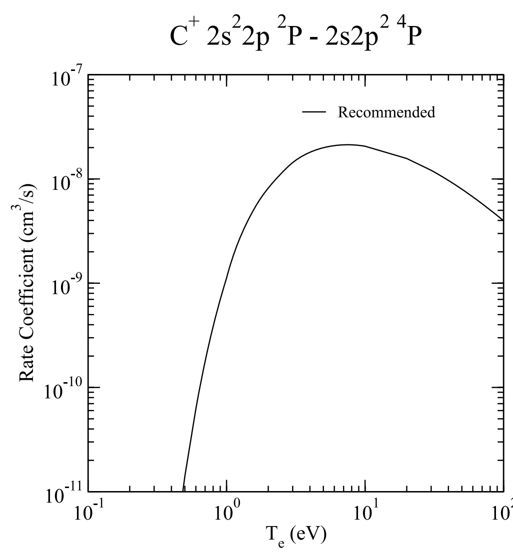

Graph 94: Rate coefficient for electron-impact excitation.

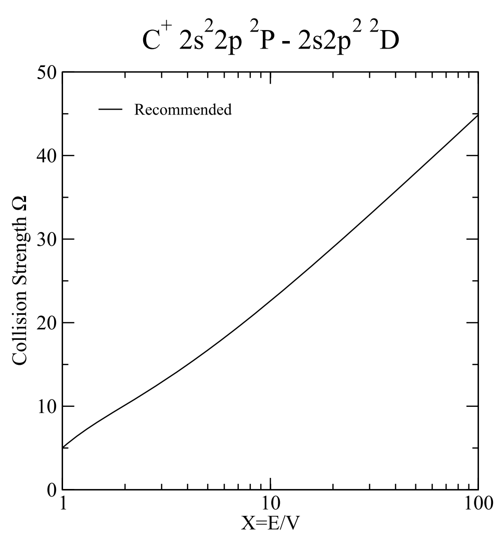

Graph 95: Collision strength for electron-impact excitation.

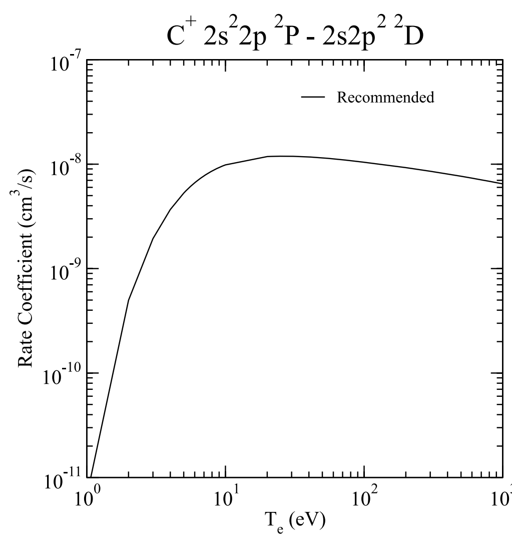

Graph 96: Rate coefficient for electron-impact excitation.

Graphs 1–124. (*continued*)

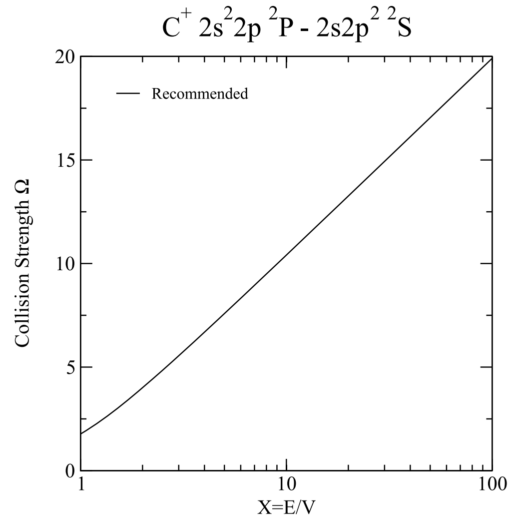

Graph 97: Collision strength for electron-impact excitation.

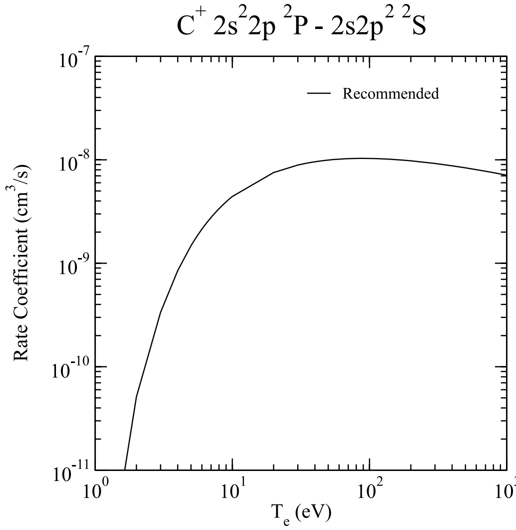

Graph 98: Rate coefficient for electron-impact excitation.

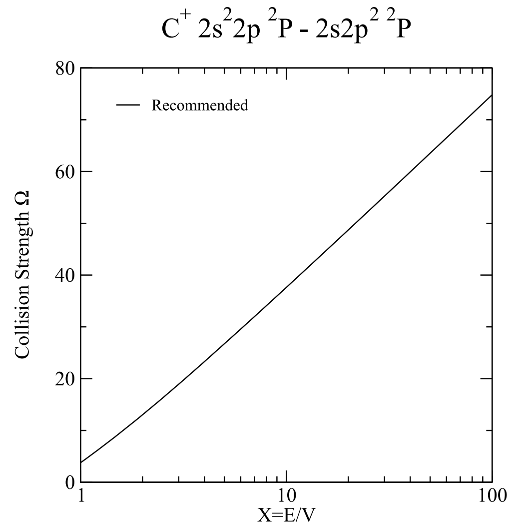

Graph 99: Collision strength for electron-impact excitation.

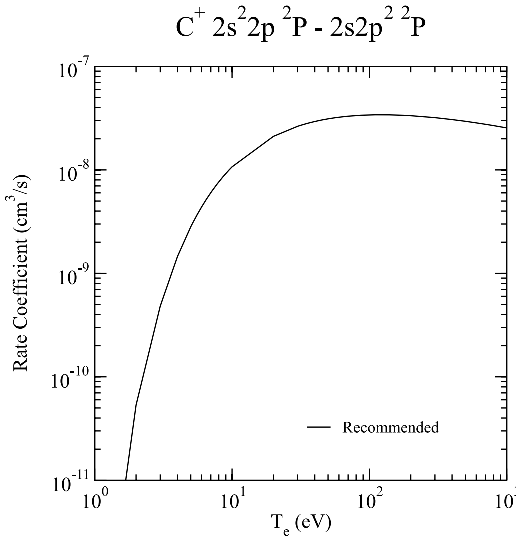

Graph 100: Rate coefficient for electron-impact excitation.

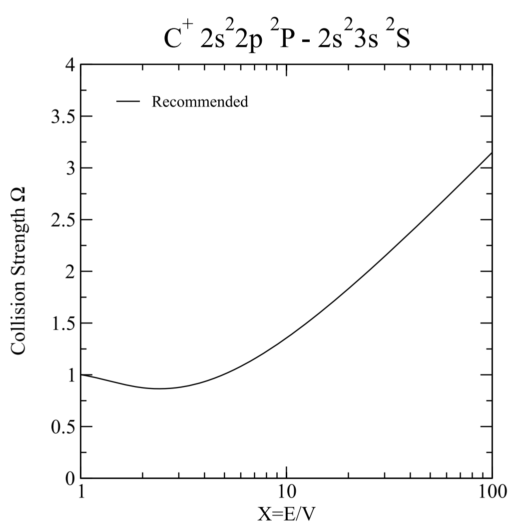

Graph 101: Collision strength for electron-impact excitation.

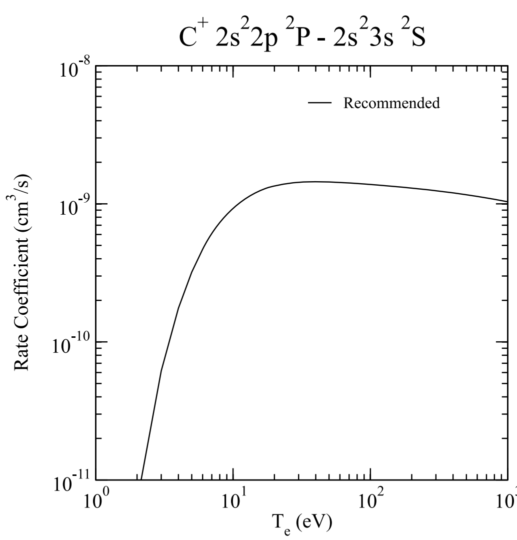

Graph 102: Rate coefficient for electron-impact excitation.

Graphs 1–124. (*continued*)

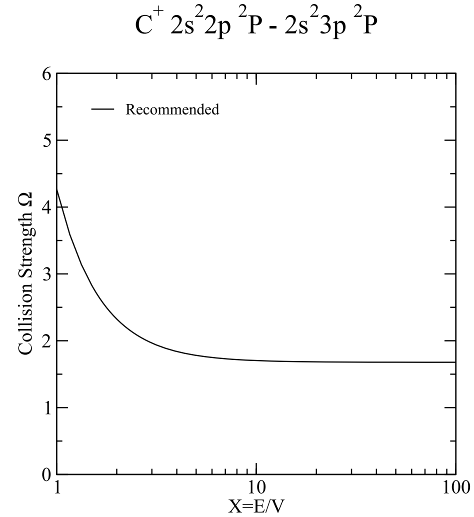

Graph 103: Collision strength for electron-impact excitation.

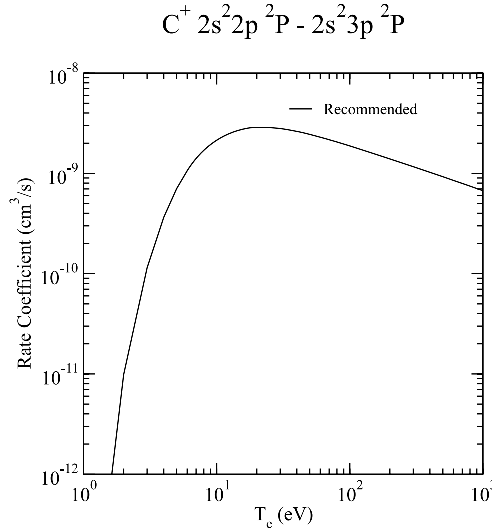

Graph 104: Rate coefficient for electron-impact excitation.

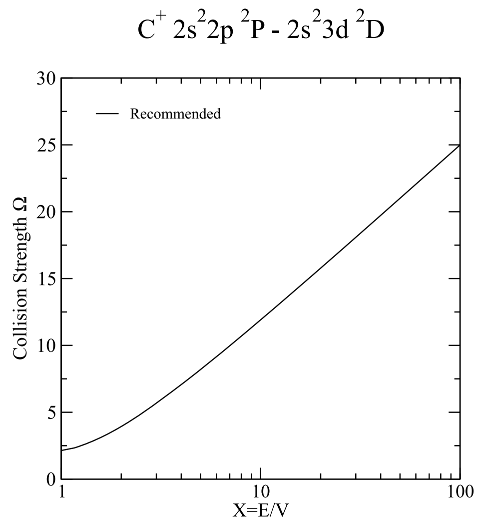

Graph 105: Collision strength for electron-impact excitation.

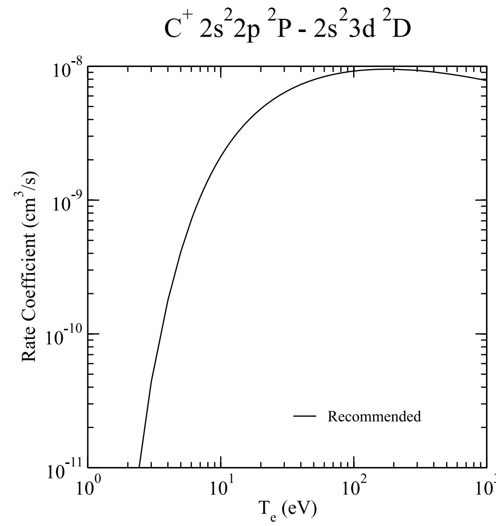

Graph 106: Rate coefficient for electron-impact excitation.

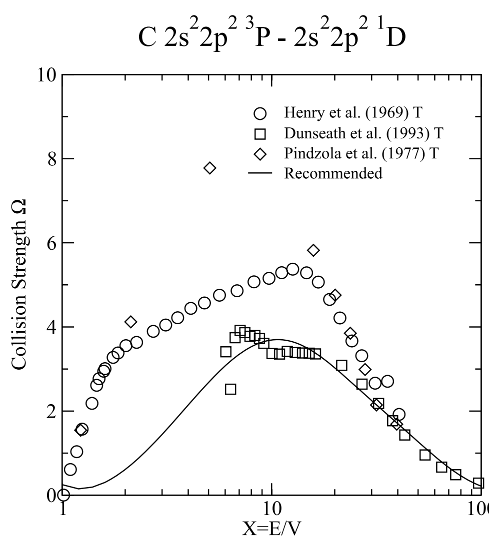

Graph 107: Collision strength for electron-impact excitation.

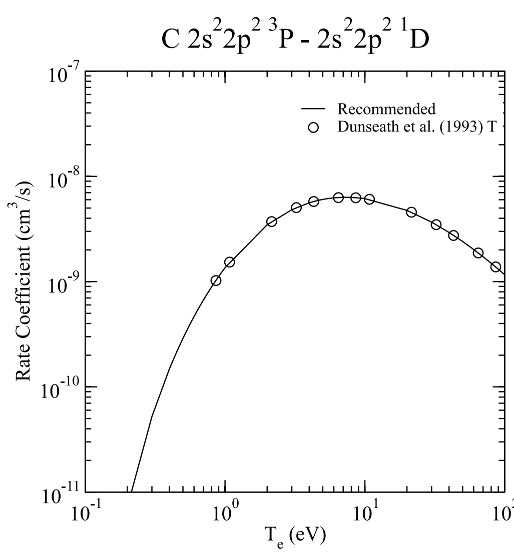

Graph 108: Rate coefficient for electron-impact excitation.

Graphs 1–124. (*continued*)

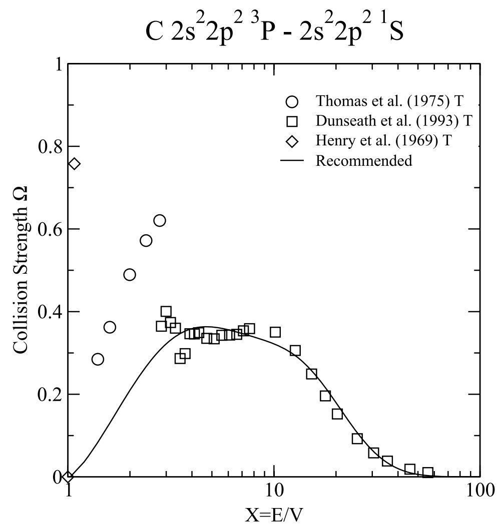

Graph 109: Collision strength for electron-impact excitation.

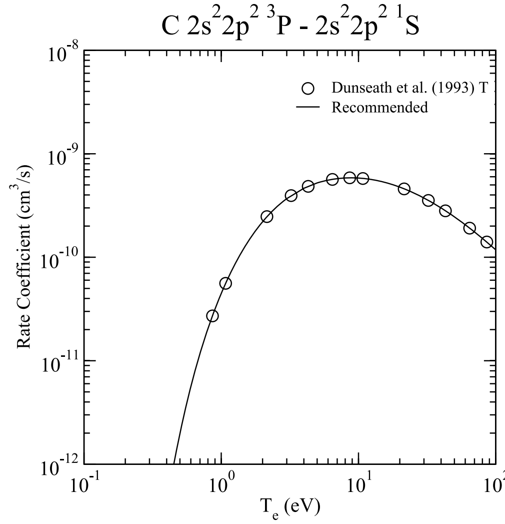

Graph 110: Rate coefficient for electron-impact excitation.

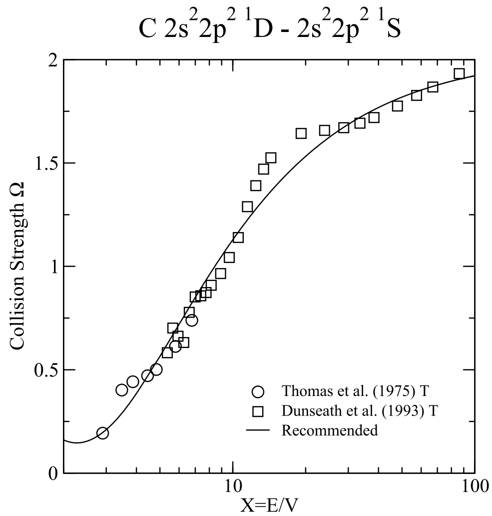

Graph 111: Collision strength for electron-impact excitation.

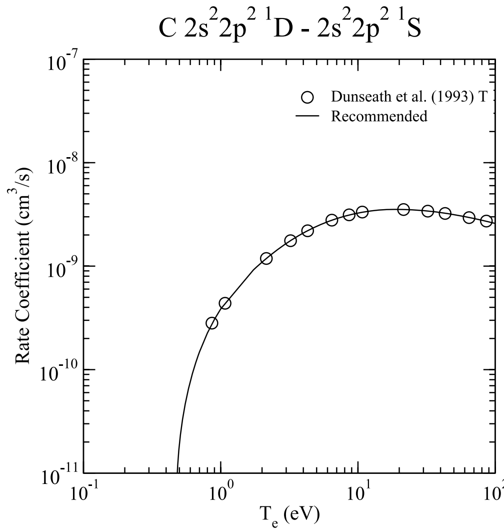

Graph 112: Rate coefficient for electron-impact excitation.

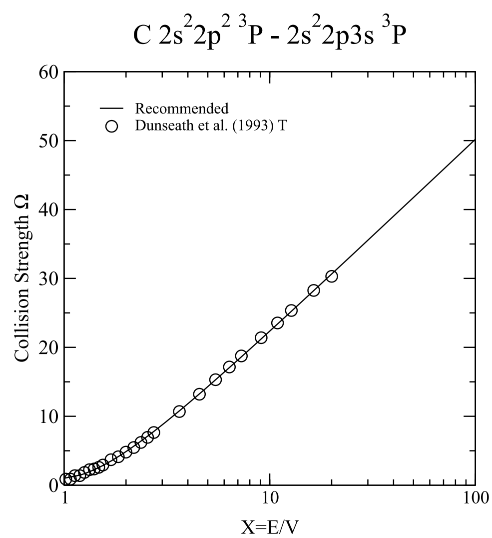

Graph 113: Collision strength for electron-impact excitation.

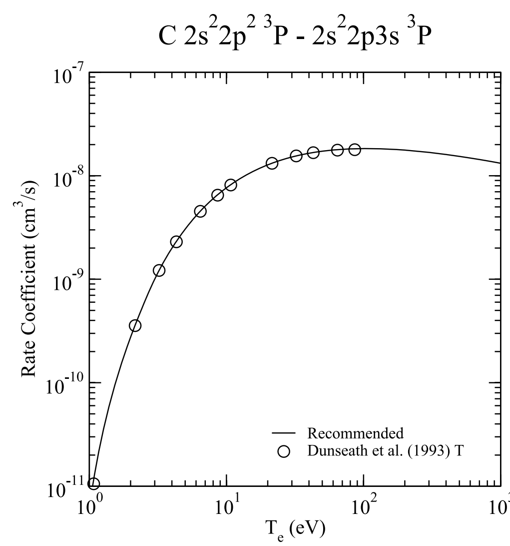

Graph 114: Rate coefficient for electron-impact excitation.

Graphs 1–124. (*continued*)

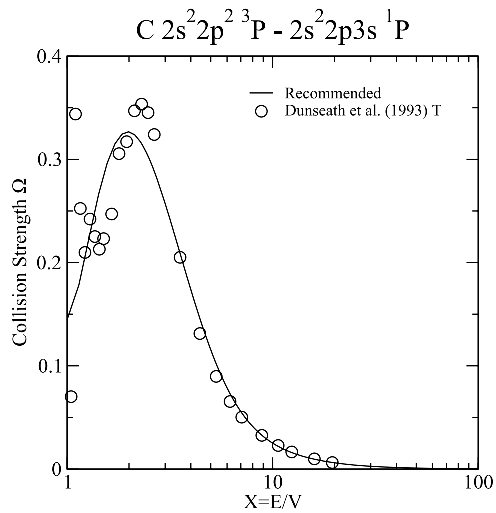

Graph 115: Collision strength for electron-impact excitation.

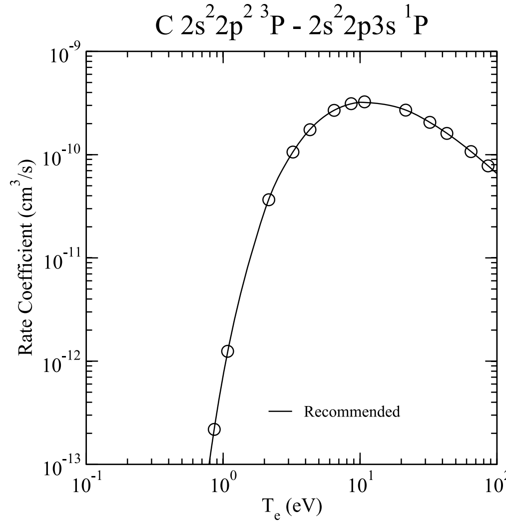

Graph 116: Rate coefficient for electron-impact excitation.

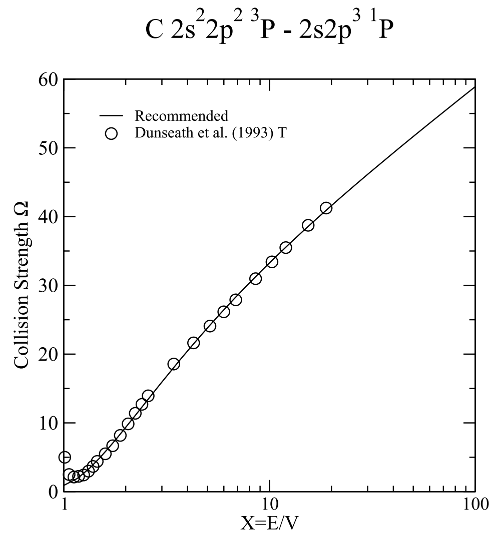

Graph 117: Collision strength for electron-impact excitation.

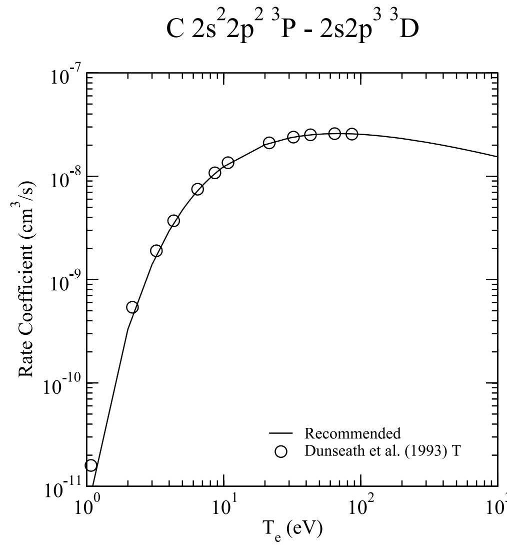

Graph 118: Rate coefficient for electron-impact excitation.

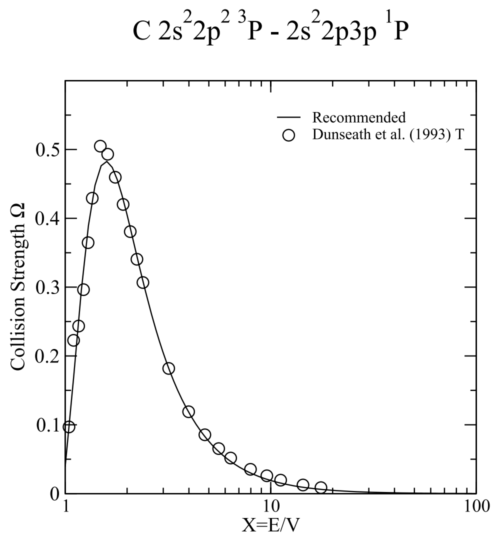

Graph 119: Collision strength for electron-impact excitation.

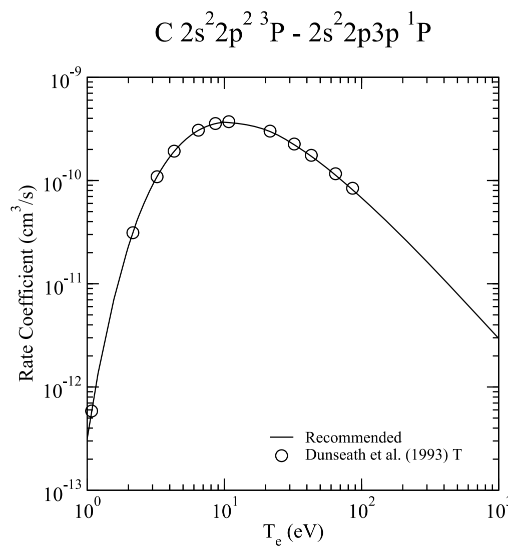

Graph 120: Rate coefficient for electron-impact excitation.

Graphs 1–124. (*continued*)

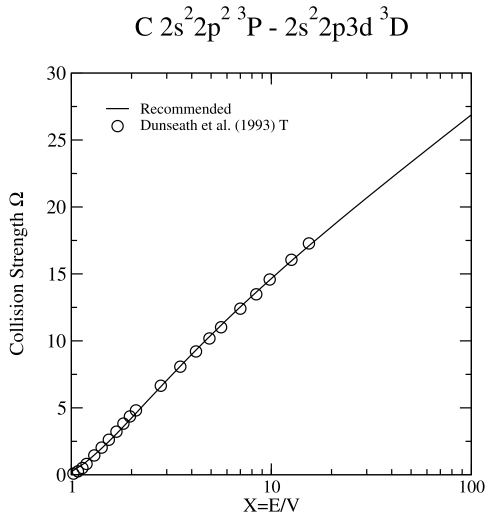

Graph 121: Collision strength for electron-impact excitation.

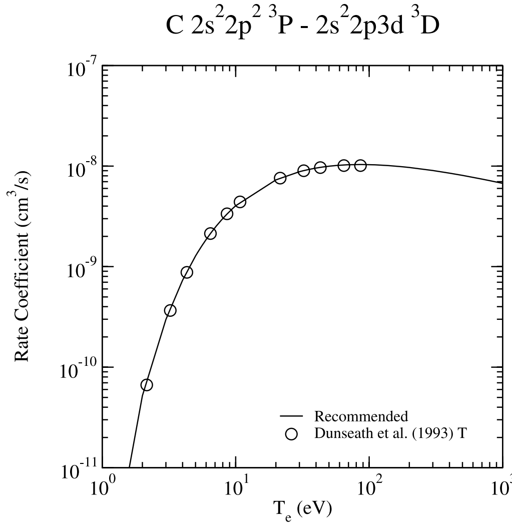

Graph 122: Rate coefficient for electron-impact excitation.

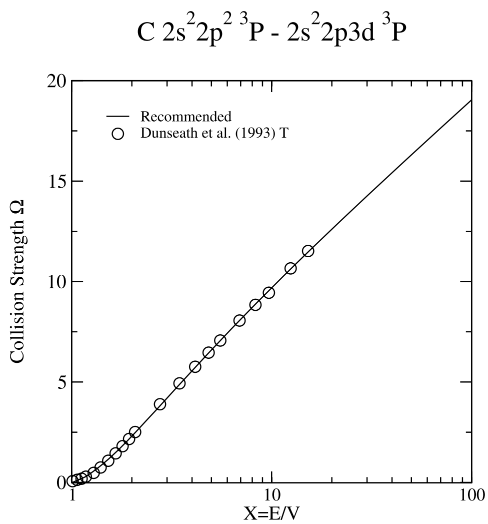

Graph 123: Collision strength for electron-impact excitation.

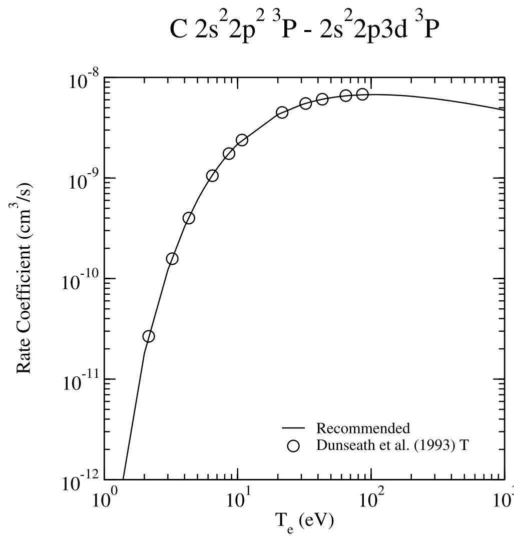

Graph 124: Rate coefficient for electron-impact excitation.

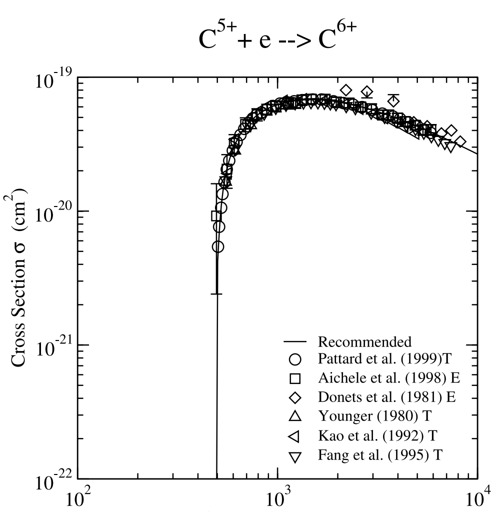

Graph 125: Cross section for electron-impact ionization.

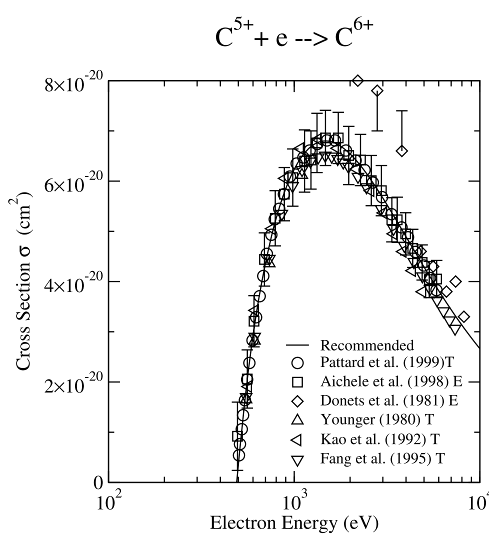

Graph 126: Same as previous Graph, but with the linear scale for the vertical axis.

Graphs 125–138. Recommended electron-impact ionization cross sections. See page 416 for Explanation of Graphs.

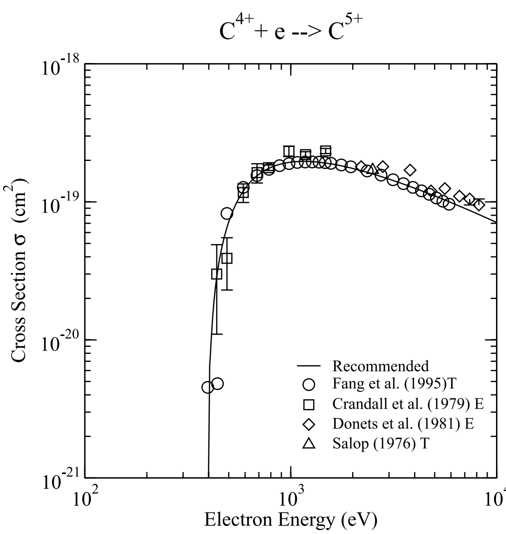

Graph 127: Cross section for electron-impact ionization.

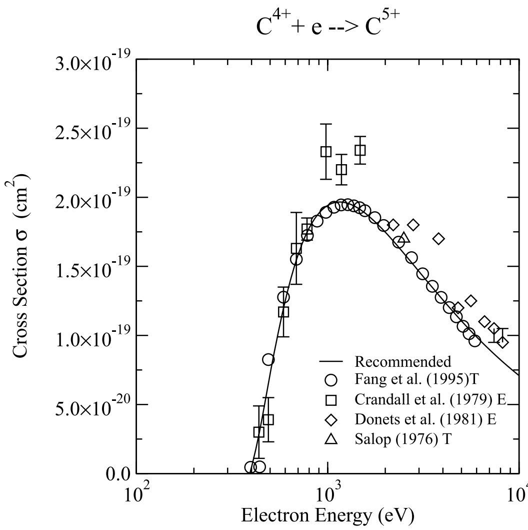

Graph 128: Same as previous Graph, but with the linear scale for the vertical axis.

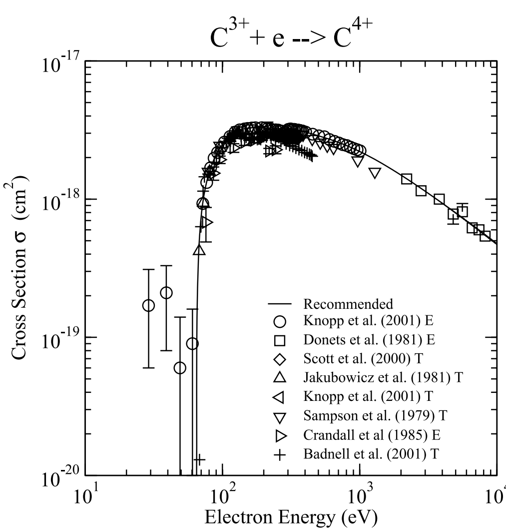

Graph 129: Cross section for electron-impact ionization.

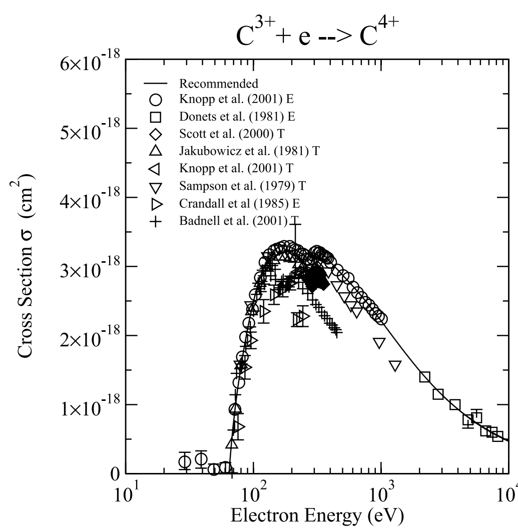

Graph 130: Same as previous Graph, but with the linear scale for the vertical axis.

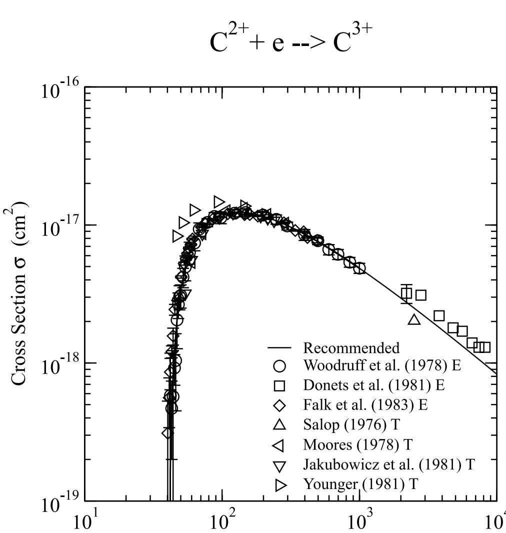

Graph 131: Cross section for electron-impact ionization.

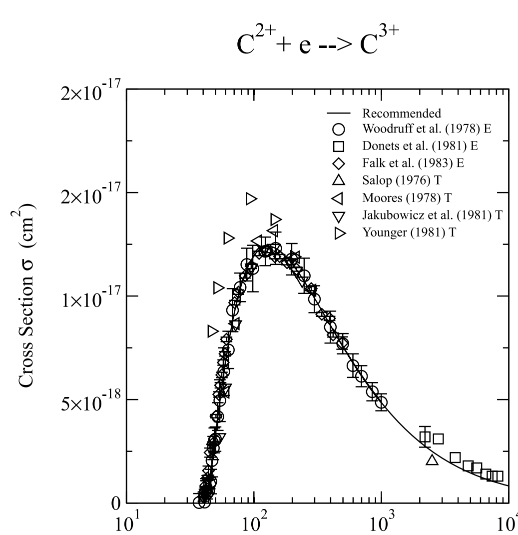

Graph 132: Same as previous Graph, but with the linear scale for the vertical axis.

Graphs 125–138. (*continued*)

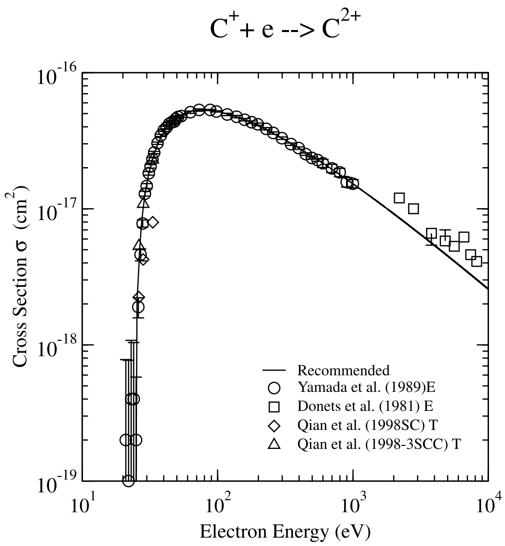

Graph 133: Cross section for electron-impact ionization.

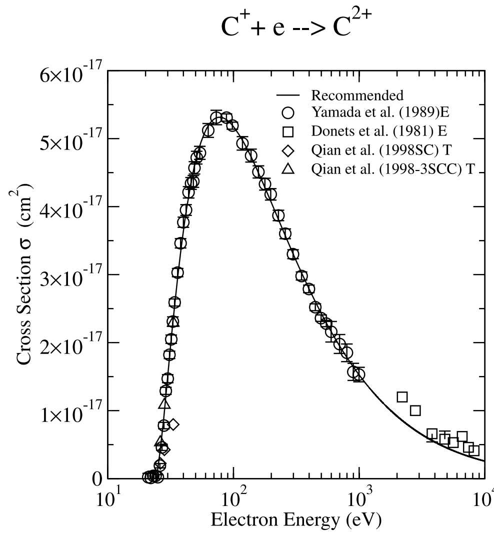

Graph 134: Same as previous Graph, but with the linear scale for the vertical axis.

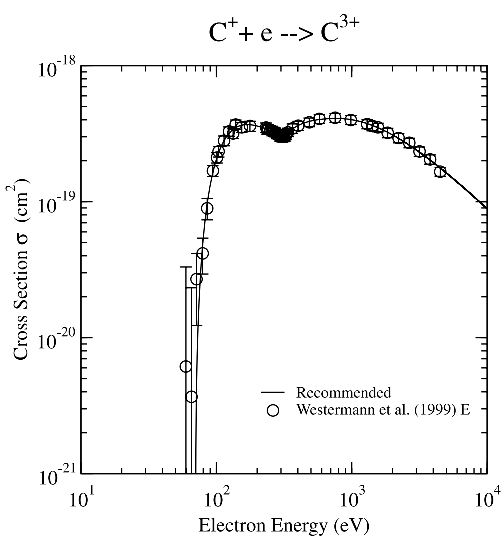

Graph 135: Cross section for electron-impact ionization.

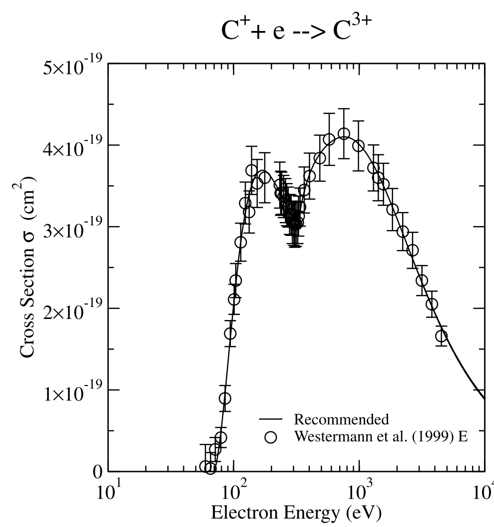

Graph 136: Same as previous Graph, but with the linear scale for the vertical axis.

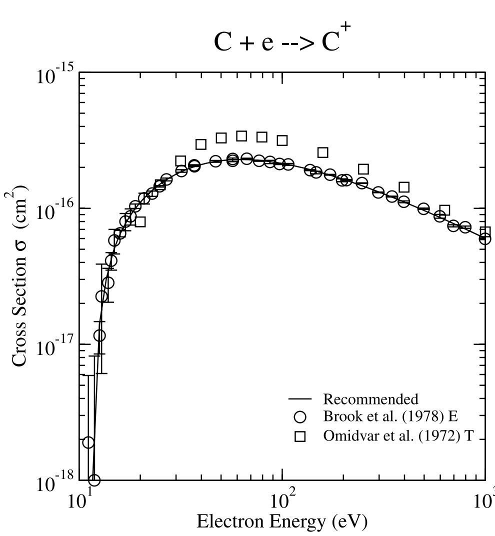

Graph 137: Cross section for electron-impact ionization.

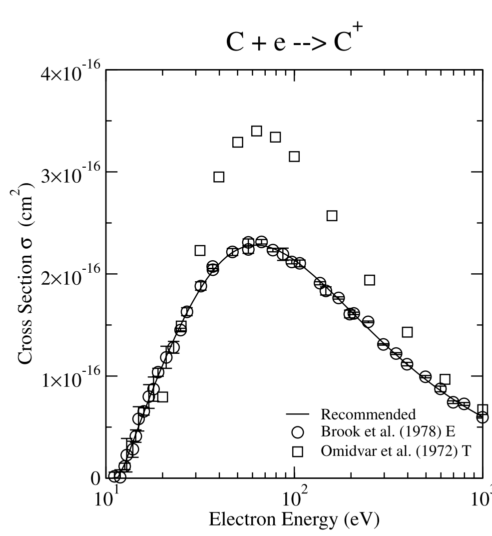

Graph 138: Same as previous Graph, but with the linear scale for the vertical axis.

Graphs 125–138. (*continued*)

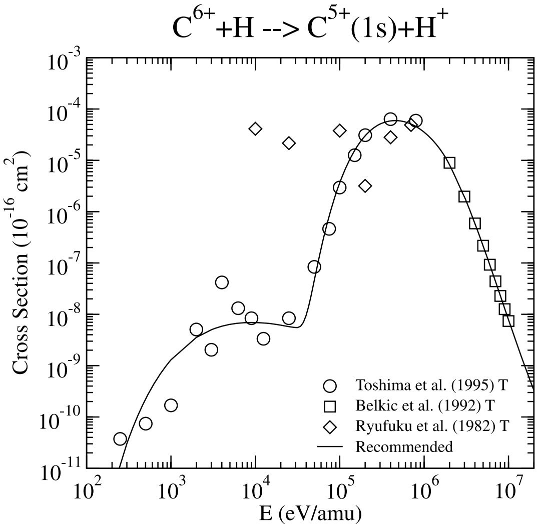

Graph 139: Cross section for charge exchange.

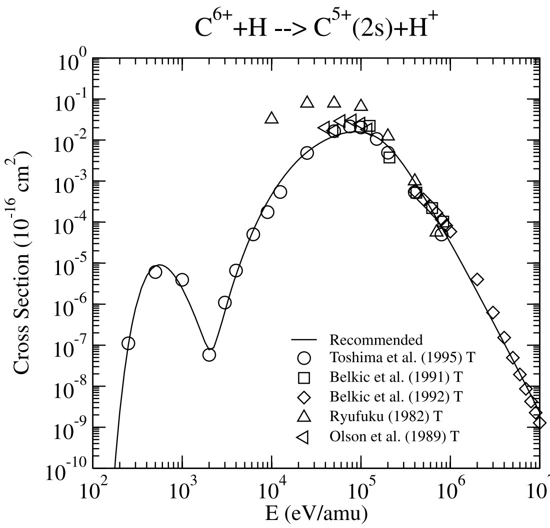

Graph 140: Cross section for charge exchange.

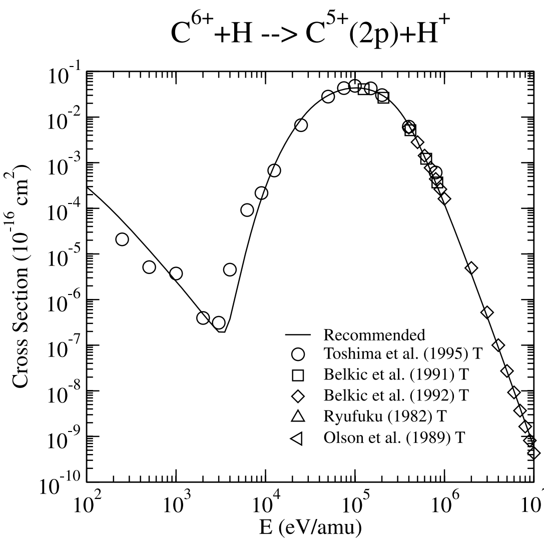

Graph 141: Cross section for charge exchange.

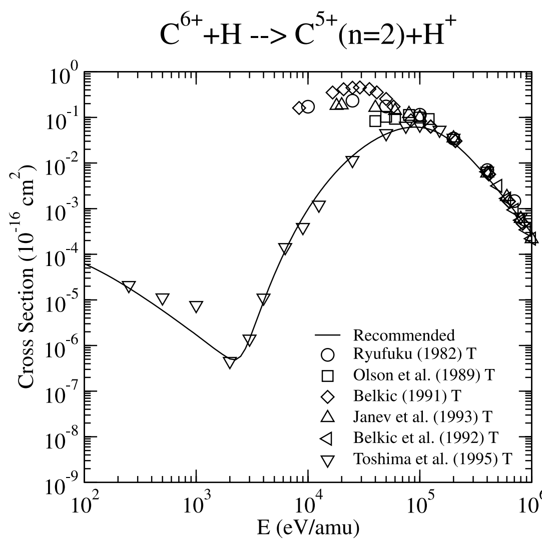

Graph 142: Cross section for charge exchange.

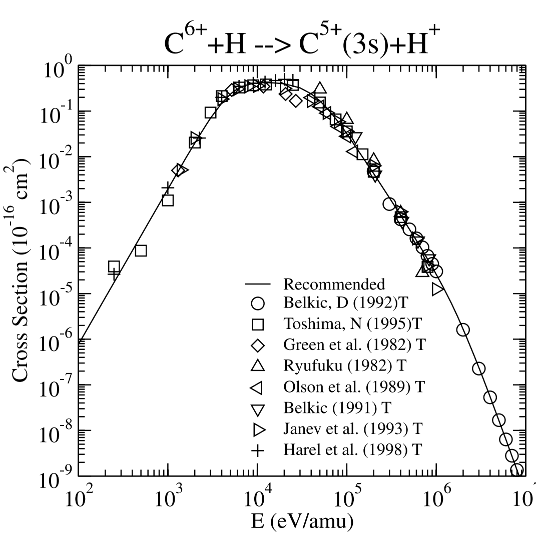

Graph 143: Cross section for charge exchange.

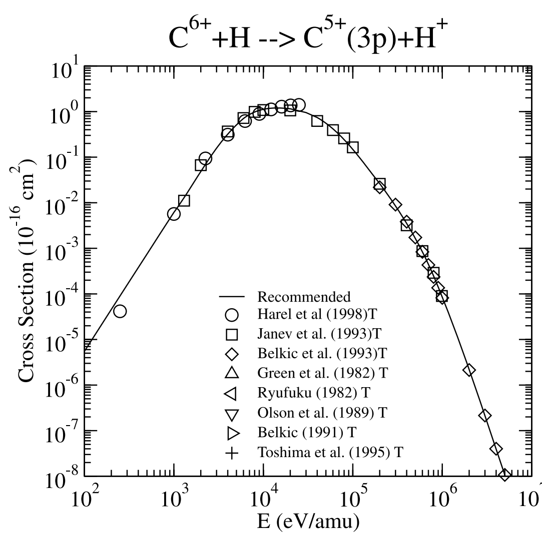

Graph 144: Cross section for charge exchange.

Graphs 139–175. Recommended charge exchange cross sections. See page 416 for Explanation of Graphs.

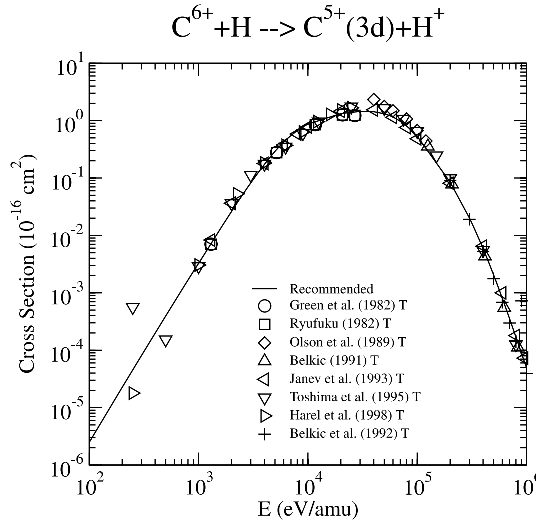

Graph 145: Cross section for charge exchange.

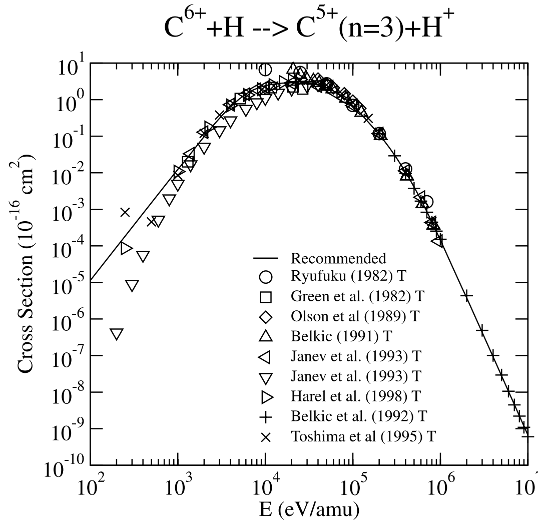

Graph 146: Cross section for charge exchange.

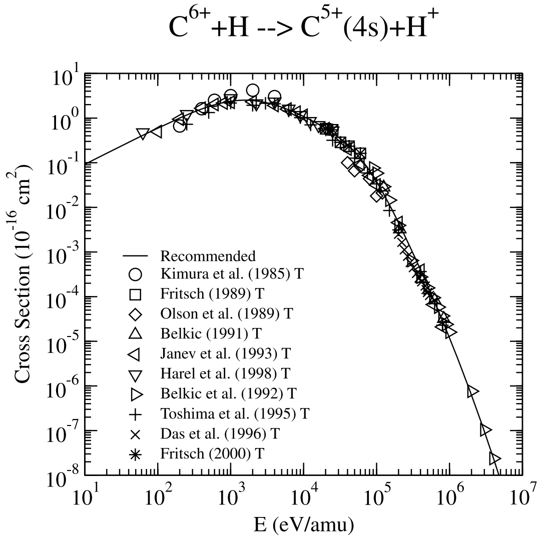

Graph 147: Cross section for charge exchange.

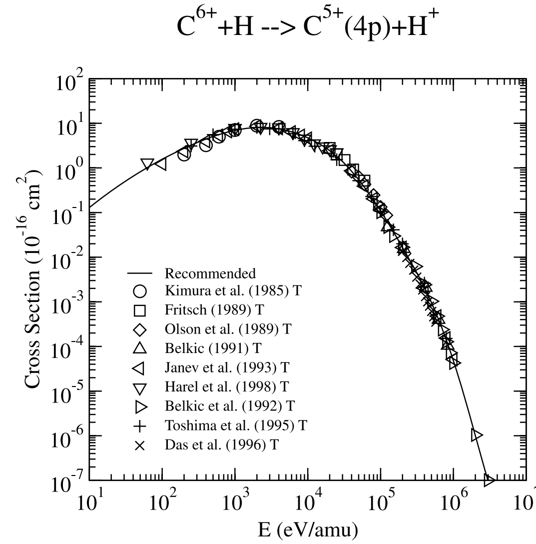

Graph 148: Cross section for charge exchange.

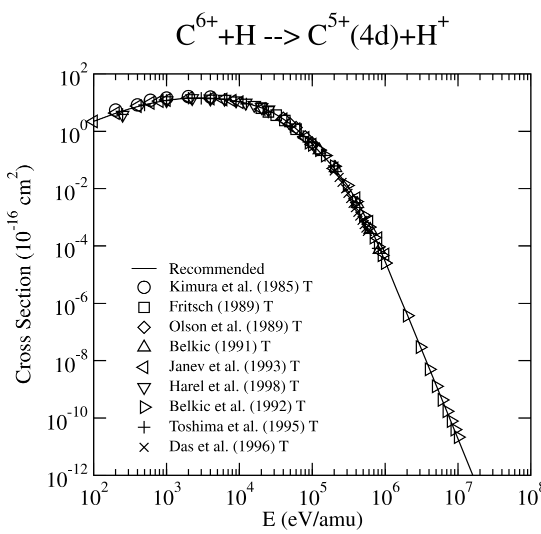

Graph 149: Cross section for charge exchange.

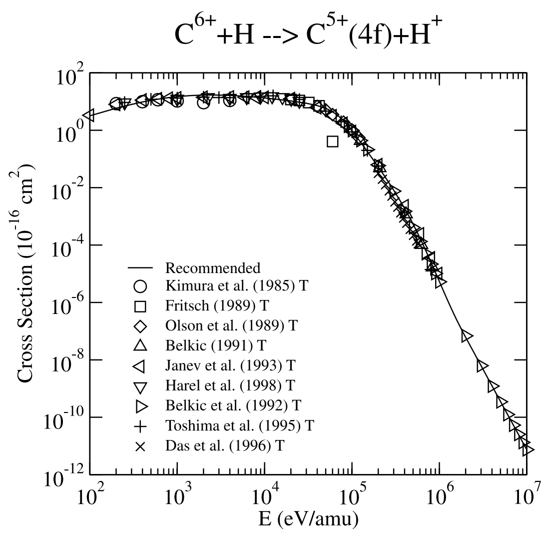

Graph 150: Cross section for charge exchange.

Graphs 139–175. (*continued*)

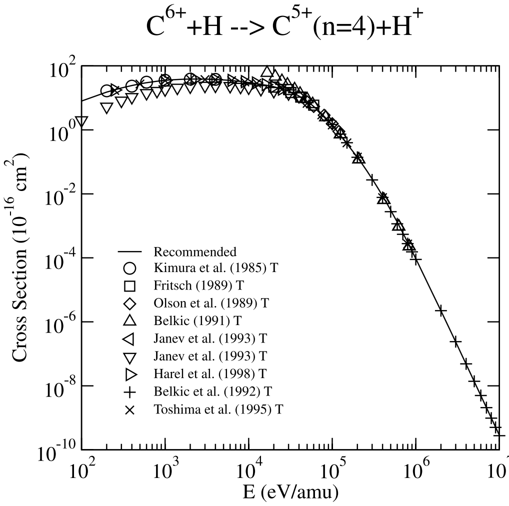

Graph 151: Cross section for charge exchange.

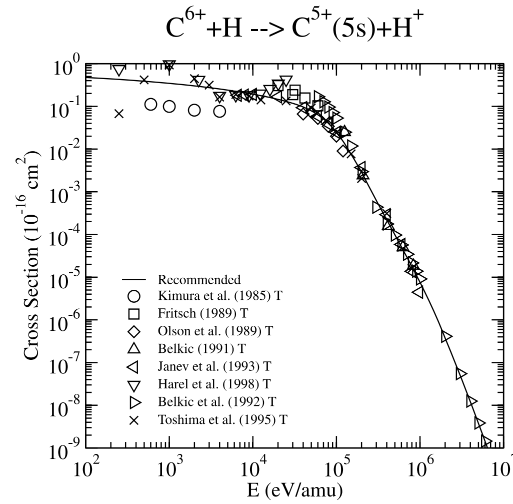

Graph 152: Cross section for charge exchange.

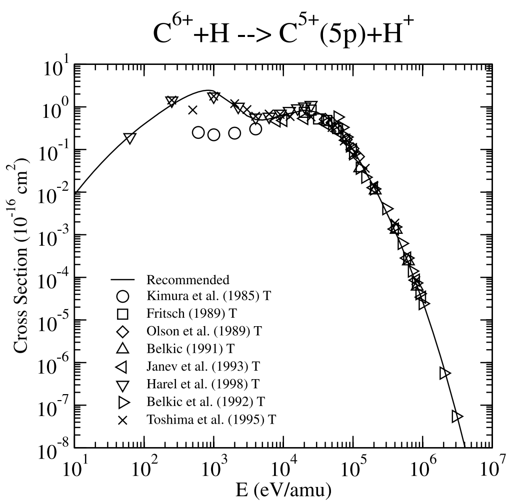

Graph 153: Cross section for charge exchange.

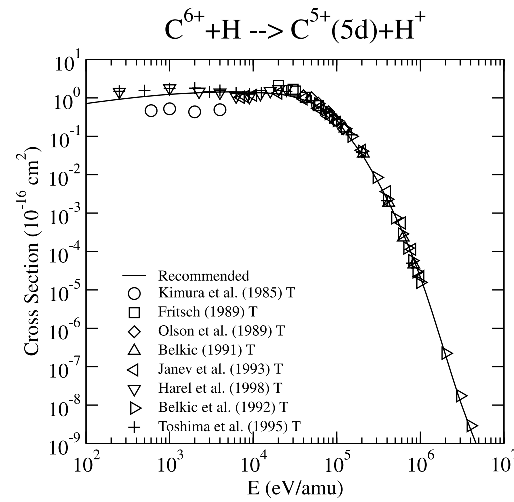

Graph 154: Cross section for charge exchange.

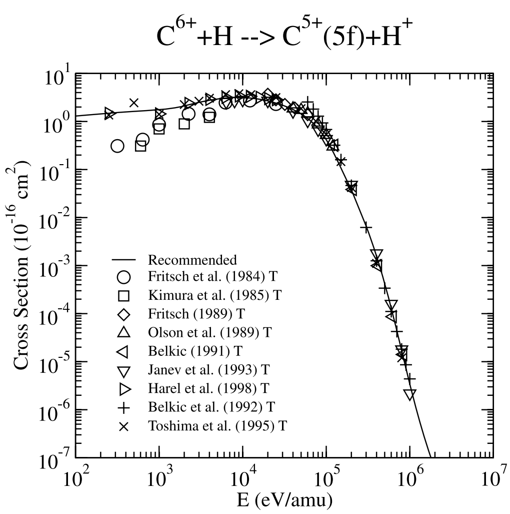

Graph 155: Cross section for charge exchange.

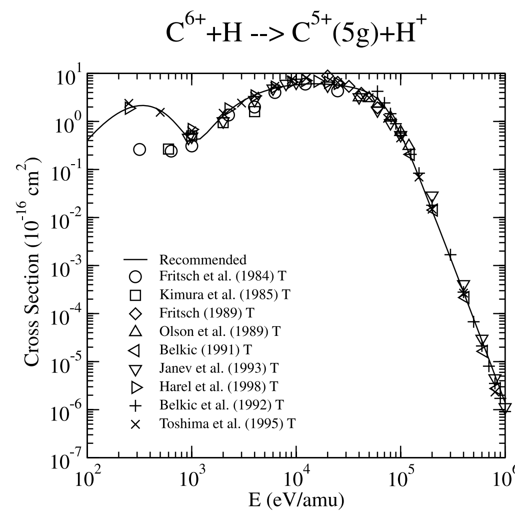

Graph 156: Cross section for charge exchange.

Graphs 139–175. (*continued*)

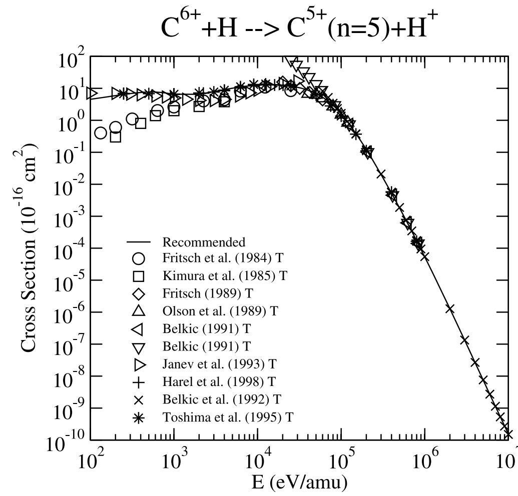

Graph 157: Cross section for charge exchange.

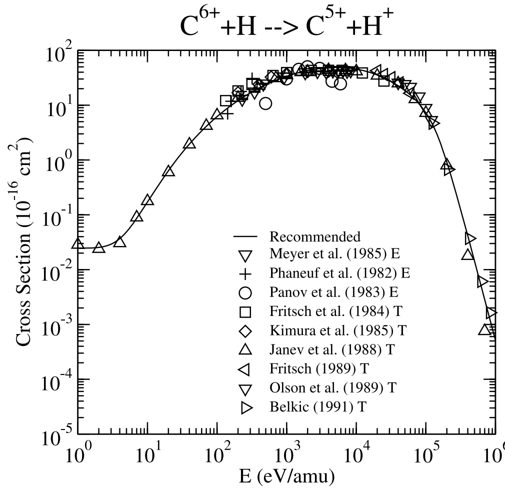

Graph 158: Cross section for charge exchange.

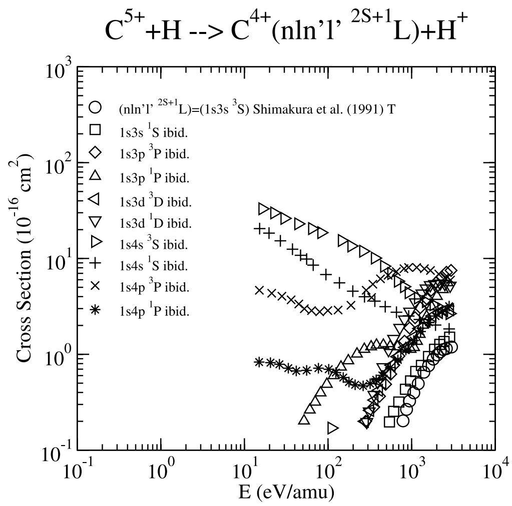

Graph 159: Cross section for charge exchange.

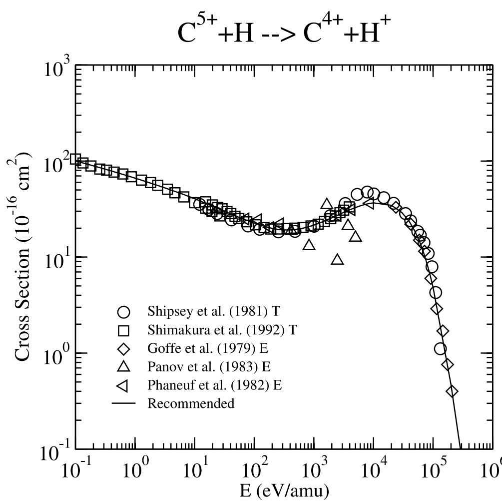

Graph 160: Cross section for charge exchange.

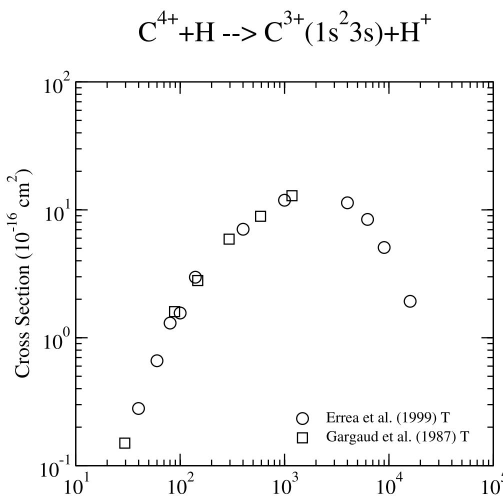

Graph 161: Cross section for charge exchange.

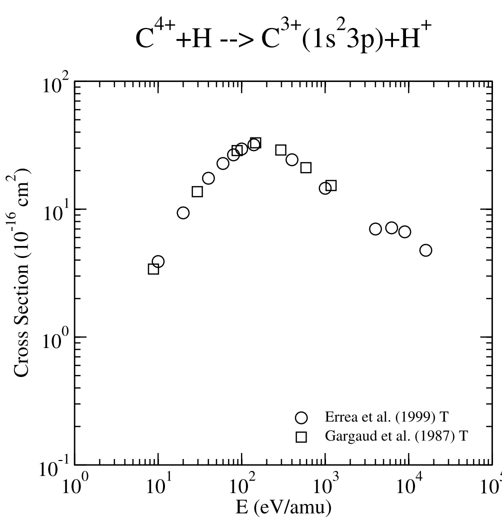

Graph 162: Cross section for charge exchange.

Graphs 139–175. (*continued*)

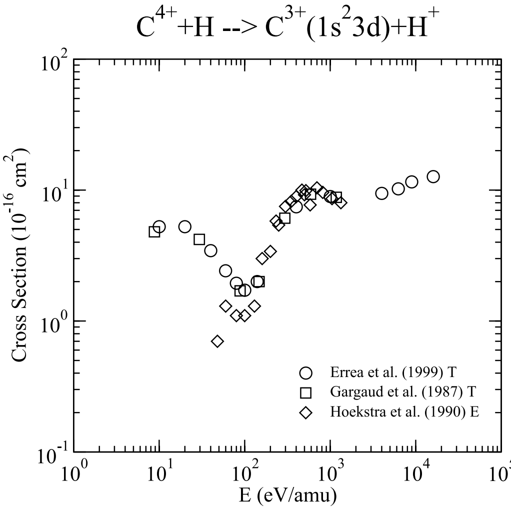

Graph 163: Cross section for charge exchange.

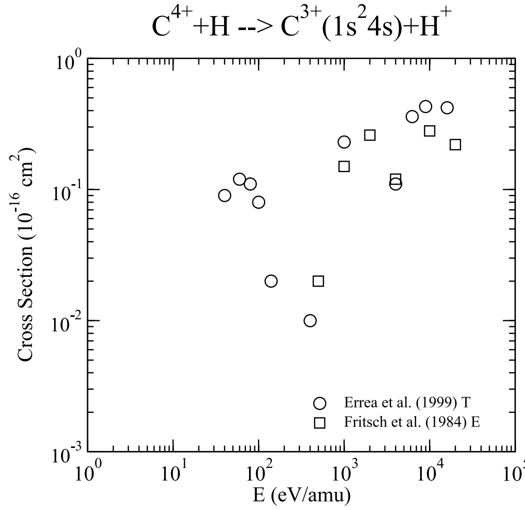

Graph 164: Cross section for charge exchange.

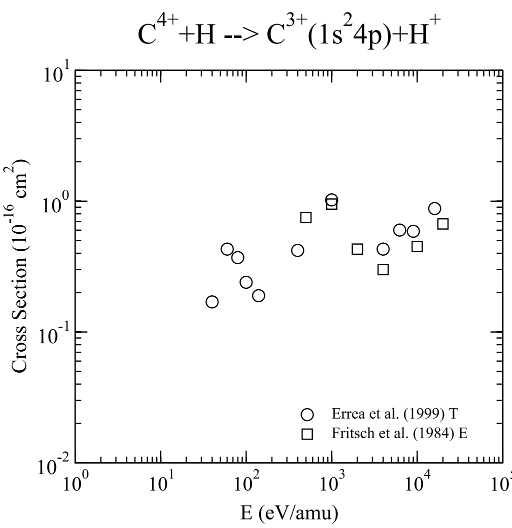

Graph 165: Cross section for charge exchange.

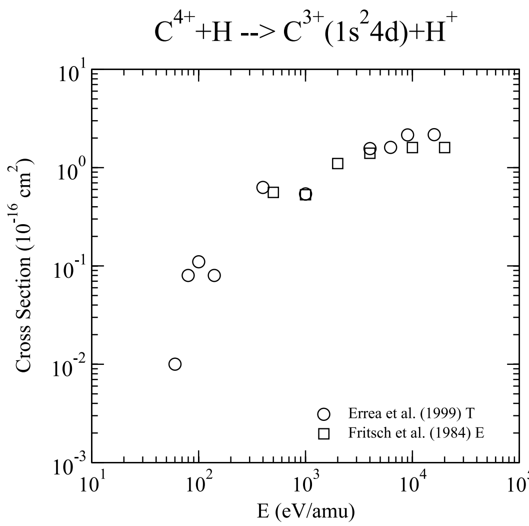

Graph 166: Cross section for charge exchange.

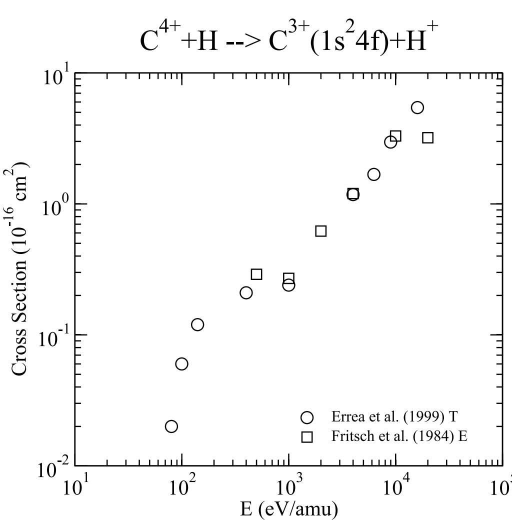

Graph 167: Cross section for charge exchange.

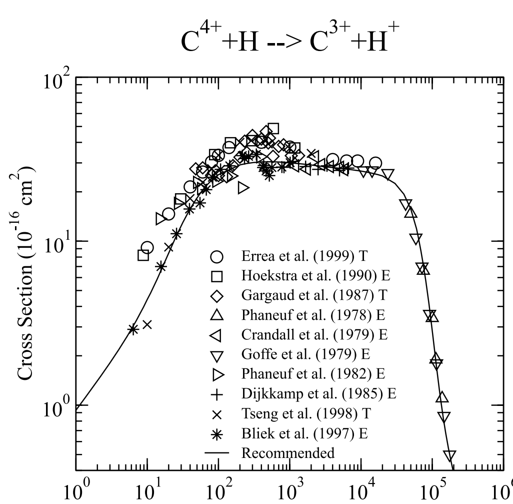

Graph 168: Cross section for charge exchange.

Graphs 139–175. (*continued*)

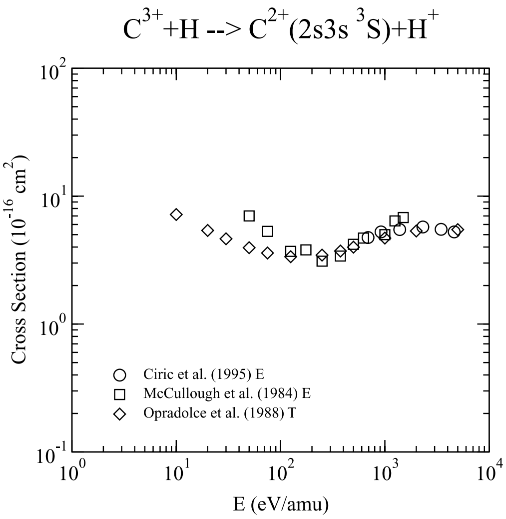

Graph 169: Cross section for charge exchange.

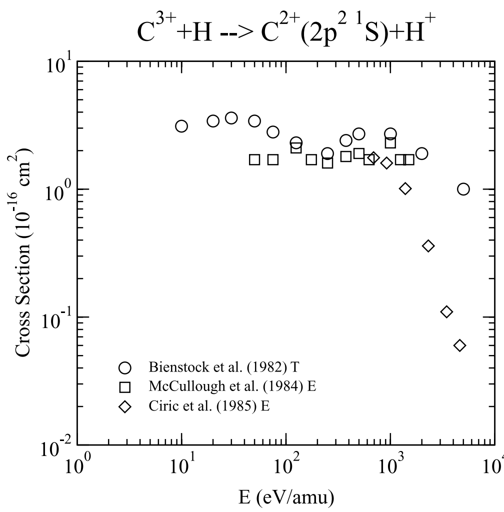

Graph 170: Cross section for charge exchange.

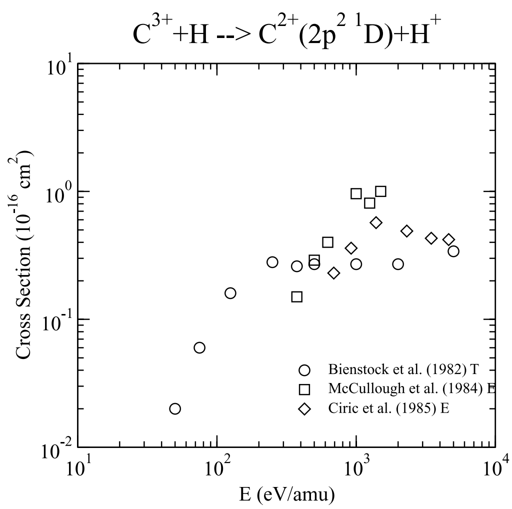

Graph 171: Cross section for charge exchange.

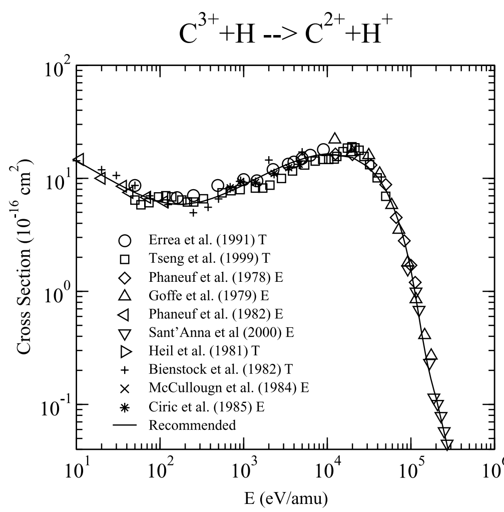

Graph 172: Cross section for charge exchange.

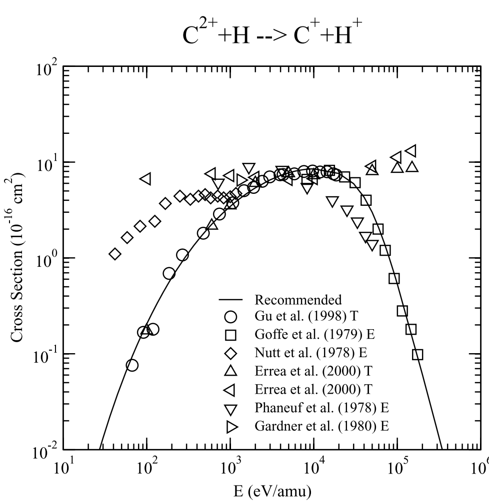

Graph 173: Cross section for charge exchange.

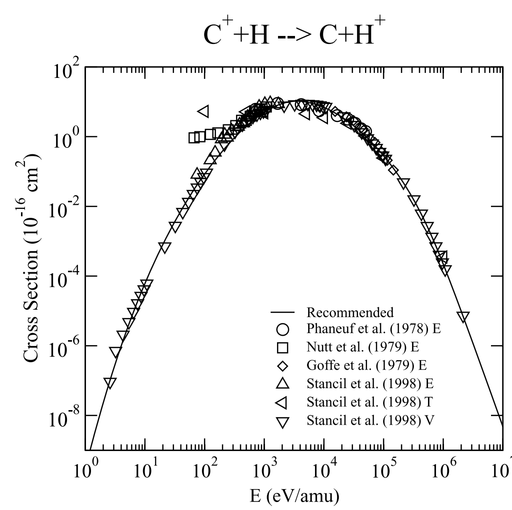

Graph 174: Cross section for charge exchange.

Graphs 139–175. (*continued*)

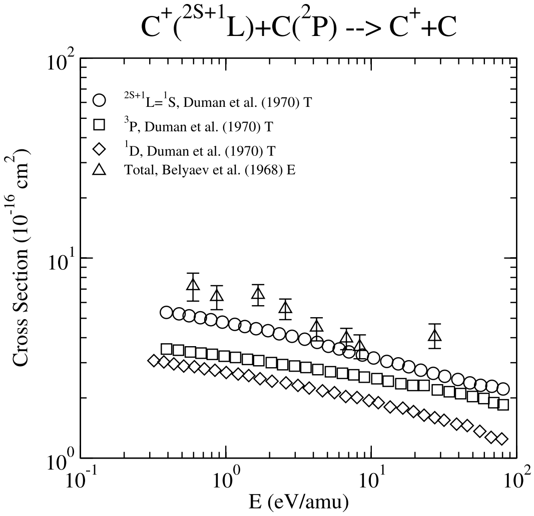

Graph 175: Cross section for charge exchange.

Graphs 139–175. (*continued*)